

**COPY-MOVE (CLONING) IMAGE FORGERY
DETECTION USING WAVELETS AND PROJECTION
PROFILING**

By

MOHD DILSHAD AHMAD ANSARI

ENROLLMENT NO. 126205

**A THESIS SUBMITTED IN FULFILLMENT OF THE REQUIREMENTS
FOR THE DEGREE OF**

DOCTOR OF PHILOSOPHY

IN

COMPUTER SCIENCE & ENGINEERING



JAYPEE UNIVERSITY OF INFORMATION TECHNOLOGY

WAKNAGHAT, H.P. - 173234 (INDIA)

FEBRUARY 2018



JAYPEE UNIVERSITY OF INFORMATION TECHNOLOGY

(Established by H.P. State Legislature vide Act No. 14 of 2002)
P.O. Wagnaghat, Teh. Kandaghat, Distt. Solan - 173234 (H.P.) INDIA
Website : www.juit.ac.in
Phone No. +91-01792-257999 (30 Lines)
Fax : +91-01792-245362

SCHOLAR DECLARATION

I hereby declare that the work reported in the Ph.D. thesis entitled, "COPY-MOVE (CLONING) IMAGE FORGERY DETECTION USING WAVELETS AND PROJECTION PROFILING" submitted at Jaypee University of Information Technology, Wagnaghat, India, is an authentic record of my work carried out under the supervision of Dr. Satya Prakash Ghrera. I have not submitted this work elsewhere for any other degree or diploma.

Mohd Dilshad Ahmad Ansari

Enrollment Number-126205

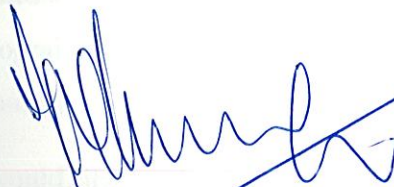
Department of Computer Science & Engineering

Jaypee University of Information Technology, Wagnaghat, India

Date: 24th February 2018

SUPERVISOR CERTIFICATE

This is to certify that the thesis entitled, “COPY-MOVE (CLONING) IMAGE FORGERY DETECTION USING WAVELETS AND PROJECTION PROFILING” which is being submitted by MOHD DILSHAD AHMAD ANSARI in fulfillment for the award of degree of Doctor of Philosophy in Computer Science & Engineering by the Jaypee University of Information Technology, Wagnaghat, India is the record of candidate's own work carried by him under my supervision. This work has not submitted partially or wholly to any other University or Institute for the award of this or any other degree or diploma.



Dr. Satya Prakash Ghrera

Professor and Head

Department of Computer Science & Engineering

Jaypee University of Information Technology, Wagnaghat, India

Date: 24th February 2018

Acknowledgements

It is by the grace of Almighty, the most beneficent, gracious and merciful. It is my privilege as well as honor to express my thankfulness to the following without whose guidance and support that I have been able to complete my doctoral work.

I express my deep sense of gratitude and respect to my supervisor Dr. Satya Prakash Ghrera, Head, Department of Computer Science & Engineering, JUIT, Wagnaghat, for his Guidance, encouragement, thought provoking, promotion, insightful comments and support during the course of this research work. He has been a strong as well as supportive adviser to me throughout my research career. His knowledge, kindness, patience, sincerity, and vision have provided me with lifetime benefits.

I express my loyal as well as admirable gratitude to JUIT administration, Prof (Dr) Vinod Kumar (Vice Chancellor), Prof (Dr) S.D. Gupta (Director & Dean, Academics & Research), Prof (Dr) Y. Medury (Former COO, JES), Maj. Gen (Retd.) Rakesh Bassi (Registrar) for providing opportunity to pursue a Doctorate Programme, infrastructural facilities as well as advanced lab to complete this scientific endeavor of my life.

I would like to thank Dr. Sunil Kumar Khah, Dr. Ravindara Bhatt, Dr. Yashwant Singh and Dr. Vivek Sehgal, Members of DPMC for their evaluation and valuable suggestions during my presentations. I take this opportunity to thank Dr. Amit Kumar Singh, Dr. P.K. Gupta, Dr. Pardeep Kumar, Dr. P.K. Singh for their constant advice, suggestions throughout my research work. I am also thankful to all faculty members and Staff of the Computer Science and Engineering Department, JUIT, Wagnaghat for their guidance and support.

I am blessed and lucky to have friends who have always stood alongside me. My heartfelt gratitude to all my friends for their continuous support and ever needed assistance.

It is my gratification to express my indebtedness to all research scholars of the Computer Science & Engineering and other Departments also for keeping me blessed with best wishes.

My special thank to Dr. R.S.Durai, Kapil Kumar, Jabir Ali, Pratiksha Gautam, Dr. Madan Sati, Dr. Tanuj Kumar, Farhina Ansari, Dr. A.R. Misrha, Dr. Ashwani, Neha, Shweta, Imran, Shivam for their kind help and support and I would also like to express my heartfelt gratitude to all those (my seniors and colleagues) who have help me directly or indirectly towards accomplishing my doctorate programme and forgive if have missed out anyone.

I wish to thank my beloved parents, Mr. Irshad Ansari and Mrs. Farikan Begum, and Grandparents, Late Haji Ali ahmad and Mrs. Islaman. Their constant love, moral support as well as motivation provided me vision and confidence, and they were the driving force to successfully finish my research. I also express my profound gratitude to my brother-in-law Mr. Mumtaz Ahmad, Sister Mrs. Reshma who have been major source of inspiration during the course of my research.

It is important to acknowledge the funding agency for providing the financial assistance. My deepest gratitude to University Grants Commission (UGC) for providing the fellowship through UGC with Maulana Azad National Fellowship (MANF) scheme. I am in the fellowship, MANF-JRF and MANF-SRF as MOMA scholar (Ministry of Minority Affairs), Govt. of India.

Last but not the least I would like to express my deepest gratitude to Mr. Mohd Wajid for their love, support and motivation throughout this research work, i am also thankful to Dr.Muhammad Usman and Dr. Ahmad Nawaz khan.

(MOHD DILSHAD AHMAD ANSARI)

Contents

| | | |
|----------|--|----------|
| 1 | Introduction and Background | 3 |
| 1.1 | Introduction | 3 |
| 1.1.1 | Pixel-Based Image Forgery Detection | 4 |
| 1.1.2 | Copy-Move (Cloning) | 5 |
| 1.1.3 | Resampling (Resize, Stretch, Rotation) | 6 |
| 1.1.4 | Splicing | 6 |
| 1.1.5 | Statistical | 7 |
| 1.2 | Related Work | 7 |
| 1.2.1 | Key-point based Approaches | 10 |
| 1.2.2 | Block Based Methods | 11 |
| 1.3 | Feature Extraction Techniques | 14 |
| 1.4 | Performance Measures | 16 |
| 1.5 | Problem Identification | 17 |
| 1.6 | Objectives of Thesis | 18 |
| 1.7 | Organization of the Thesis | 19 |

| | | |
|----------|--|-----------|
| 2 | Projection Profiling based Copy-Move Forgery Identification | 20 |
| 2.1 | Summary | 20 |
| 2.2 | Introduction | 21 |
| 2.3 | Proposed Algorithm | 22 |
| 2.4 | Results and Discussion | 24 |
| 2.5 | Conclusion | 33 |
| 3 | Modified Fast Discrete Haar Wavelet and Ring Projection Transform based Cloning detection | 35 |
| 3.1 | Summary | 35 |
| 3.2 | Introduction | 36 |
| 3.3 | Modified Fast Haar Wavelet Transform | 37 |
| 3.3.1 | Features Extraction using Ring Projection Transform (RPT) | 39 |
| 3.4 | Proposed Algorithm | 42 |
| 3.5 | Results and Discussion | 44 |
| 3.6 | Conclusion | 51 |
| 4 | Cloning Detection Using Direct Fuzzy and Ring Projection Transform | 52 |
| 4.1 | Summary | 52 |
| 4.2 | Introduction | 53 |
| 4.3 | Fuzzy Transform | 54 |
| 4.3.1 | Fuzzy Partition - Basic Functions | 54 |

| | | |
|----------|---|-----------|
| 4.3.2 | Direct Fuzzy Transform | 57 |
| 4.3.3 | F-Transform in Two Variables | 58 |
| 4.4 | Image Compression using F-Transform Method | 60 |
| 4.5 | Proposed Algorithm | 61 |
| 4.6 | Results and Discussion | 64 |
| 4.7 | Conclusion | 69 |
| 5 | Intuitionistic Fuzzy Local Binary Pattern using Texture Feature Extraction | 70 |
| 5.1 | Summary | 70 |
| 5.2 | Introduction | 71 |
| 5.3 | Local Binary Pattern | 71 |
| 5.4 | Intuitionistic Fuzzy Local Binary Pattern | 73 |
| 5.5 | Performance Metrics: Entropy of IFLBP Features | 76 |
| 5.6 | Experimental Results and Analysis | 77 |
| 5.7 | Conclusion | 86 |
| 6 | Conclusions and Future Scope | 87 |
| 6.1 | Conclusions | 87 |
| 6.2 | Future Scope | 88 |

List of Figures

| | | |
|-----|--|----|
| 1.1 | <i>Types of digital image forgery techniques</i> | 4 |
| 1.2 | <i>Pixel based image forgery</i> | 5 |
| 1.3 | <i>Copy-move(cloning)image forgery</i> | 6 |
| 1.4 | <i>Spliced image forgery</i> | 7 |
| 1.5 | <i>Image forgery detection techniques</i> | 10 |
| 1.6 | <i>Block based image forgery detection techniques</i> | 11 |
| 2.1 | <i>(a) Original image (b) Doctored image (c) Results of Cloning forgery.</i> | 26 |
| 2.2 | <i>Horizontal and filtered horizontal projection profile depicts in figure 2.1(b).</i> | 26 |
| 2.3 | <i>Vertical and filtered vertical projection profile depicts in figure 2.1(b).</i> | 27 |
| 2.4 | <i>(a) Original image (b) Doctored image (c) Results of Cloning forgery.</i> | 27 |
| 2.5 | <i>Horizontal and filtered horizontal projection profile depicts in figure 2.4(b).</i> | 28 |
| 2.6 | <i>Vertical and filtered vertical projection profile depicts in figure 2.4(b).</i> | 28 |
| 2.7 | <i>(a) Original image (b) Doctored image (c) Results of Cloning forgery.</i> | 29 |

| | | |
|------|--|----|
| 2.8 | <i>Horizontal and filtered horizontal projection profile depicts in figure 2.7(b).</i> | 29 |
| 2.9 | <i>Vertical and filtered vertical projection profile depicts in figure 2.7(b).</i> | 30 |
| 2.10 | <i>(a) Original image (b) Doctored image (c) Results of Cloning forgery.</i> | 30 |
| 2.11 | <i>Horizontal and filtered horizontal projection profile depicts in figure 2.10(b).</i> | 31 |
| 2.12 | <i>Vertical and filtered vertical projection profile depicts in figure 2.10(b).</i> | 31 |
| 2.13 | <i>(a) Original image (b) Doctored image (c) Results of Cloning forgery.</i> | 32 |
| 2.14 | <i>Horizontal and filtered horizontal projection profile depicts in figure 2.13(b).</i> | 32 |
| 2.15 | <i>Vertical and filtered vertical projection profile depicts in figure 2.13(b).</i> | 33 |
| 3.1 | <i>MFHWT decomposition</i> | 39 |
| 3.2 | <i>Concept of RPT template</i> | 41 |
| 3.3 | <i>(a) Real image, (b) Doctored image, (c) Cloning identification with CTR=2 and (d) Forgery detection with CTR=1.</i> | 46 |
| 3.4 | <i>Detection of identical object with a rotation attack (a) Real image, (b) Doctored image and (c) Cloning identification</i> | 46 |
| 3.5 | <i>Gaussian blurring (with mean = 0; $\sigma = 0.01$), Rotation with angle 180 degree and scale factor=120; (a) Real image, (b) Doctored image and (c) Cloning identification</i> | 47 |
| 3.6 | <i>Multi-paste forgery identification(a) Real image, (b) Doctored image and (c) Cloning detection</i> | 47 |
| 3.7 | <i>(a) Original image, (b) Doctored image, (c) Cloning detection</i> | 48 |

| | | |
|------|--|----|
| 3.8 | <i>(a) Real image, (b) Doctored image, (c) Cloning detection</i> | 48 |
| 3.9 | <i>(a) Real image, (b) Doctored image, (c) Cloning detection</i> | 49 |
| 3.10 | <i>(a) Real image, (b) Doctored image, (c) Cloning detection</i> | 49 |
| 4.1 | <i>A non-uniform fuzzy partition of interval [1, 4] by triangular membership functions.</i> | 56 |
| 4.2 | <i>Uniform fuzzy partition of interval [1, 4] by sinusoidal membership functions.</i> | 56 |
| 4.3 | <i>Proposed model</i> | 63 |
| 4.4 | <i>(a) Real image, (b) Doctored image (c) Fuzzy Transform image and (d) Forgery detection</i> | 66 |
| 4.5 | <i>(a) Real image, (b) Doctored image (c) Fuzzy Transform image and (d) Forgery detection</i> | 66 |
| 4.6 | <i>Forgery detection on MICC-220 Database (a) Real image, (b) Forgery image (c) Fuzzy Transform image and (d) Forgery detection</i> | 67 |
| 4.7 | <i>Forgery detection on MICC-220 Database (a) Real image (b) Forgery image (c) Fuzzy Transform image and (d) Forgery detection</i> | 67 |
| 4.8 | <i>Forgery detection on MICC-220 Database (a) Real image (b) Forgery image (c) Fuzzy Transform image and (d) Forgery detection</i> | 67 |
| 5.1 | <i>IFLBP calculation scheme for a 3×3 pixel neighborhood. (a) Gray-levels of a 3×3 pixels neighborhood. (b) Intuitionistic Fuzzy threshold values along with membership as well as non-membership values. (c) Binomial weights matrix. (d) IFLBP codes and CIFLBP.</i> | 75 |
| 5.2 | <i>Proposed model</i> | 76 |

| | | |
|-----|--|----|
| 5.3 | Histograms Plot of IFLBP Codes for X-Ray Image | 81 |
| 5.4 | Histograms Plot of IFLBP Codes for Thyroid Image | 82 |
| 5.5 | Histograms Plot of IFLBP Codes for Brain CT-Scan Image | 83 |
| 5.6 | Histograms Plot of IFLBP Codes for Lena Image | 84 |
| 5.7 | Histograms Plot of IFLBP Codes for JUIT Logo | 85 |

List of Tables

| | | |
|-----|---|----|
| 2.1 | Execution Time (In seconds) Comparison with Existing Algorithm | 33 |
| 3.1 | Accuracy Results | 50 |
| 3.2 | Accuracy Comparison on Test Images | 50 |
| 3.3 | Feature Dimension Comparison with Existing Algorithm | 50 |
| 3.4 | Execution Time (In seconds) Comparison with Existing Algorithm | 51 |
| 4.1 | Accuracy Results | 68 |
| 4.2 | TPR, FPR and Execution Time Comparison for every Technique on MICC-F220 Database | 68 |
| 4.3 | Feature Dimension Comparison with Existing Algorithm | 68 |
| 5.1 | The Entropy Values at Different Threshold and Hesitation for X- Ray image | 79 |
| 5.2 | The Entropy Values at Different Threshold and Hesitation for Thy- roid Image | 79 |
| 5.3 | The Entropy Values at Different Threshold and Hesitation for Brain CT Scan Image | 79 |

| | | |
|-----|---|----|
| 5.4 | The Entropy Values at Different Threshold and Hesitation for Lena Image | 80 |
| 5.5 | The Entropy Values at Different Threshold and Hesitation for JUIT Logo | 80 |

Abstract

Digital images play an extensive role in our daily life as we are living in the digital and technical era. The images can be a personal or official and can also be used for various important purposes such as evidence in court of law, a news item, financial record etc. Forged images are being used as original images to disguise and can be presented as false evidence. Furthermore, image processing softwares, editing tools and internet makes this process quite easy. Anyone can doctor the digital images without leaving visual clues. The activity of doctoring images is decreasing the trust-worthiness of digital images. Therefore, there is an essential and effective algorithm which can detect image forgery automatically for authenticity or genuineness of the digital images.

The copy-move (cloning) is a very popular type of forgery which is used to create a digital image doctoring. In this approach, a specific block of image or object is copied and then pasted to the other portion of the same image to accomplish information hiding. Additionally, the copied area moves from the same image, its significant properties namely noise, texture and color palette will be well matched with the remaining part of the image. It will lead to a great remonstrance in identifying and locating the forgery regions.

Although various approaches have been proposed by a number of researchers to detect copy-move image forgery (CMFD), still there are some research gaps such as false detection, high execution time and poor accuracy due to various forgery attacks. We have addressed all these issues in proposed algorithms, and new improvements have been suggested to enhance the accuracy as well as reduce the execution time.

This thesis has been divided into six chapters. Chapter 1 introduces the concept of image forgery, classification of forgery, important characteristics and various applications of image forgery. This is followed by a literature review of copy-move image forgery detection techniques along with their merits and demerits.

The method of copy-move image forgery along with major performance metrics namely Accuracy, True Positive Rate (TPR) and False Positive Rate (FPR) has been discussed. An identification of CMFD using image projection profiling with improved performance in accuracy and execution time is discussed in chapter 2.

Chapter 3 and 4 discuss robust and hybrid techniques with their performance in respect of accuracy, TPR, FPR, execution time, dimension reduction as well as after applying various attacks. We have also tested proposed algorithm on public database MICC-220. This database is having total 220 images. Total images are a combination of original image, copy-move forgery images and various attacks are also applied on forge images such as rotation, scaling, compression etc. Chapter 5 presents texture feature extraction method, which is used in various application areas of image processing. Finally, the summery of all work along with contribution and future scope are discussed in chapter 6 followed by list of publications and references at the end.

Chapter 1

Introduction and Background

1.1 Introduction

Digital image forgery is not new to the human being but a very old issue. Previously, it was restricted to art and literature although did not affect the common people. Nowadays the rapid growth of internet, image processing software plus sophisticated editing tools make this task pretty easy where a digital image could be effortlessly modified or forged [1]. Further, it is almost impossible for human vision system to recognize visually either the image is original or doctored with naked eye. The rapid improvement have been found in the digital forgeries in mainstream media as well as on the internet and in social media [2]. This trend shows grave susceptibility as well as decreases the trustworthiness of the digital images. Consequently, developing better algorithms to authenticate the honesty as well as genuineness of digital images is essential, specifically taking into consideration that images can be conferred as an evidence in a court of law, as a part of a medical records, as news item and as financial documents. So, detecting forgery in a image is one of the prime objective of digital image forensics. The classification of image forgery is shown in figure 1.1.

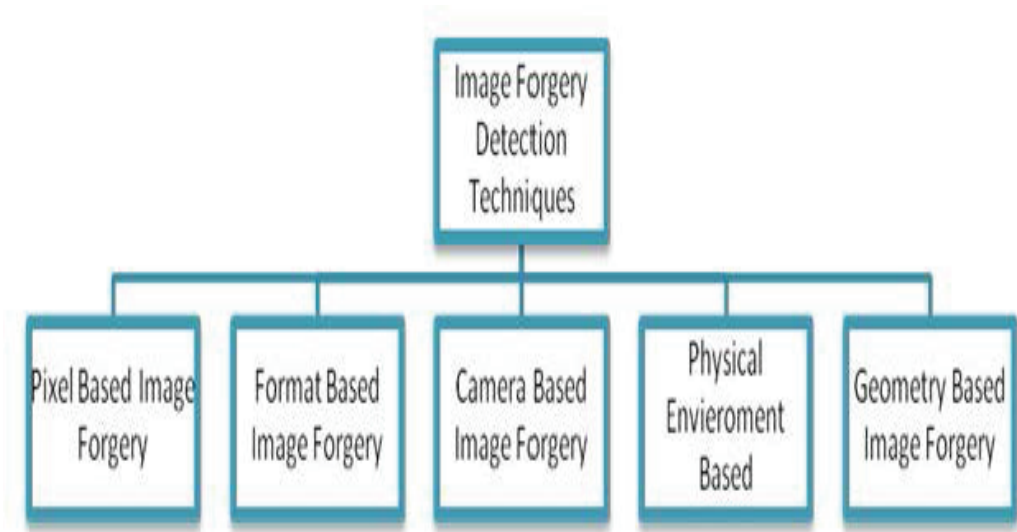


Figure 1.1: *Types of digital image forgery techniques*

1.1.1 Pixel-Based Image Forgery Detection

Pixel based approaches emphasis to pixels of the image. Pixel-based approaches are also known as passive image tampering detection techniques. Further, this method is classify into four types. In this work, our focus is on copy-move image forgery. This technique is one of the most trivial method for image forgery. Figure 1.2 display the classification of pixel based image forgery method.

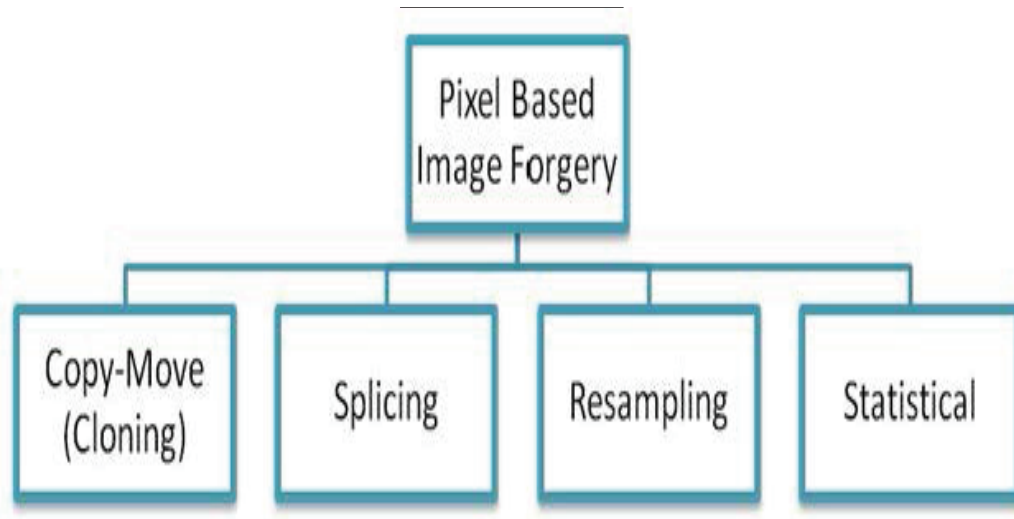


Figure 1.2: *Pixel based image forgery*

1.1.2 Copy-Move (Cloning)

Copy-move is one of the widely used as well as trivial method of image forgery and it is also known as cloning. In this type of forgery, the area or object of image is copied and then pasted into someplace within the image. Figure 1.3 depicts the original image with its doctored version. The original image is having six balloons and copy-move image with nine balloons.

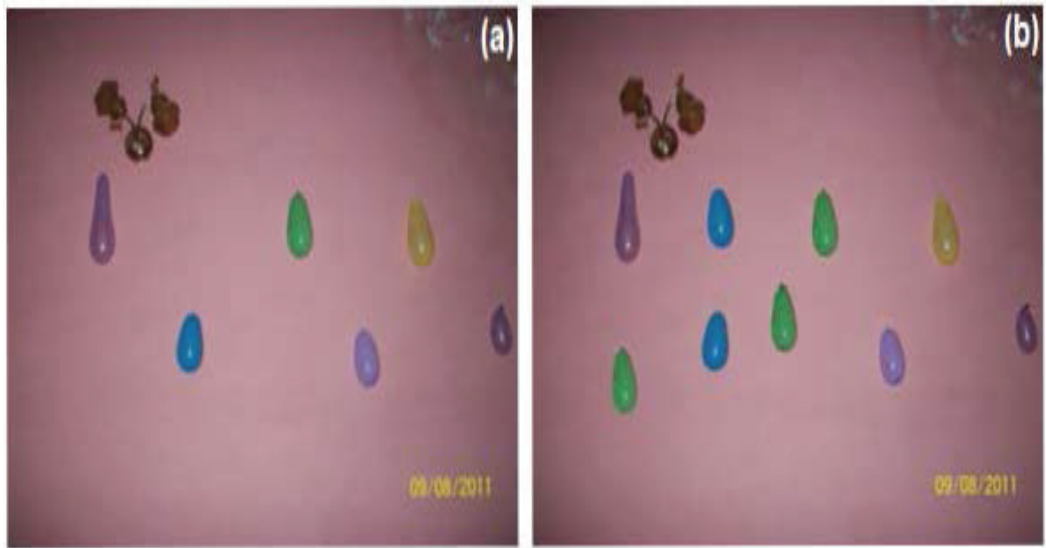


Figure 1.3: *Copy-move (cloning) image forgery*

1.1.3 Resampling (Resize, Stretch, Rotation)

For combining two objects or people into a single, it is likely to perform various operations such as we have to resize as well as stretch one person or object to match with the other object or people. Additionally, in this process we have to resample original image into a new sampling lattice.

1.1.4 Splicing

This is a different type and widely used technique of image forgery. In this approach, two or more than two images will be converted into a single composite image. Suppose we have two images shown in Figure 1.4. We have made a composite of these two into a single image. If this is done carefully than the border between spliced are impossible to identify visually.

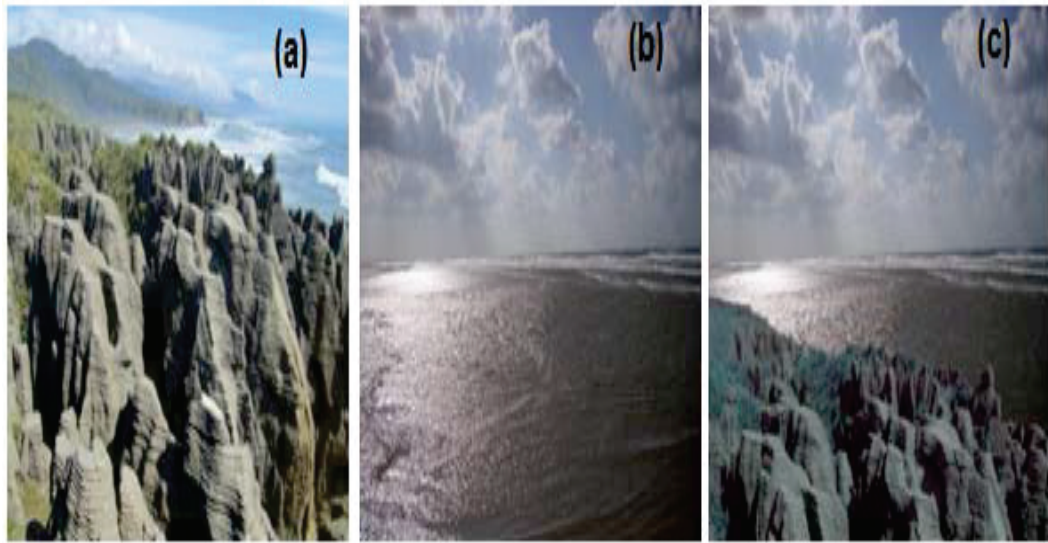


Figure 1.4: *Spliced image forgery*

1.1.5 Statistical

The statistical model is basically used to detect all things from basic image alterations such as resizing as well as filtering to perceptive photographic from computer generated photo and finding the hidden messages.

1.2 Related Work

Various algorithms have been proposed for detecting copy-move region by various researchers, few algorithms are efficient in term of detection of actual forgery region but taking too much execution time. Some algorithms are not efficient detecting forgery but having less execution time. However, very few algorithms are efficient in term of detecting forgery with less execution time but not robust in term of various attacks such as rotation, scaling, blurring, multiple copy-paste attack etc.

The detection of digital image forgery algorithms are divided into active and passive techniques. In the active technique, digital image needs preprocessing of image namely signature generation as well as embedding of watermark, which restricts their application or usefulness in systems. Contrasting, watermarking and signature based techniques; the passive techniques do not require the generation of digital signature or embedding of watermark. Further, passive approaches of detecting image forgery are separated into five types as display in Figure 1.1 Additionally, pixel based approaches mainly identify the statistical anomalies applied at the pixel level; on the other hand, format based approaches control the statistical correlations employed by a specific lossy compression system; Further, camera based approaches utilize artifacts introduced by the camera lens or sensor as well as on-chip post-processing; In physical environment based approaches, we unambiguously model and notice anomalies in the three-dimensional interaction among physical objects or light as well as camera; Lastly, geometry based approaches formulate dimensions of objects in the world and their locations reciprocal to the camera.

a) Pixel Based Techniques are mainly emphasized on the detecting pixel irregularities that were introduced at the time of forgery process. These are the most popular technique in image forensics, further categorize in three categories i.e. Cloning (copy-move), Splicing and Retouching.

b) Format Based Techniques are mainly depend on image formats as well as work in the JPEG format, this techniques are further classify into three categories i.e. JPEG Quantization, Double JPEG and JPEG Blocking.

c) Camera Based Approaches are focus on identifying the clues of forgery by exploiting the artifacts applied by various step of the image capturing process. Further divided in four categories i.e. Chromatic Aberration, Color Filter Array, Camera Response and Sensor Noise.

d) Physics Based Techniques are dependent on calculating the lighting directions and differences in lighting between image areas in the image as a telltale sign of image doctoring, further divides into three types i.e. Light Direction 2D, Light Direction 3D and Light Environment.

e) Geometric Based Technique is dependent on calculating principal points of image areas across an image, and the discrepancy between principal points. This technique is further categorized into two categories i.e. Principal point and metric measurement.

The copy-move (Cloning) image tampering is the most common approach practiced to create an image tampering, in which a particular block or object of an image is copied and then pasted into some other place of the similar image to accomplish information hiding. As the copied block arrives from the similar image, its significant characteristics namely noise texture and color palette will be reconcilable with the remaining part of the image and hence it will lead to a great threat whenever we are going to detect it as well as in locating the doctored region. The detection of copy-move (cloning) image forgery various approaches have been developed that are mainly dependent on either block based technique or key point matching techniques are shown in figure 1.5[3, 4, 9, 12, 18, 24, 26].

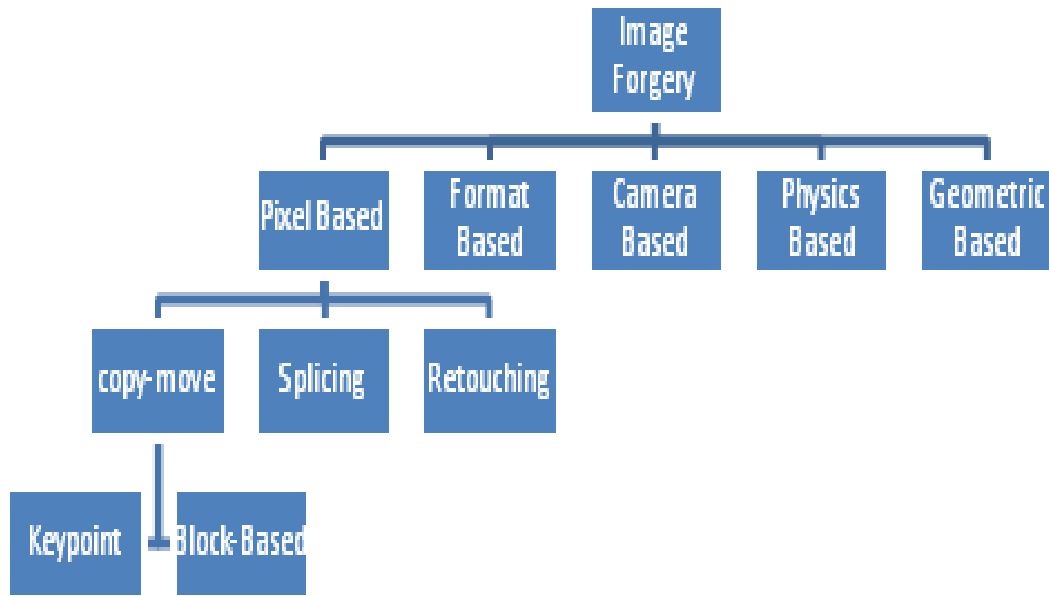


Figure 1.5: *Image forgery detection techniques*

1.2.1 Key-point based Approaches

The key point based approaches are mainly reckon on the extracting local interest points. These points are also known as key-points. Further, extracting the local points with high entropy without any image sub-blocking. The best key-points are able to identify distinct locations in a image areas are considered as efficient key points. They should be robust in terms of detecting noise, geometric transformations, illumination changes and other distortions. The major benefits of key-point approaches are that the detecting tampered region with high rate, which illustrate a rich structure namely image regions, though struggling to decrease the false matches in the flat regions such as sky and ocean.

Huang et al. [15] developed copy move forgery detection using scale invariant feature transform (SIFT) technique in 2009. Firstly, the authors have used SIFT technique to find the duplicate region with scale as well as rotation. Further, best

bin first search (BBF) techniques have been used for finding possible duplicate key-points. Additionally, nearest neighbor distance ratio(NNDR) is applied to increase the detection rate or accuracy. This technique is able to find key-points even if image is noisy or compressed. Similar methods have been developed by various authors using SIFT and SURF algorithm such as, Amerini et al.[22] and Battiato et al.[53].

1.2.2 Block Based Methods

Block based approaches are very popular and able to detect forgery regions accurately. First image is separated into a overlapping sub blocks. Further, efficient features (feature vector) are extracted from every block with the help various feature extraction and dimension reduction methods (DWT, DCT, SVD and PCA etc.) as shown in figure 1.6. Compared these feature vectors to find the possible forgery regions.

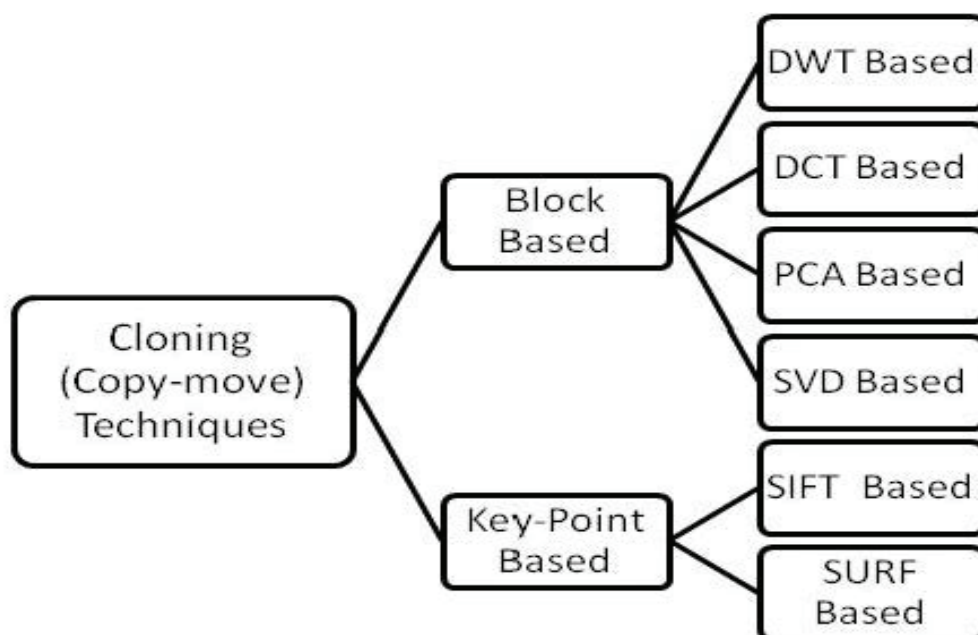


Figure 1.6: *Block based image forgery detection techniques*

The first block based method is introduced by Fridrich et al. [1] for detecting image tampering in 2003. This technique have divided the image into overlapping blocks (16×16) for extracting features. Further, extracted DCT coefficients are used as feature vector. Moreover, lexicographically sort the DCT coefficients of each blocks. After lexicographically sorting, identical blocks are nearby and forgery region are detected. Authors have perform retouching operations But any other robustness test have not performed .This method is taking too much computational time and not able to detect tampered region if attack are applied on image like rotation and scaling.

Next, Popescu et al. [2] initiated a technique for exposing digital forgeries by detecting duplicated image regions in 2004. Principal component analysis (PCA) is applied on fixed size image blocks (16×16 , 32×32). Further, eigenvalues as well as eigenvectors have been calculated of every block. Moreover, lexicographical sort is applied and duplicated regions have been detected. This technique provides better results compare to fridhrich methods. This technique is capable of detecting tampered region even if the image is compressed as well as noisy.

Gouhui Li et al. [7] introduced a sorted neighborhood technique for the detection of duplicate region with the help of DWT and SVD in 2007. First, DWT is used to decompose image into four sub-bands. Further, low frequency sub band is chosen for further processing. Moreover, singular value decomposition (SVD) is applied to extract feature vector on reduced dimension representation. Lexicographical sort is applied on singular value vector and similar vectors are nearby. These vectors are matched and forged region detected. They have used gray scale as well as color images for detecting duplicate region.

Mehdi Ghorbani et al. [8] developed DWT-DCT (QCD) method for detecting copy-move image forgery in 2011. Initially, authors have applied DWT to get low, high frequency sub bands of image. Further, DCT-QCD (Quantization Coefficient Decomposition) is employed in row vectors to decrease vector

length. Then, lexicographically sort is applied to the row vectors and shift vector is calculated. Finally, the comparison of shift vector with the preset threshold is performed and the tampered region is located.

Jing Zhang et al. [13] introduced a new technique for copy-move image forgery detection from digital images in 2008. Firstly, authors have applied DWT, the image is splitted into low frequency four sub bands. Further, low frequency sub band is chosen and divided into non-overlapping blocks. Moreover, the phase correlation utilize to calculate the spatial offset betwixt the copy-move areas. Finally, pixel matching is employed for detecting tampered area. developed technique provides better results even if the image is highly compressed and also considered as very effective technique which is taking less computational time comparatively.

Li kang et al. [15] designed the algorithm for detecting tampering from digital image in 2010. Firstly, the image is divided into small blocks as well as improved singular value decomposition (SVD) is applied for feature extraction. Further, lexicographically sort is applied on SV vectors, similarity matching is employed to located forged region from the input image.

Zhouchen Lin et al. [17] developed a fast as well as automatic technique and fine-grained forgery region detection with the help of DCT coefficient in 2009. First of all DCT coefficient have applied for extracting feature from image and then bayesian method is employed for locating possible forgery. Finally, the forgery region is location successfully.

Further, Wang et al. [43] developed hybrid approach, used DWT and DCT for detecting copy-move forgery region. Similarly, distinct techniques have been developed for detecting copy move image forgery. [4, 5, 6, 11, 12, 15, 17, 18, 19, 20, 23, 24, 25, 26, 45, 46, 55, 56, 57]

1.3 Feature Extraction Techniques

The most common features available in the image include color, texture and Shape etc. Feature extraction is mainly dependent on these three types of features and performance of any desired task is also dependent on these extracted features. Generally, feature representation methods are divided in three categories namely region-based, global based and block-based features [44, 101]. Additionally, less concentration has been given to image feature extraction related to a meaningful research on annotation as well as retrieval model itself developed. In this present work, our attention is only on texture based feature extraction. we have tested our algorithm on various medical images i.e. X-Ray, thyroid and Brain CT scan, and image processing images i.e. Lena image and JUIT logo.

A number of textural feature extraction methods were developed [62, 63]. The local binary pattern (LBP) method [63] is working on the idea of binary patterns for illustration of texture. It is extensively accepted due to simplicity of LBP and effective in representing the local spatial structure of an image. Further, the LBP techniques were enlarged as well as joined with different techniques. In results, the wide range of texture demonstration algorithm are convenient for various image analysis assignments. Conventional examples contain LBP expansion featuring scale invariance [66] as well as rotation invariance [66, 67] Further, the combination of both inter plus intra spatial structure of the LBP patterns [68] as well as fusion of micro LBP and macro Gabor features [69].

A very first study on visual inspection [73] has demonstrated that the LBP features were efficiently adopted in surface defect detection. Afterwards, BP-based features[74] have also adopted for wood quality discrimination. Moreover, more recently these features have been employed on automatic defect detection [75, 76] as well as in remote sensing [77]. Additionally, a diversified inspection has presents, the extraction of features with the help of BP approaches are found to be useful for content based image retrieval [78, 79]. Though, recently the LBP

technique has been utilized in a discriminative model for image ranking from text queries [80]. In addition to that, texture representation technique is also considered as highly efficient and effective in the area of face recognition. Afterwards, it is proficiently employed in invariant face recognition [81, 82], recognition of facial expressions [84] and face authentication [83]. Wonderful results are achieved from its various application of biomedical imaging including classification of protein images [86], video endoscopy [85], computer aided neuroblastoma prognosis system [87]. Further, it is also successfully used in various area of motion analysis such as underwater image matching [88], object tracking [90], modeling and detection of moving objects [89].

The research community has lot of interest on LBP texture representation, various approaches have been proposed with the help of BP model. The technique was developed for the assessment of local contrast measure [64]. Later, the LBP/C technique was establish by using the joint distribution of LBP codes as well as local contrast measures, which shows support to diversity of the illumination. This is also employed to improve the differentiation capacity of the original LBP technique. In addition to that, other version of LBP is Local edge patterns (LEP) technique which was designed for image segmentation [70]. This technique explain the spatial structure of local texture through the spatial orientation of edge pixels. Afterwards, similar method median binary pattern (MBP) was developed by Hafiane et al.[71], which is intensity-shift invariant. It is works on the texture primitives are resolved with localized thresholding contrary to local median. Following this analysis, a hashed variant of MBP to a binary chain has been figure out, in results another resolution as well as rotation invariant MBP (MBP-ROT) texture descriptor found [72].

Fuzzy sets provide a adaptable framework for dealing with indeterminacy characterizing real world problems, originating mainly from the unprecise as well as imperfect nature of information. However, fuzzy sets do not deal with the hesitancy (intuitionistic index) in images originated out of distinct factors. In which

their majority are caused by intrinsic vulnerability of the acquisition and imaging mechanisms. Further, distortions arises as a result of the restraint of acquisition chain namely the non-linear nature of mapping system, quantization noise, affect certainty with respect to the “brightness” or “edginess” of a pixel, the suppression of dynamic range. Hence, introduce a degree of hesitancy connected with the corresponding pixel.

Next, fuzzy sets theory introduced by Zadeh [96] by extracting the texture spectrum features [91] as well as their proficient successors. Additionally, the LBP features are able to improve their robustness to noise [30, 92, 93, 94, 95]. Though, these practice can only be treated as preliminary because they incorporate only a restricted experimental assessment. Further, Keramidas, Iakovidis et al [30, 95] proposed a generic as well as uncertainty aware technique for the derivation of fuzzy local binary pattern (FLBP) texture models. Additionally, intuitionistic fuzzy set theory proposed by Atanassov [97] provides a impressionable mathematical structure to deal with uncertainty as well as the hesitancy originating from imperfect as well as imprecise information. A extrusive property of IFS is that it appoint to each element a membership degree as well as a non membership degree with certain amount of hesitation degree.

1.4 Performance Measures

The performance of the forgery detection techniques can be observe by calculating Accuracy, True Positive Rate (TPR) and False Positive Rate (FPR). They can be estimated as follows:

True Positive (TP): Tempered image detected as tempered

False Positive (FP): Original image detected as tempered

True Negative (TN): Original image detected as original

False Negative (FN): Tempered image detected as original

From these above measures, we can define various performance evolution metrics: Accuracy, True Positive Rate (TPR) and False Positive Rate (FPR) as follows:

$$\text{Accuracy} = \frac{\text{Number of identified images}}{\text{Number of forged images}} \times 100$$

$$\text{True Positive Rate(TPR)} = \frac{\text{Number of forged images identified as forged}}{\text{Number of forged images}}$$

$$\text{False Positive Rate(FPR)} = \frac{\text{Number of original images identified as original}}{\text{Number of original images}}$$

1.5 Problem Identification

In this thesis, we have focused to design robust algorithms which are able to detect forgery with less execution time and also able to detect forgery on images subjected to scaling, rotation, blurring, and multiple copy-paste attacks. We have focused on the following issues:

1. In the literature survey of image forgery, we have found that the number of existing approaches, which are not able to detect actual forgery region. So, the false matches are the major limitation. Detecting actual region with good accuracy rate is the challenging tasks. We have addressed this issue and proposed an algorithm based on projection profiling.
2. We have processed the image block by block and extracted the feature vector for each block then compared similar the feature vector to find the possible duplication. The extraction process will take lot of computational time so improving computational time is other major challenge of this research domain. We have suggested a hybrid algorithm based on direct fuzzy transform and ring projection which reduces the execution time as well as improve the accuracy.

1.6 Objectives of Thesis

Image processing software's, editing tools and internet makes image forgery process quite easy. Anyone can doctor images without leaving any visual clues. Therefore, there is necessity of some effective algorithm which can detect image forgery automatically with good accuracy rate. Objective of the thesis are given as follows:

1. To propose a robust and efficient forgery detection algorithm, which is able to detect forgery region successfully. Also reduce the false matches and suggest new improvements in the accuracy rate.
2. To develop a lightweight and fast technique for detecting copy-move image forgery. The algorithm will take less execution time for detecting copy-move region compare to existing approaches.
3. To introduce a hybrid scheme which provide better result compare to other reported algorithms if various attacks are applied. And also able to detect copy-move forgery region accurately with less execution time.
4. To propose an efficient scheme for feature extraction from digital image, these extracted features can be applied in many application areas of image processing including image forgery detection.

We design a forgery detection technique with less execution time and robust to various forgery attacks. Proposed algorithms obtain the several objectives and identified number of problems in existing forgery detection techniques and their solutions.

1.7 Organization of the Thesis

The thesis has been organized into six chapters as follows:

chapter 1 provides the introductory part of the thesis as well as literature review and background. In chapter 2, we have presented an approach for identification of copy-move image forgery based on projection profiling for reducing the execution time. In chapter 3, a hybrid scheme for copy-move image forgery detection using ring projection and modified fast discrete haar wavelet transform is discussed. Chapter 4 presents a copy-move image forgery detection using direct fuzzy and ring projection transform. This algorithm is efficient in term of accuracy of detecting forgery as well as reducing the execution time. Further, chapter 5 demonstrates a texture features extraction technique using intuitionistic fuzzy local binary pattern. Finally, the conclusions and future scope are discussed in chapter 6. List of publications and references are depicted at the end.

Chapter 2

Projection Profiling based Copy-Move Forgery Identification

2.1 Summary

Image forgery is a very common issue which causes the negative impact on the society. In the past, it was not affecting the general public because the sophisticated software as well as editing tools are not getatable quickly, the fast progress of the image processing software make this task pretty simple. It is strenuous for humans to perceive visually whether the image is original or doctored if it is done with care. The genuineness of image is very essential in present digital scenario. Cloning doctoring is trivial form of tampering, such type of tampering an object is copied and than pasted into other place within the same image in order to hide some essential features of the image. In the present chapter, we discuss detecting of cloning technique using image projection profiling. Firstly, the input image is converted into binary then horizontal as well as vertical projection profiles have been calculated, which is employed in calculating the rectangular area of copy-move image forgery. The experimental analysis demonstrate that

the developed technique is capable in term of detecting copy-move region and meaningful enhancement have been suggested in computational time.

2.2 Introduction

If image forgery is done with care without leaving any traces then it is strenuous to human visionary framework to perceive whether the digital image is original or doctored. Further, the quick progress of the digital image processing software and internet make this task pretty easy, anybody can easily doctored digital image using these getatable editing softwares. This tendency illustrate serious susceptibility as well as diminishing the trustworthiness of the digital images. Thus, new algorithms should be developed to authorize the integrity as well as the persuasiveness of digital images. Additionally, it is awfully crucial in present digital scenario, specifically obtaining in this regards the image is conferred as an evidence in a court of law, as financial documents, as a component of medical records and can be utilize in some other important places. Hence, the detection of digital forgery is very critical.

The most common type of image forgery is cloning forgery which is frequently used for doctoring digital image. Additionally, in cloning, an object or an region of an image is copied and pasted onto the another section of the same image to cover some eminent feature of the image. The task of detecting image forgery becomes more complicated due to the copied section have the same properties of the image namely texture, noise component and color palette etc. Further, these properties show the detection approach search for copy-move forgery section with the help of inconsistencies in statistical measures will fail. The number of techniques are available which provides the solution of copy-move image forgery. These techniques provides a result under set of circumstances as well as assumptions; these approaches will not perform if these presumption are not realized [1, 2, 4, 6].

In the direct technique for identifying clone image is splitted into small overlapping blocks and then all the blocks are compared with one another. If two blocks are found to be similar, then these blocks represent potential forgeries. Suppose the image is having ss pixels, the block size pp pixels and the blocks are compared pixel by pixel, then there are $((s-m+1) (s-p)/2)p^2$ comparisons. If $s=256$ and $p=16$, then there are 7.4 million comparisons. Thus, we can say that these direct techniques are too slow for identifying doctoring from the digital images. In order to make the computation fast and overcome direct technique for identifying forgeries, we have introduced the concept of projection profiling. The main advantage of this technique is it doest require features extractions as well as so much calculations of blocks and comparisons of blocks.

2.3 Proposed Algorithm

The projection profiling of an image accommodate essential peculiarity of an image. This may be employed in the detection as well as estimation various features of an image. Additionally, it take less computation time compare to another image representing approaches. The image profiling is attempted for identifying Braille character pattern [35]. In this chapter, we have also utilize image projection profiling. This technique will help in identifying the copy-move forgery from digital images.

The proposed method has been applied on binary images as follows:

1. An Image \mathbf{X} (color/gray) of order (P,Q) converted to binary image \mathbf{Y} .
2. Horizontal $r(n)$ and vertical $s(m)$ are the projection profile of Image \mathbf{Y} respectively, may be expressed as

$$r(n) = \sum_{m=1}^P Y(m, n)$$

and

$$s(m) = \sum_{n=1}^Q Y(m, n)$$

3. By using impulse response, moving average filter of order L is calculated

$$g(a) = \frac{1}{L} \sum_{l=0}^{L-1} \delta(a - l)$$

assume, $L \lll \min (P, Q)$

4. Horizontal (r) and vertical projection profile (s) passed through moving average filter and r' , s' be the outputs after applying the filter:

$$r'(n) = \sum_{k=1}^L g(k)r(n - k)$$

and

$$s'(m) = \sum_{k=1}^L g(k)s(m - k)$$

5. Calculate the mean outputs of the filter

$$z_r = \frac{1}{Q} \sum_{n=1}^Q r'(n)$$

$$z_s = \frac{1}{P} \sum_{m=1}^P s'(m)$$

6. Find the rectangular corner indexes of cloning region. Let $r_s=r_e=s_s=s_e=\phi$, such that ϕ is a void set.

for $n \rightarrow 1:Q$

if $r'(m) < z_r$

$r'(n)=1$

else

$r'(n)=0$

$r''(n)=r'(n) - r'(n - 1)$

if $r''(n)=1$

```

 $r_s = [r_s, n]$ 
if  $r''(n) = -1$ 
 $r_e = [r_e, n]$ 
end
for  $m \rightarrow 1:P$ 
if  $s'(m) < z_s$ 
 $s'(m) = 1$ 
else
 $s'(m) = 0$ 
 $s''(m) = s'(m) - s'(m-1)$ 
if  $s''(m) = 1$ 
 $s_s = [s_s, m]$ 
if  $s''(m) = -1$ 
 $s_e = [s_e, m]$ 
end

```

7. Finally, Find the rectangular area cloning region of the image \mathbf{X}

$$R_1 = \mathbf{X}(r_s(1,1):r_e(1,1):s_s(1,1):s_e(1,1))$$

and

$$R_2 = \mathbf{X}(r_s(1,2):r_e(1,2):s_s(1,2):s_e(1,2))$$

Here R_1 and R_2 are the similar regions.

2.4 Results and Discussion

The experimental results were carried out on MATLAB 2013a, 4GB RAM and core i3 processor. To check the robustness and feasibility of our proposed algorithm, we have tested proposed algorithm on more than 20 forged images with various image sizes i.e. 128×128 , 256×256 and 512×512 etc.

Figure 2.1(a) shows original image with the forged version of original are shown in figure 2.1(b). Further, the doctored image is transformed to binary image. After that, the horizontal as well as vertical projection profile of the input image is computed and depicted in figure 2.2, figure 2.3 respectively. Moreover, moving average filter has been used on these obtained projection profiles, which is used to smoothen these curves (depicted in figure 2.2 and figure 2.3). Further, the x-coordinate of corners index of the rectangle boxes have been computed with the help of filtered horizontal projection profile as describe in proposed approach. Similarly, y-coordinate has been estimated with the help of filtered vertical projection profile.

Proposed technique is also employed on various tampered images as depicted in figures 2.4 to 2.15. The developed algorithm is works well despite multiple area or objects are presents in the image which is depend on the recurrence of valleys of the projection profile. Additionally, we can recognize the cloning area in the tampered image with the help of projection profile. In addition to that, if various objects are presents in the image then it will provide a valley in the projection profile however it will not be identical with another valley in the similar projection profile. Though, the developed algorithm is also having limitation as it works well when the object is having high contrast to the background of the image.

The computational time efficiency is compared with the existing method are shown in Table 2.1. It has been shown that computation time is relatively less for the proposed method for different sizes of images. For the proposed algorithm, there is tremendous improvement in the computation time for the bigger image sizes. The Complexity of this algorithm is $O(n^2)$.

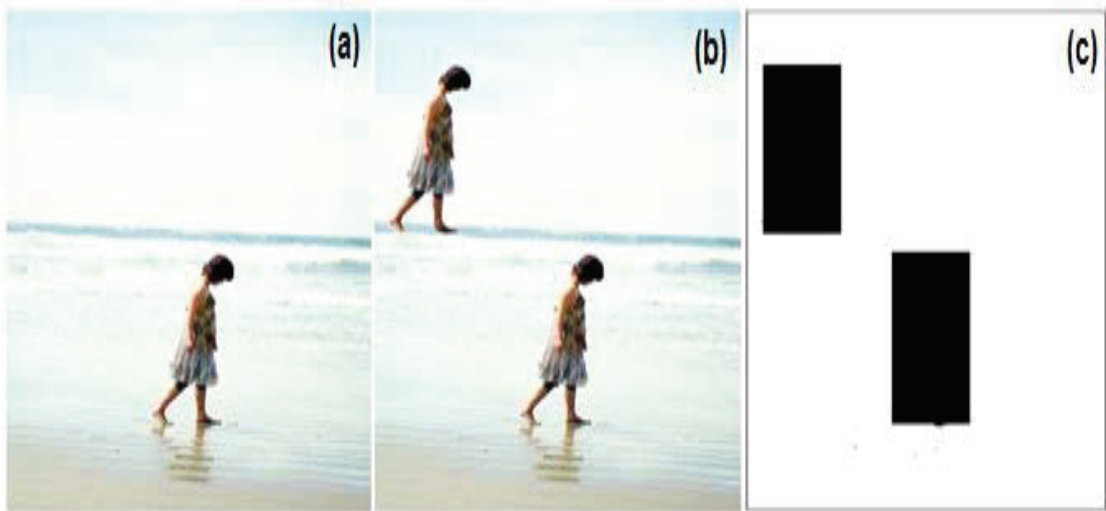


Figure 2.1: (a) Original image (b) Doctored image (c) Results of Cloning forgery.

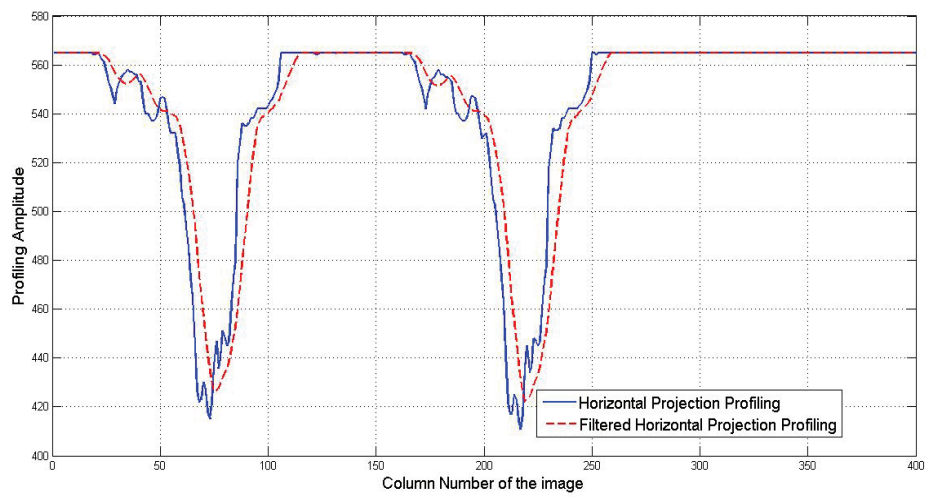


Figure 2.2: Horizontal and filtered horizontal projection profile depicts in figure 2.1(b).

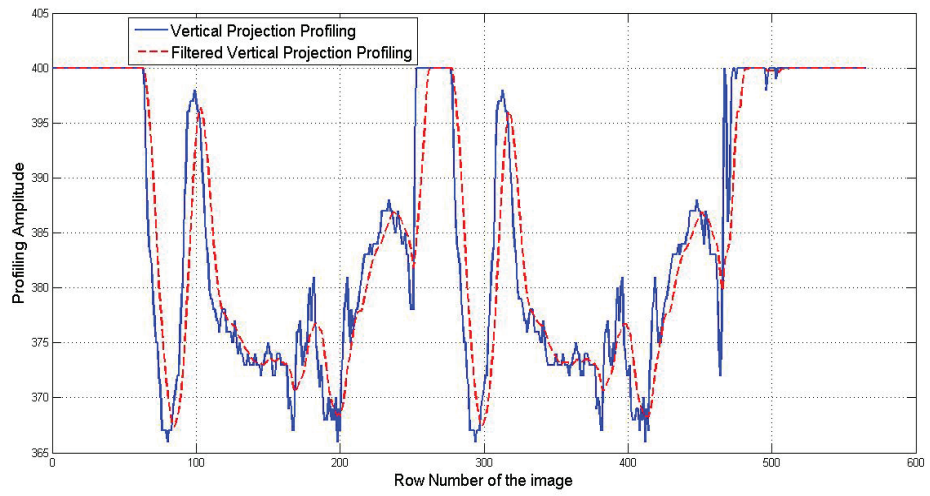


Figure 2.3: *Vertical and filtered vertical projection profile depicts in figure 2.1(b).*

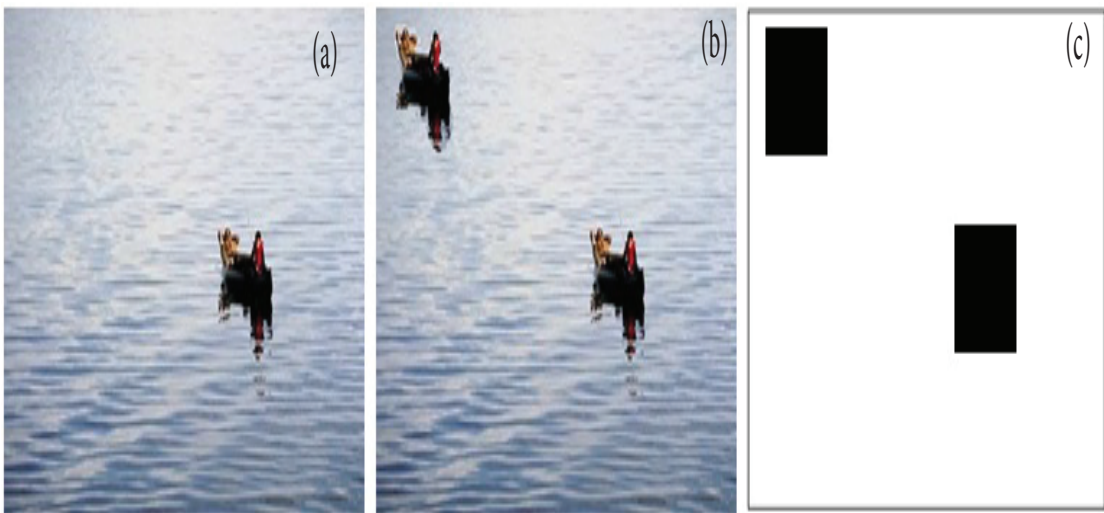


Figure 2.4: *(a) Original image (b) Doctored image (c) Results of Cloning forgery.*

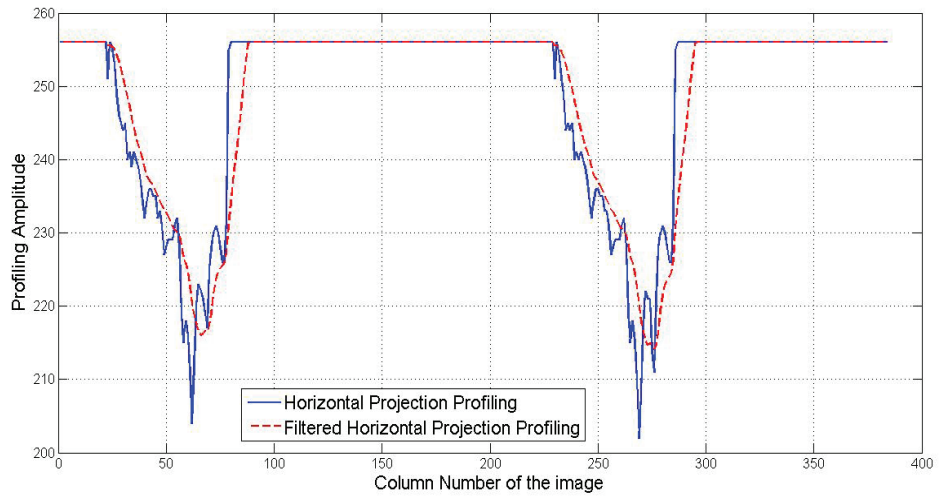


Figure 2.5: *Horizontal and filtered horizontal projection profile depicts in figure 2.4(b).*

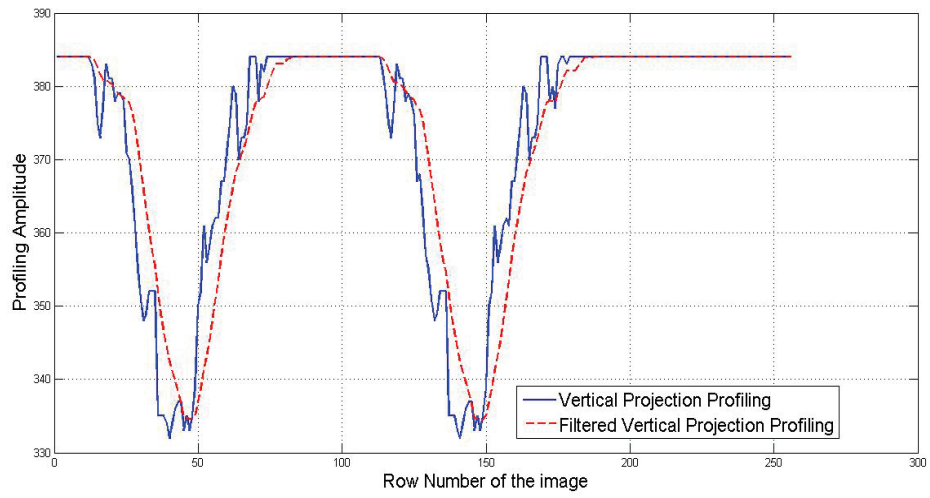


Figure 2.6: *Vertical and filtered vertical projection profile depicts in figure 2.4(b).*



Figure 2.7: (a) Original image (b) Doctored image (c) Results of Cloning forgery.

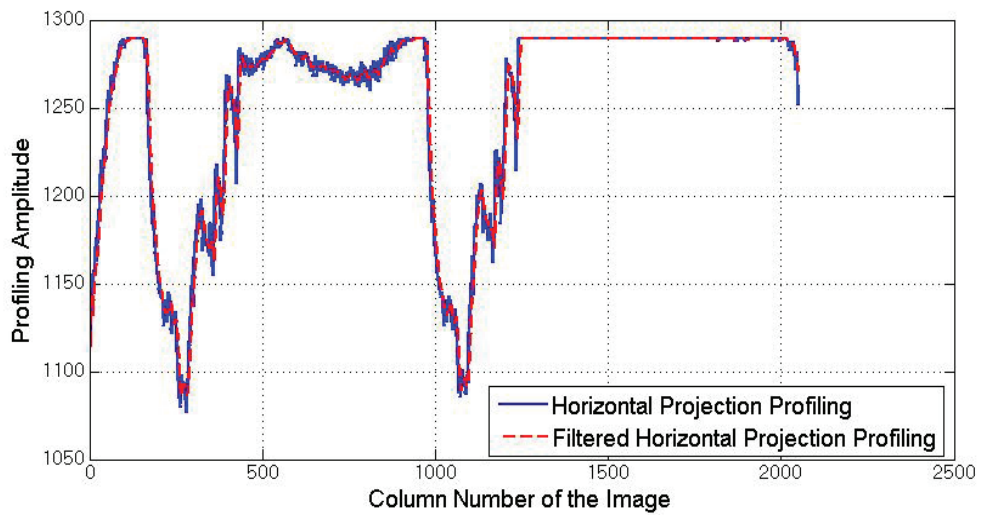


Figure 2.8: Horizontal and filtered horizontal projection profile depicts in figure 2.7(b).

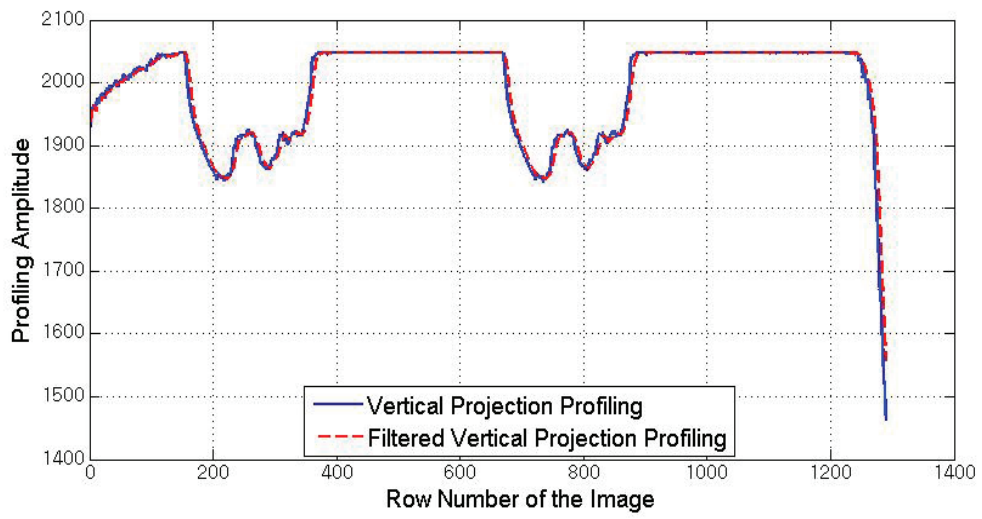


Figure 2.9: *Vertical and filtered vertical projection profile depicts in figure 2.7(b).*

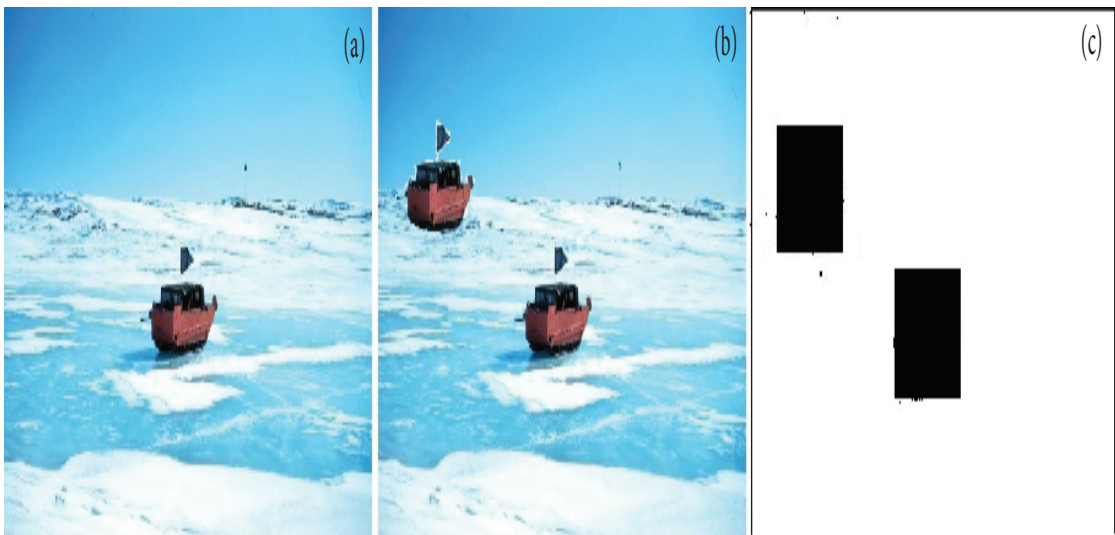


Figure 2.10: *(a) Original image (b) Doctored image (c) Results of Cloning forgery.*

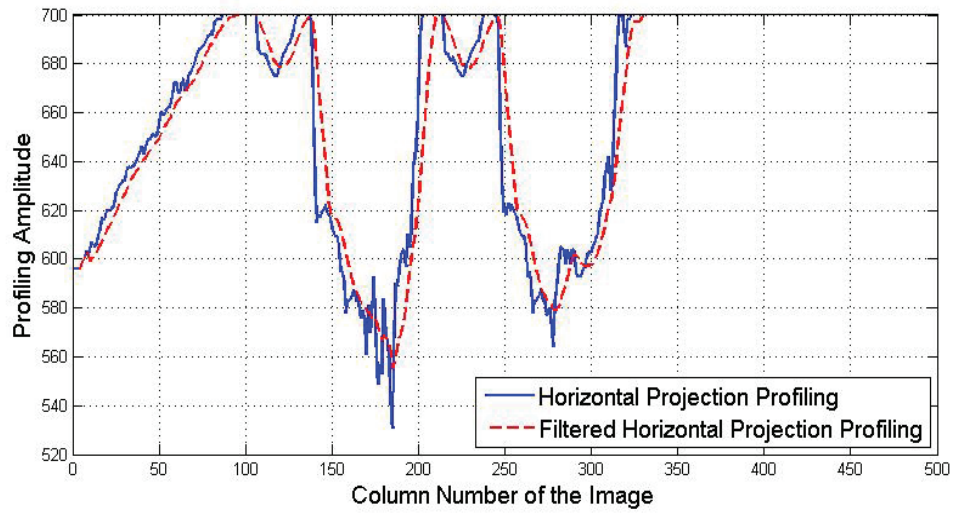


Figure 2.11: *Horizontal and filtered horizontal projection profile depicts in figure 2.10(b).*

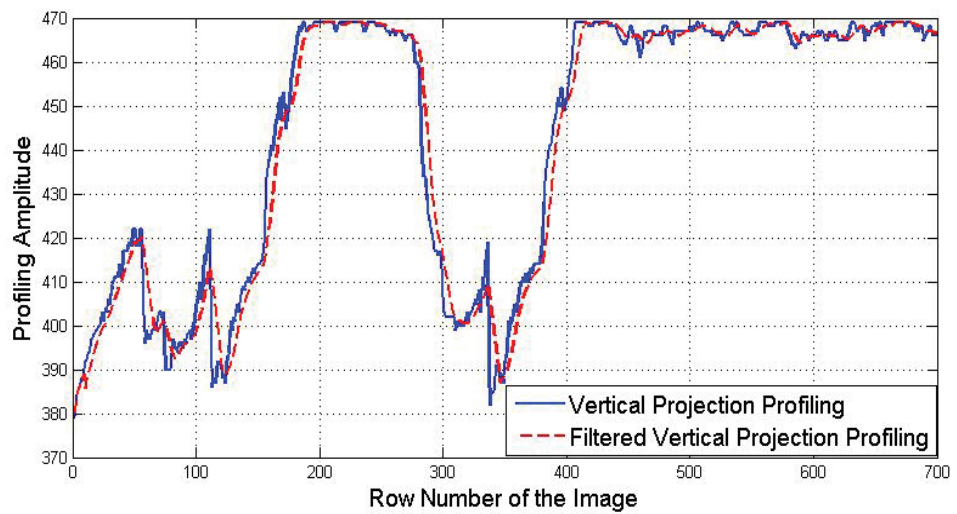


Figure 2.12: *Vertical and filtered vertical projection profile depicts in figure 2.10(b).*

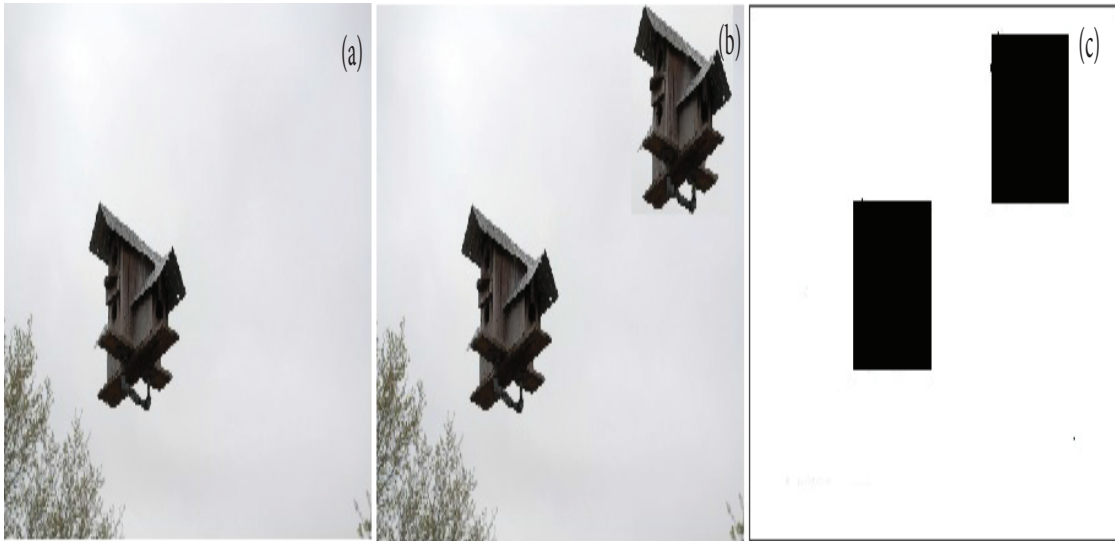


Figure 2.13: (a) Original image (b) Doctored image (c) Results of Cloning forgery.

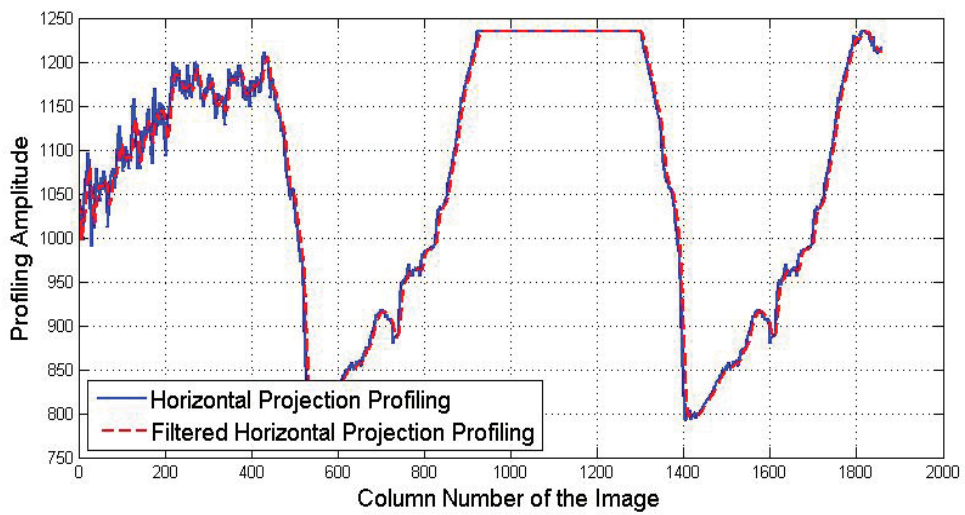


Figure 2.14: Horizontal and filtered horizontal projection profile depicts in figure 2.13(b).

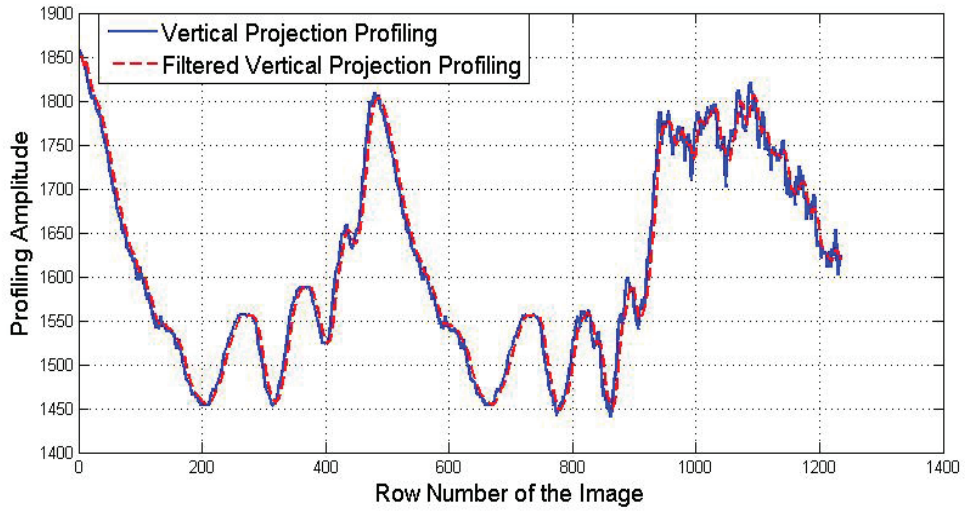


Figure 2.15: Vertical and filtered vertical projection profile depicts in figure 2.13(b).

Table 2.1: Execution Time (In seconds) Comparison with Existing Algorithm

| Image Name | Image 1 | Image 2 | Image 3 | Image 4 | Image 5 | Image 6 |
|-----------------|-------------|-------------|-------------|-------------|-------------|-------------|
| Image Size | 128 ×128 | 256 ×256 | 384 ×384 | 424 ×424 | 512 ×512 | 656 ×656 |
| Wang et al.[43] | 4.96 | 39.70 | 171.09 | 239.48 | 478.109 | 1259.35 |
| Proposed Method | 3.29 | 4.27 | 4.81 | 5.33 | 5.69 | 6.12 |

2.5 Conclusion

We have developed a new approach for image forensics using projection profiling. As the block-based cloning forgery identification techniques are computationally intensive. Hence, any improvement in execution time will help in checking forgery from the given image. The proposed method successfully addresses this issue and is noticeably faster than the existing methods.

To check the robustness of our proposed approach it has been implemented on distinct forge images. The results demonstrate that the proposed technique is capable in detecting copy-move region effectively and new enhancements have been suggested in computational time shown in table 2.1. In future, we can improve the copy-move forgery detection approach with applying various attacks namely rotation, added Gaussian noise, JPEG Compression and scaling.

Chapter 3

Modified Fast Discrete Haar Wavelet and Ring Projection Transform based Cloning detection

3.1 Summary

In the recent years, Wavelet transform has been considered to be a very effective tool for image processing. Modified fast haar wavelet transform (MFHWT) is very useful approach which reduces the computation work in haar transform (HT) as well as fast haar transform (FHT). In this current work, we applied modified fast haar wavelet on an input image to yields a highly minimized dimension representation. In that manner, the number of image blocks of an image can be drastically reduced which improves the time proficiency of successive lexicographical sorting as well as similarity matching.

This reduced dimension representation is splitted into fixed size overlapping blocks, then ring projection transform is executed to every block for extract the features into a row vector. These extracted feature vectors are arranged in a matrix. Further, the feature vectors are lexicographically sorted so that identical blocks would be successive. Lastly, the similar blocks are filtered out by calculating the similarity value of correlation coefficient between two adjacent blocks. Obtained results demonstrate the performance of proposed technique, which is able to reduces dimension drastically as well as decreases the time, memory required for the identification process of copy move forgery.

3.2 Introduction

In the recent years, the recognition of digital cameras, tablets and smart phones have made the acquirement of digital images simple. Additionally, sophisticated photo editing tools and packages namely Photoshop makes it somewhat easy to generate image doctoring, on which people almost unattainable to distinguish the dissimilarities between the original image as well as doctored image. There is speedy enlarge in digitally manipulated image forgeries in social media as well as on the internet. These kinds of activities decreasing the credibility of digital image, so there must be some algorithm which can provide the authenticity of digital images.

In literature, there are mainly two types of image authentication methods: Active as well as passive method. In the active methods, the digital image requires preprocessing of image namely watermark embedding and signature generation, which restrictions their application in practice. To overcome active methods passive method came into the picture, approaches do not require any digital signature to be generated or to insert any watermark. Additionally, passive methods are further categories into five categories.[1, 2]

3.3 Modified Fast Haar Wavelet Transform

In this section, we discuss the concept of modified fast haar wavelet and ring projection transforms. Further, Haar Transform (HT) is memory proficient and exactly reversible without the edge effects. Nowadays haar transform technique is widely used in image compression. The HT is one of the effortless as well as simple transformation from the space domain to a local frequency domain. Further, HT disintegrate signal into two components, the first one is known as average (approximation) as well as trend and second one is called difference (detail) as well as fluctuation.

An explicit formula for the values of first average sub-signal, $a^1 = (a_1, a_2, \dots, a_{n/2})$ at one level for a signal $f = (f_1, f_2, \dots, f_n)$ of length n is given by

$$a_k = \frac{f_{2k-1} + f_{2k}}{\sqrt{2}}, \quad k = 1, 2, \dots, n/2. \quad (3.3.1)$$

and the first detail sub-signal, $d^1 = (d_1, d_2, \dots, d_{n/2})$ at the similar level is defined as

$$d_k = \frac{f_{2k-1} - f_{2k}}{\sqrt{2}}, \quad k = 1, 2, \dots, n/2. \quad (3.3.2)$$

Wavelet decomposition of the images is adopted because of its inherent multi-resolution properties. Additionally, the basic concept of employing discrete wavelet transform is to minimize the size of a image at every level. Assume a square image of size $2^j \times 2^j$ pixels at level L minimizes to size $2^{j/2} \times 2^{j/2}$ pixels at level $L + 1$. Further, at every level, the image is divided into four sub bands or images. Additionally, the sub bands or images are knows as LL, LH, HL and HH. Further, LL band (approximation region) consist information regarding the global properties of evaluated image and elimination of spectral coefficients against that region have more chances of the immense distortion in the original image.

Moreover, LH (horizontal region) are having information regarding the vertical lines which is hidden in a image and elimination of spectral coefficients against that region remove horizontal details of the original image. On the other hand, HL (vertical region) consist information regarding vertical lines which is hidden in a image and elimination of spectral coefficients against that region remove vertical details of the original image. Lastly, HH (diagonal region) includes information regarding the diagonal details which is hidden in a image and elimination of spectral coefficients against that region leads to less distortions in the original image.

Roeser and Jernigan [33] introduced the Fast Haar Transform computation-ally efficient and effective techniques which are able to minimize the laborious work of calculations. Further, FHT incorporate addition, subtraction along with division by 2.

Additionally, the FHT are applied in atmospheric turbulence analysis, image analysis, signal and image compression [34]. Moreover, modified fast as well as exact algorithm for fast haar transform has been explain in [49].

In MFHWT, first average sub-signal, $a^1 = (a_1, a_2, \dots a_{n/4})$ at one level for a signal $f = (f_1, f_2, \dots f_n)$ of length n is given by

$$a_k = \frac{f_{4k-3} + f_{4k-2} + f_{4k-1} + f_{4k}}{4}, \quad k = 1, 2, \dots, n/4 \quad (3.3.3)$$

and the first detail sub-signal, $d^1 = (d_1, d_2, \dots d_{n/4})$ at the same level is given as

$$a_k = \begin{cases} \frac{(f_{4k-3}+f_{4k-2})-(f_{4k-1}+f_{4k})}{4}, & k = 1, 2, \dots, n/4 \\ 0, & k = n/2, 2, \dots, n. \end{cases} \quad (3.3.4)$$

Bhardwaj and Ali [50] used the same concept of finding averages and differences to extended for 2-D images in addition of acknowledging the detail coefficients 0 as $n/2$ elements at every level.

The MFHWT is faster than FHT, it is also minimize the computation effort. Additionally, MFHWT provides the values of approximation as well as detail coefficients one level ahead than the FHT and HT. Moreover, At every level in MFHWT, we require only half of the original data employed in FHT because of this it becomes more and more memory proficient. The most noticeable fact is that the MSE as well as PSNR values of reconstructed images are as wonderful as in HT as well as in FHT. Figure 3.1 depicts an image along with its wavelet transform applied up to level 3.

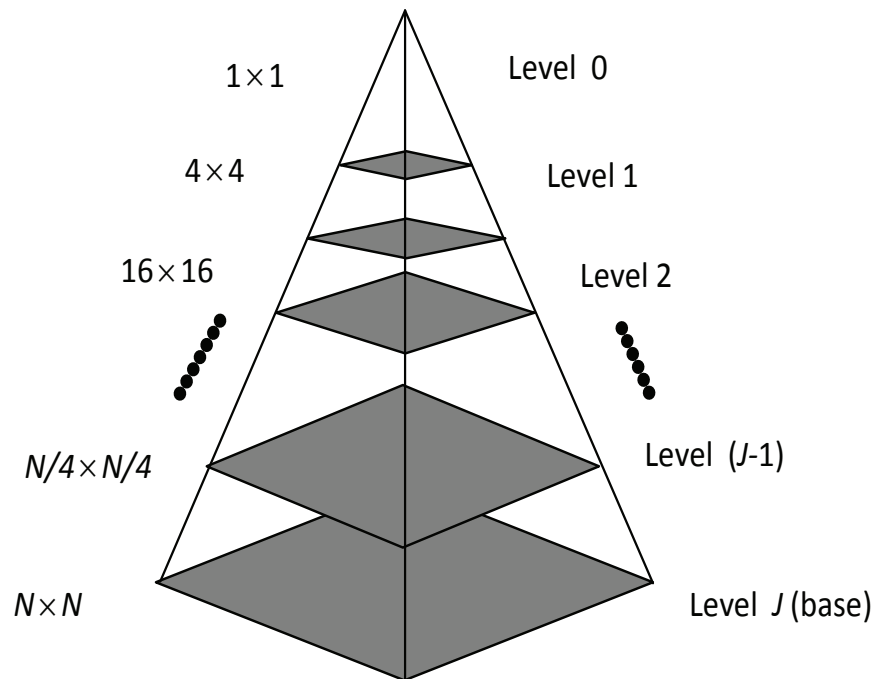


Figure 3.1: *MFHWT decomposition*

3.3.1 Features Extraction using Ring Projection Transform (RPT)

The RPT [36, 37, 51, 52] was proposed to make pattern matching invariant to rotation. The RPT converts a 2-D image in the rotation-invariant representation

of 1-D ring projection space. Further, let say a template whose dimension is $m \times n$, by $T(x, y)$. Moreover, the template will be processed by RPT as above: Firstly, the center point of $T(x, y)$ is represented as (x_c, y_c) . Afterwards, the template $T(x, y)$ Cartesian frame is converted into a polar frame using the given relations:

$$x = r \cos \theta, \quad (3.3.5)$$

$$y = r \sin \theta, \quad (3.3.6)$$

where, $r = \text{Int}[(x - x_c)^2 + (y - y_c)^2]^{1/2}$, $r \in [0, R]$, $R = \min(M, N)$ and $\theta \in [0, 2\pi]$.

The ring-projection of image $T(x, y)$ at radius r , denoted by $P_T(r)$, is defined as the mean value of $T(r \cos \theta, r \sin \theta)$ at the specific radius r . That is,

$$P_T(r) = \frac{1}{2\pi r} \int_0^{2\pi} T(r \cos \theta, r \sin \theta) \quad (3.3.7)$$

The effect of noise can be minimize by taking the mean of stimulus values of every particular ring. The discrete illustration of $P_T(r)$ is given by

$$P_T(r) = \frac{1}{S_r} \sum_{i=1}^n T(r \cos \theta_k, r \sin \theta_k) \quad (3.3.8)$$

where, S_r is the total number of pixels tumbling on the circle of radius $r = 0, 1, 2, \dots, R$. Because $P_T(r)$ is describe as the mean of pixel intensities values along with circle, centered on the template, whose radius is r as depicted in Figure 3.2. Further, $P_T(r)$ values of all rings in the template have proportionate significance in the calculation of correlation [37]. Additionally, as RPT is formulated along circular rings by maximizing radii, the derived one dimensional ring projection template is invariant to rotation of its corresponding two dimensional image template.

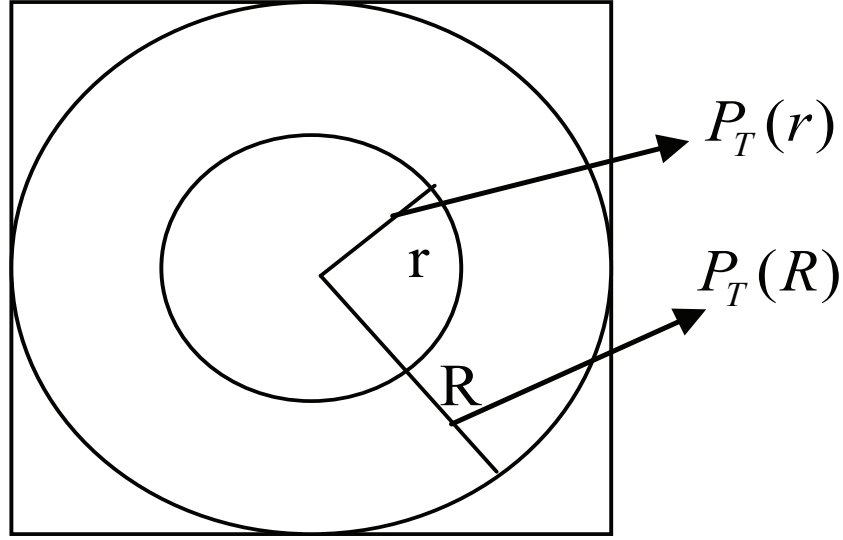


Figure 3.2: *Concept of RPT template*

The correlation coefficient is a measurement of the strength of the linear relationship between two variables or sets of data. To extract the similar pattern or matching, normalized correlation (NC) is applied.

Let $P_T = [P_T(0), P_T(1), P_T(2), \dots, P_T(R)]$ and $P_S = [P_S(0), P_S(1), P_S(2), \dots, P_S(R)]$.

Then normalized correlation coefficient between two different RPTs P_T and P_S is given by the formula:

$$\langle P_T, P_K \rangle = \frac{\left[(R+1) \sum_{r=0}^R P_T(r)P_S(r) - \sum_{r=0}^R P_T(r) \sum_{r=0}^R P_S(r) \right]^2 \times 100}{\left\{ (R+1) \sum_{r=0}^R P_T(r)^2 - \left[\sum_{r=0}^R P_T(r) \right]^2 \right\} \left\{ (R+1) \sum_{r=0}^R P_S(r)^2 - \left[\sum_{r=0}^R P_S(r) \right]^2 \right\}} \quad (3.3.9)$$

The value of $\langle P_T, P_K \rangle$ is undamaged by rotations as well as linear changes (constant improvement and offset) between two different RPTs P_T and P_S . Additionally, the dimensional size of the ring projection vector is only $R+1$. However, this notably minimizes the computation complexity of $\langle P_T, P_K \rangle$.

3.4 Proposed Algorithm

In the block based cloning algorithms, most of the technique frameworks are similar to the approach developed by Popescu and Farid [2]. In these approaches lot of computational effort are required for dimension reduction as well as matching control and similarity filtering. Generally, as the input images grow bigger, the nature of CMFD algorithms required many iterations and comparisons e.g., Suppose that a gray-scale image of dimension $m \times n$ pixels could be splitted into overlapping blocks of size $b \times b$ pixels, then total number of image blocks are $N = (m - b + 1) \times (n - b + 1)$ produced by sliding the window of $b \times b$ pixels above the entire image by one pixel every time from upper left to bottom right corner. MATLAB excels in working with matrices, however is less optimized when faced with multiple loops. Therefore, it will be highly important that the loops were kept to a minimum as possible. Moreover, CMFD technique would become computationally restrictive when the bigger number of image blocks which inescapably leads to drastically high computation work for consequent feature extraction as well as similarity matching. Therefore, the key point to decreases the computational work, the process of CMFD is usually applied on a highly minimized dimension of image; however, information loss is undeniable.

Based on this idea, we have develop a boosting approach to reduce the computational overhead as well as number of obtained blocks every time and it turns out to decrease time and memory considerably. The developed technique has been applied on gray image as follows:

1. Read the input image, if the input image is *RGB*, then converts it into gray scale version by $I = 0.228R + 0.587G + 0.114B$.
2. Apply MFHWT up to particular level '*L*' to the gray image.
3. Overlapping blocks of size $b \times b$ are created in the LL_L image with one

pixel shifting and the total number of overlapping blocks is presented by $N_{ovr} = (M - b + 1) \times (N - b + 1)$.

4. The blocks with minimum contrast value are ignored as they are unstable over image variations and leads to false positive results. Therefore, in order to reduce the false positive results, we ignore those blocks, where contrast value is less than the predefined threshold. Hence, if the contrast value of each overlapping $b \times b$ is less than the predefined ' CTR ', then we ignore it, otherwise we apply the following steps:
 - (a) Transform each overlapping $b \times b$ into a $1-D$ RPT vector of size $R+1$.
 - (b) The extracted features from Step (a) are managed in a matrix which is denoted by A of size $(M - b + 1)(N - b + 1) \times R + 1$.
 - (c) In the mean while, we form another matrix P of two columns for storing top-left coordinates.
5. Apply lexicographical sort to the matrix A so that identical blocks are consecutively sorted.
6. For every adjacent rows of matrix A ,
 - (a) Compute the normalized correlation coefficient between the pair of sorted rows using the equation (3.3.9)
 - (b) If the calculated correlation coefficient is exceeded from a preset threshold ' C'_t ', then extract the corresponding blocks position from the matrix P , and marked the location of these doctored blocks are in the original image by setting pixel values to zero.
7. Finally, the copy-move region is detected automatically.

3.5 Results and Discussion

This section present the experimental procedure and determine the performance of developed approach in terms of accuracy, true positive rate (TPR)and false positive rate(FPR).The experimental results were carried out on Matlab R2013a, 4 GB RAM and core i3 processor. To determine the performance of proposed method and its quality, a realistic database can be constructed. We have composed a database of 100 images, where 50 images are forged and 50 images are original. This database having different type of image format and various resolutions like 256×256 , 512×512 , 640×480 etc. The forged images are constructed with the help of Photoshop, In which the forge area or object is randomly selected and pasted into the same image. Also, we have applied various attacks on tempered image like scaling, rotation and blurring. The performance of the proposed technique has been observe by calculating Accuracy, True Positive Rate (TPR) and False Positive Rate (FPR).

The performance of the developed method is shown in Table 3.1, Table 3.2, Table 3.3 and Table 3.4, which shows the proposed method perform better than state of the art techniques [1, 2]. Table 3.1 shows the accuracy of proposed algorithm with normal forgery and various attacks. The accuracy of proposed algorithm in normal forgery, blurring attack and rotation attack were 95 %, 89 % and 87 % respectively. The overall accuracy of proposed method was 90.75 %. Additionally, Table 3.2 shows the accuracy with other reported algorithm on same images. Table 3.3 shows proposed algorithm is able to reduce dimensions drastically in comparison to other reported methods[1, 2, 8, 12, 21, 22]. If the dimension of the algorithm is less, then definitely it will take less computational time, that is why proposed algorithm is taking less computational time as compare to other existing algorithm as shown in Table 3.4.

The images shown in Figure 3.3 represents the result of cloning detection marked on the tampered image with predefined threshold CTR and without CTR. The row consist of four images: original image, doctored image, result image with CTR 2 as well as CTR 1 from left to right. First, the original image is decomposed at level 1 by applying MFHWT. The parameters in this experiment were set as: $C_t = 0.98$, $CTR = 2$, $b = 7$. The detection process taking 6 seconds which shows that proposed method is highly efficient with respect to computational time and successfully able to detect forgery region. However, if we apply proposed algorithm by taking the blocks whose contrast is minimum, then we obtained false positive results and more time are required for forgery detection process. The detection result with following parameter values $C_t = 0.98$, $CTR = 1$, $b = 7$ and the required time is 8 seconds.

Further, we have applied various attacks such as rotation, scaling and blurring attack. The forgery detection results are depicted in figure 3.4, figure 3.5 and figure 3.6. For testing algorithm on robustness against rotation attack, one duplicate object is rotated with angles of 45 degree and developed technique is capable is detecting forgery region as depicted in figure 3.4. Further, figure 3.5 display tampered image was distorted by different processing operations such as Gaussian blurring (with mean =0; $\sigma = 0.01$), Rotation with angle 180 degree and scale with some factor. Figure 3.6 shows copy of a single object is pasted multiple times in the forged image and developed approach is capable in detecting all objects efficiently without any postprocessing operation. Similarly, forgery are being identified on other images also as shown in figure 3.7 to 3.10. The complexity of this algorithm is $O(n^2 \log n)$

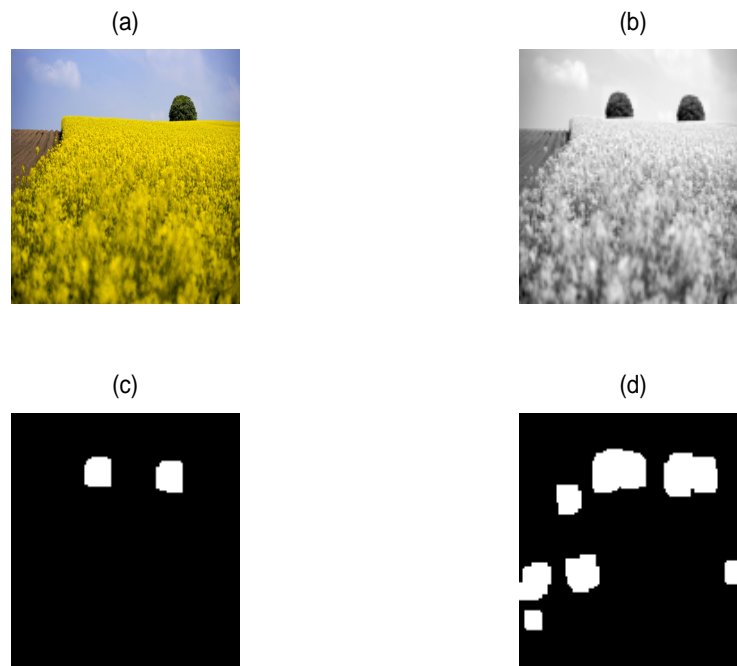


Figure 3.3: (a) Real image, (b) Doctored image, (c) Cloning identification with $CTR=2$ and (d) Forgery detection with $CTR=1$.

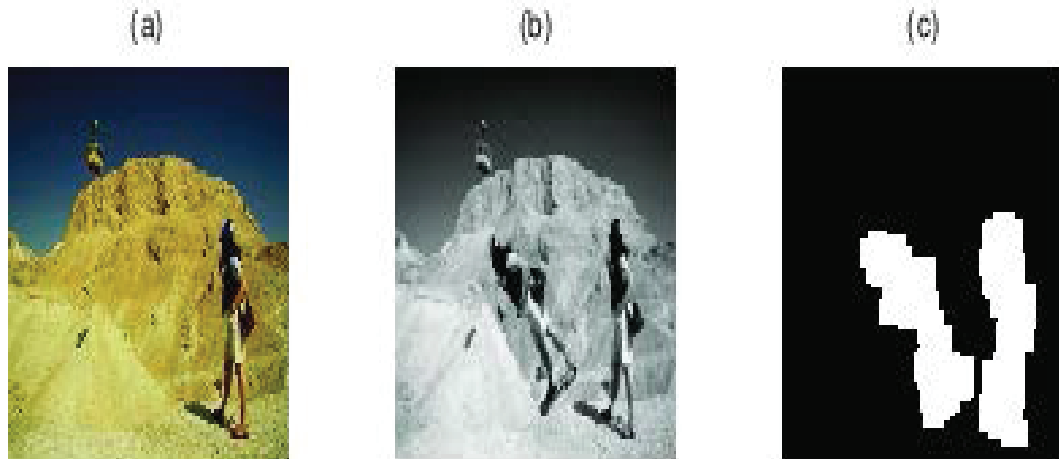


Figure 3.4: Detection of identical object with a rotation attack (a) Real image, (b) Doctored image and (c) Cloning identification

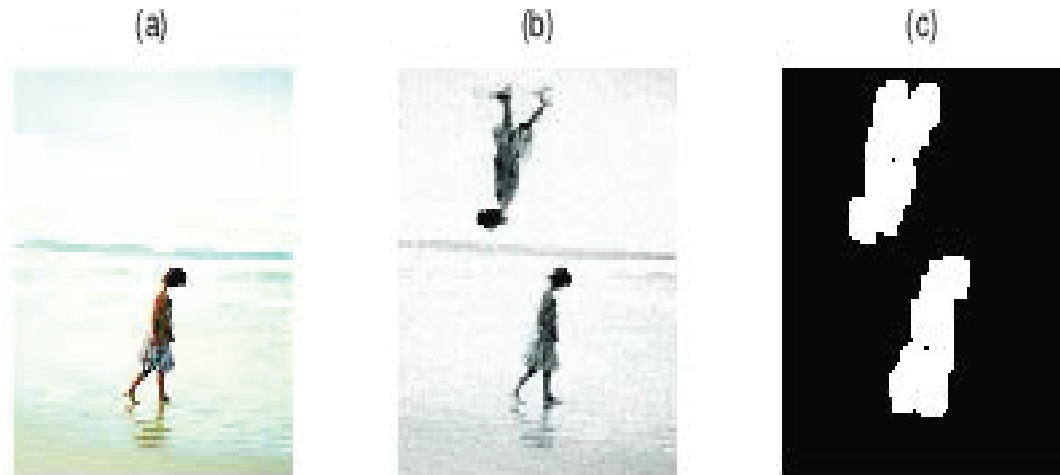


Figure 3.5: *Gaussian blurring (with mean = 0; $\sigma = 0.01$), Rotation with angle 180 degree and scale factor=120; (a) Real image, (b) Doctored image and (c) Cloning identification*

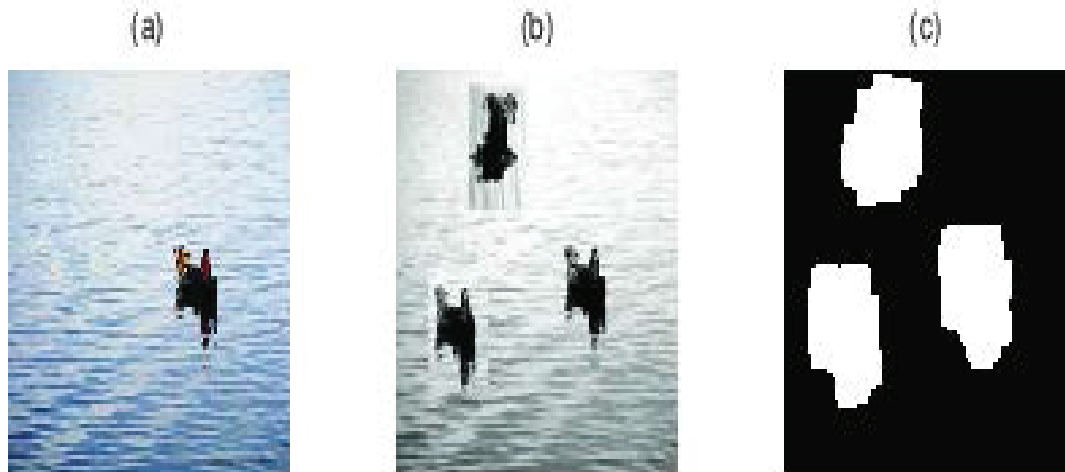


Figure 3.6: *Multi-paste forgery identification (a) Real image, (b) Doctored image and (c) Cloning detection*

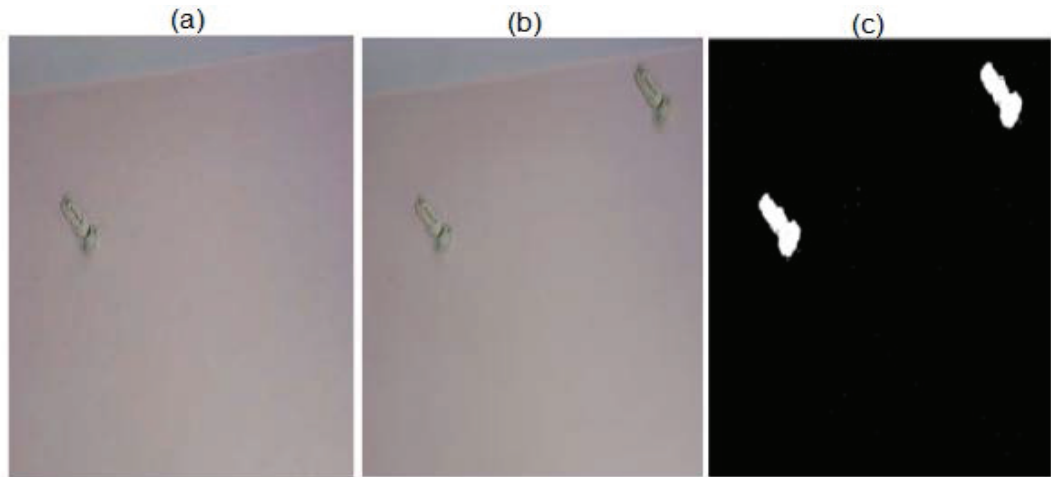


Figure 3.7: (a) *Original image*, (b) *Doctored image*, (c) *Cloning detection*

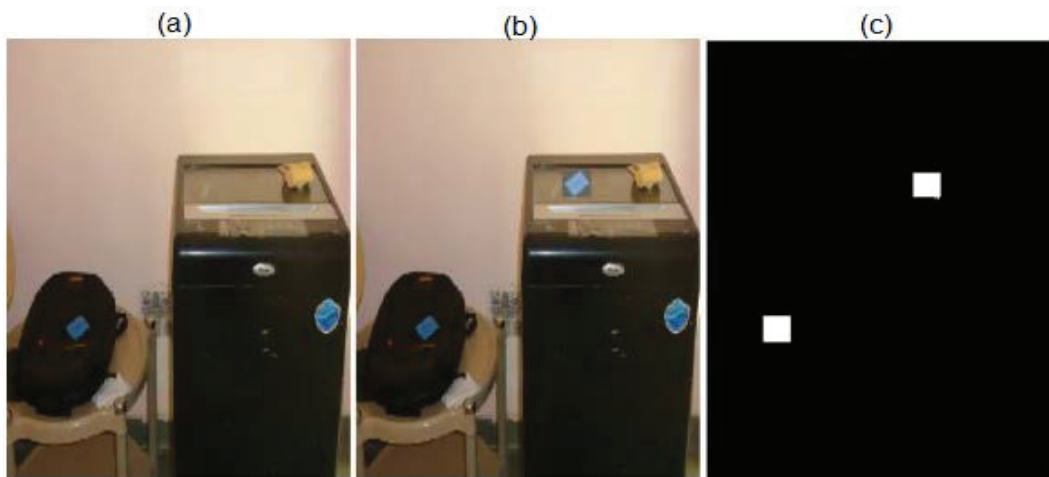


Figure 3.8: (a) *Real image*, (b) *Doctored image*, (c) *Cloning detection*

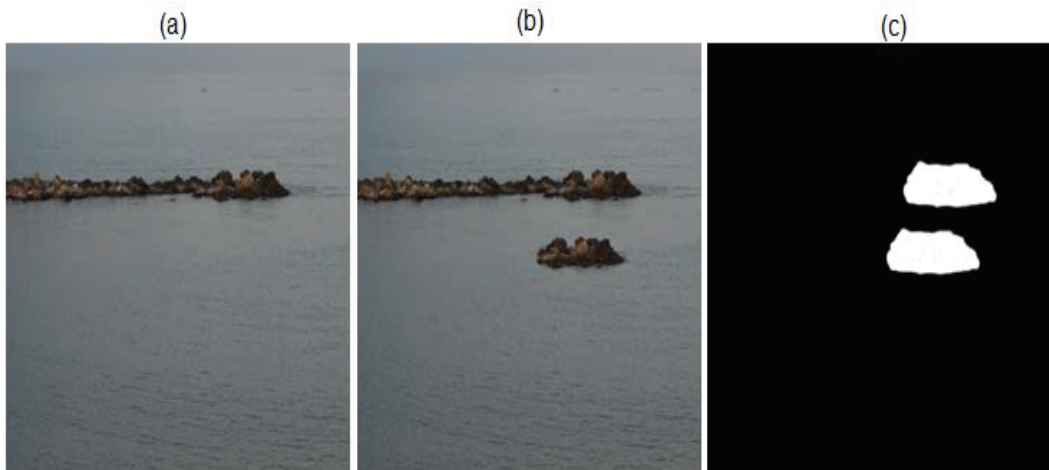


Figure 3.9: (a) *Real image*, (b) *Doctored image*, (c) *Cloning detection*



Figure 3.10: (a) *Real image*, (b) *Doctored image*, (c) *Cloning detection*

Table 3.1: Accuracy Results

| Forgery Type | No. of Images | Identified Correctly | Identified Incorrectly | Accuracy |
|------------------------------------|---------------|----------------------|------------------------|----------|
| Normal Forgery(50) | 100 | 95 | 5 | 95 % |
| Forgery with Blurring (25) | 100 | 89 | 11 | 89 % |
| Forgery with Rotation (25) | 100 | 87 | 13 | 87 % |
| Forgery with Multiple objects (25) | 100 | 92 | 8 | 92 % |
| Total | 400 | 363 | 37 | 90.75 % |

Table 3.2: Accuracy Comparison on Test Images

| Images | Proposed method | Method in [45] | Method in [17] | Method in [1] |
|-----------|-----------------|----------------|----------------|---------------|
| Deer | 87.85 | 84.15 | 67.17 | 68.58 |
| Extension | 76.74 | 72.15 | 25.54 | 40.25 |
| Red tower | 94.26 | 91.75 | 55.49 | 70.16 |
| Tree | 81.92 | 77.13 | 61.02 | 57.91 |
| Truck | 80.25 | 74.06 | 57.64 | 55.53 |
| CRW | 65.84 | 62.45 | 20.81 | 24.00 |

Table 3.3: Feature Dimension Comparison with Existing Algorithm

| Technique | Extraction Method | No. of Blocks | Feature Dimension |
|---------------------|-------------------|-----------------|-------------------|
| Fridrich et al. [1] | DCT | 62001 | 64 |
| Popescu & Farid [2] | PCA | 62001 | 32 |
| Amerini et al. [22] | SIFT | 2700 key points | 128 |
| Zimba et al. [21] | DWT-PCA | 12789 | 16 |
| Ghorbani et al. [8] | DWT-DCT | 12769 | 16 |
| Jiu Hu et al. [55] | Grouped DCT | 45024 | 8 |
| Lou et al. [12] | Spatial Domain | 61009 | 5 |
| Proposed Method | MFHWT-RPT | 14641 | 4 |

Table 3.4: Execution Time (In seconds) Comparison with Existing Algorithm

| Methods | Extraction Domain | Blocks Size | Execution Time |
|---------------------|-------------------|-------------|----------------|
| Fridrich et al. [1] | DCT | 8 | 294.96 |
| Popescu et al. [2] | PCA | 8 | 70.97 |
| Wang et al. [43] | DWT-DCT | 8 | 39.70 |
| Proposed | MFHWT-RPT | 8 | 5.80 |

3.6 Conclusion

This chapter presents a novel technique for detecting copy-move forgery using haar wavelet and ring projection transform. By the comprises scheme of haar wavelet and ring projection transform, the time and memory proficiency can be significantly enhanced. Because of the inherently rotation-invariant feature of the RPT technique, large angle rotation of doctored area are easily detected. The obtained results show the feasibility and effectiveness of the proposed method. In future work, one can apply the proposed method to detection the forgery in color, highly compressed and noisy images.

Chapter 4

Cloning Detection Using Direct Fuzzy and Ring Projection Transform

4.1 Summary

Cloning detection is a real image processing method without reinforcement of embedded security information. Fuzzy Transform (F-Transform) is a powerful tool that encompasses both classical transforms (Fourier, Laplace, DCT and Wavelet) as well as approximation technique using fuzzy IF-THEN rules investigated in fuzzy modeling. Ring projection transform (RPT) for features extraction is very effective tool as it transform two dimensional data into one dimensional with a very few components which significantly reduces the computational complexity. Additionally, in order to form matching invariant to rotation. Further, RPT converts a 2-D image into a rotation-invariant illustration in the 1-D ring projection space. We propose a new and comprise scheme by using fuzzy and ring projection transform for cloning detection.

Firstly, fuzzy transform is employed on input image to yield highly reduced dimension illustrations which is splitted into a fixed size overlapping blocks. Further, ring projection transform is employed to every block for calculating their features. These feature vectors are lexicographically sorted to make identical blocks sequentially. Ultimately, the identical blocks are identified using correlation coefficient, and copy-move regions were detected automatically without applying postprocessing operations. Proposed algorithm is faster and efficient in terms of execution time and accuracy.

4.2 Introduction

Digital images play a wide role in our daily life as we are living in the digital and technical era. These images can be personal or official and can be used as various important purposes such as evidence in court of law, a news item, financial record etc. Forge image are being used as original image to disguise and can be presented as false evidence. Furthermore, image processing softwares, editing tools and internet make this process quite easy. Anyone can doctored images without leaving any visual clues. Therefore, there is necessity of some effective algorithm which can detect image forgery automatically for authenticity of the digital images.

Forgeries were extremely hard when computers, digital camera and smart phone are not easily available. Nowadays the recognition of smart phones as well as digital cameras has made the task acquirement of digital images effortless. Moreover, current image editing tools namely photoshop made this task comparatively easy to produce digital image forgeries. Additionally, humans essentially cannot distinguish the dissimilarities between the original and its forged image. The clone image forgery is the very popular type of technique, perform to create a digital image doctoring. Additionally, in which a specific block of image or

object is copied and then pasted it to the other section of the similar image to accomplish information hiding. Moreover, the copied region move from the similar image so its essential properties namely noise texture and color palette will be well-matched with the remaining part of the image. It will leads to a great remonstrance in identifying and locating the forgery regions.

4.3 Fuzzy Transform

Fuzzy Transform was developed by Perfilieva [38] and Perfilieva [39]. It is a factual technique of the fuzzy approximation of a continuous function. In this section, we present the overviews of main definitions and concept of the F -transform technique.

4.3.1 Fuzzy Partition - Basic Functions

Definition 1 *A fuzzy partition of a specified interval $[c, d]$ is defined by a decomposition $\mathbb{P} = \{c = u_1 < u_2 < \dots < u_n = d\}$ of $[c, d]$ into $n - 1$ subintervals $[u_{k-1}, u_k]$, $k = 2, \dots, n$ and by a family $\xi = \{\xi_1, \xi_2, \dots, \xi_n\}$ of n fuzzy numbers (basic functions), recognize by their membership functions $\xi_k : [c, d] \rightarrow [0, 1]$, $k = 1, \dots, n$, if they carry out the mentioned conditions:*

- (i) $\xi_k : [c, d] \rightarrow [0, 1]$ is continuous with $\xi_k(u_k) = 1$;
- (ii) $\xi_k(u) = 0$ if $u \notin (u_{k-1}, u_{k+1})$;
- (iii) for $k = 2, \dots, n$, f_k is increasing on $[u_{k-1}, u_k]$ and decreasing on $[u_k, u_{k+1}]$;
- (iv) ξ_1 is decreasing on $[c, u_2]$ and ξ_n is increasing on $[u_{n-1}, d]$
- (v) for all $u \in [c, d]$ the partition of unity condition holds $\sum_{k=1}^n \xi_k(u) = 1$.

Let a fuzzy partition of $[c, d]$ be provided by the fuzzy numbers $\xi_1, \xi_2, \dots, \xi_n$ in the sense of Definition 2. We say that it is uniform if the nodes $u_1 < \dots < u_n$, $n \geq 3$, are equidistant, i.e., $u_k = c + h(k-1)$, $k = 1, \dots, n$, where $h = (d-c)/(n-1)$ and the following two additional characteristics are met:

- (i) $\xi_k(u_k - u) = \xi_k(u_k + u), \forall u \in [0, h], k = 2, \dots, n-1$;
- (ii) $\xi_{k+1}(u) = \xi_k(u - h), \forall u \in [c + h, d], k = 2, \dots, n-1$.

Remark 1 *In the case of a uniform partition, h is a length of the support of ξ_1 or ξ_n , while $2h$ is a length of the support of other basic functions ξ_k , $k = 2, \dots, n-1$.*

An example of non-uniform partition of an specified interval by fuzzy sets with triangular shaped membership functions is depicted in Figure 4.1 while Figure 4.2 shows a uniform partition of an interval by fuzzy sets with sinusoidal shaped basic functions. The above formulas provide the formal representation of such triangular and sinusoidal shaped membership functions, respectively:

$$\xi_1(u) = \begin{cases} 1 - \frac{(u-u_1)}{h_1}, & u \in [u_1, u_2]; \\ 0 & \text{otherwise,} \end{cases}$$

$$\xi_2(u) = \begin{cases} \frac{(u-u_{k-1})}{h_{k-1}}, & u \in [u_{k-1}, u_k]; \\ 1 - \frac{(u-u_k)}{h_k} & \text{if } u \in [u_k, u_{k+1}]; \\ 0 & \text{otherwise,} \end{cases}$$

$$\xi_n(u) = \begin{cases} \frac{(u-u_{n-1})}{h_{n-1}}, & u \in [u_{n-1}, u_n]; \\ 0 & \text{otherwise,} \end{cases}$$

where $k = 2, \dots, n-1$ and $h_k = u_{k+1} - u_k$.

$$\xi_1(u) = \begin{cases} 0.5 \left(\cos \frac{\pi}{h} (u - u_1) + 1 \right), & u \in [u_1, u_2]; \\ 0 & \text{otherwise,} \end{cases}$$

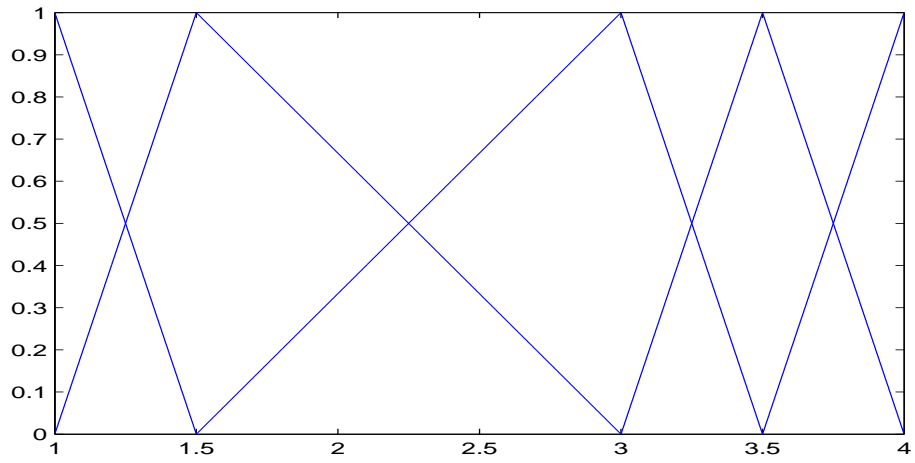


Figure 4.1: *A non-uniform fuzzy partition of interval $[1, 4]$ by triangular membership functions.*

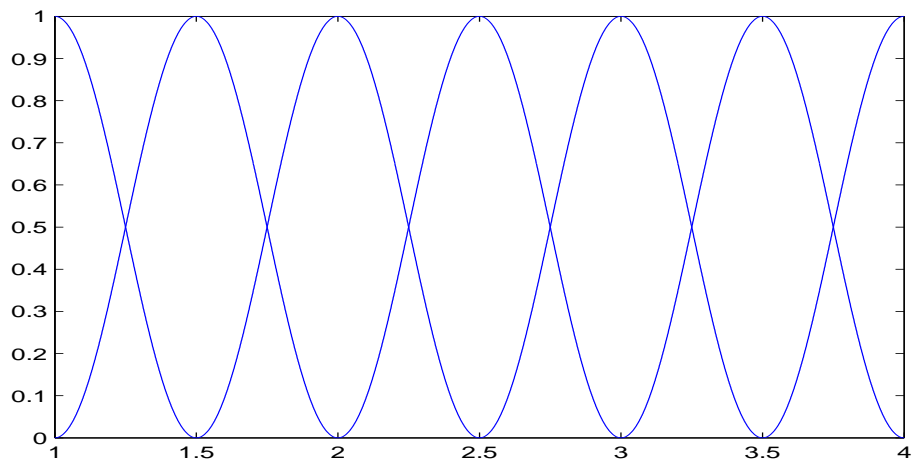


Figure 4.2: *Uniform fuzzy partition of interval $[1, 4]$ by sinusoidal membership functions.*

$$\xi_k(u) = \begin{cases} 0.5 \left(\cos \frac{\pi}{h}(u - u_k) + 1 \right), & u \in [u_{k-1}, u_{k+1}]; \\ 0 & \text{otherwise,} \end{cases}$$

where $k = 2, \dots, n-1$ and

$$\xi_n(u) = \begin{cases} 0.5 \left(\cos \frac{\pi}{h}(u - u_n) + 1 \right), & u \in [u_{n-1}, u_n]; \\ 0 & \text{otherwise.} \end{cases}$$

Firstly, remember the following lemma which is demonstrate in [39] verify that the definite integral of a basic function from a uniform fuzzy partition does not rely upon its shape.

Lemma 1 *Let a uniform fuzzy partition of $[c, d]$ be given by basic functions $\xi_1, \xi_2, \dots, \xi_n$, $n \geq 2$. Then $\int_c^d \xi_1(u)du = \int_c^d \xi_n(u)du = \frac{h}{2}$ and for $i = 2, \dots, n-1$, $\int_c^d \xi_n(u)du = h$.*

4.3.2 Direct Fuzzy Transform

Definition 2 *Let a fuzzy partition of $P = [c, d]$ be given by basic functions $\xi_1, \dots, \xi_n \subseteq P$, $n > 2$ and let $f : \rightarrow R$ be an arbitrary function from $C(D)$. The n -tuple of real numbers $[F_1, F_2, \dots, F_n]$ described by*

$$F_i = \frac{\int_c^d f(u)\xi_i(u)du}{\int_c^d \xi_i(u)du}, \quad i = 1, 2, \dots, n \quad (4.3.1)$$

is the direct fuzzy transform (F -transform) of f with respect to the provided fuzzy partition and $[F_1, F_2, \dots, F_n]$ are the components of the F -transform of f .

Definition 3 *Let $\xi_1, \xi_2, \dots, \xi_n$ be basic functions which form a fuzzy partition of $[c, d]$ and f be a function from $C([c, d])$. Let $F_n[f] = [F_1, F_2, \dots, F_n]$ be the*

integral F -transform of f with respect to $\xi_1, \xi_2, \dots, \xi_n$. Then the function

$$f_{F,n}(u) = \sum_{k=1}^n F_k A_k(u) \quad (4.3.2)$$

is known as inverse F -transform.

Definition 4 Let a fuzzy partition of $P = [c, d]$ be given by basic functions $\xi_1, \dots, \xi_n \subseteq P$, $n > 2$ and let $f : P \rightarrow R$ be a function known at nodes p_1, p_2, \dots, p_N such that for each $i = 1, 2, \dots, n$, there exists $k = 1, 2, \dots, N$: $\xi_i(p_k) > 0$. The n -tuple of reals $[F_1, F_2, \dots, F_n]$ given by

$$F_i = \frac{\sum_{k=1}^N f(p_k) \xi_i(p_k)}{\sum_{k=1}^N \xi_i(p_k)}, \quad i = 1, 2, \dots, n \quad (4.3.3)$$

is the discrete direct F -transform of f with respect to the provided fuzzy partition.

Similarly as in (4.3.2), we call the discrete inverse F -transform of f with respect to $\xi_1, \xi_2, \dots, \xi_n$ for defining the above function in the similar points p_1, p_2, \dots, p_N of $[c, d]$:

Definition 5 Let $\xi_1, \xi_2, \dots, \xi_n$ be basic functions which form a fuzzy partition of $[c, d]$ and f be a function from $C([c, d])$. Let $F_n[f] = [F_1, F_2, \dots, F_n]$ be the integral F -transform of f with respect to $\xi_1, \xi_2, \dots, \xi_n$. Then the function

$$f_{F,n}(p_j) = \sum_{k=1}^n F_k \xi_k(p_j) \quad (4.3.4)$$

is known as inverse F -transform.

4.3.3 F-Transform in Two Variables

The direct as well as inverse F -transforms of a function with two and more than two variables may be presented as a direct generalization of the case of

one variable. Further, we provide its brief review and refer to [40] for additional details.

Assume that our universe of discourse is the rectangle $[c_1, d_1] \times [c_2, d_2]$ and let $n, m > 2$, $u_1, u_2, \dots, u_n \in [c_1, d_1]$ and $v_1, v_2, \dots, v_m \in [c_2, d_2]$ be $n + m$ assigned points, called nodes, such that $c_1 = u_1 < u_2 < \dots < u_n = d_1$ and $c_2 = v_1 < v_2 < \dots < v_m = d_2$. Furthermore, let $\xi_1, \xi_2, \dots, \xi_n : [c_1, d_1] \rightarrow [0, 1]$ be a fuzzy partition of $[c_1, d_1]$ and $\psi_1, \psi_2, \dots, \psi_m : [c_2, d_2] \rightarrow [0, 1]$ be a fuzzy partition of $[c_2, d_2]$ and $f(u, v)$ be a continuous function on $[c_1, d_1] \times [c_2, d_2]$. Then we can define the $n \times m$ matrix $[F_{kl}]$ as the F -transform of f with respect to $\{\xi_1, \xi_2, \dots, \xi_n\}$ and $\{\psi_1, \psi_2, \dots, \psi_m\}$ if we have for each $k = 1, 2, \dots, n$ and $l = 1, 2, \dots, m$, $u \in [c_1, d_1]$ and $v \in [c_2, d_2]$:

$$F_{kl} = \frac{\int_{c_1}^{d_1} \int_{c_2}^{d_2} f(u, v) \xi_k(u) \psi_l(v) \, du \, dv}{\int_{c_1}^{d_1} \int_{c_2}^{d_2} \xi_k(u) \psi_l(v) \, du \, dv}. \quad (4.3.5)$$

In the case of discrete, we assume that the function f calculate values in some points $(p_i, q_j) \in [c_1, d_1] \times [c_2, d_2]$, where $i = 1, 2, \dots, N$ and $j = 1, 2, \dots, M$. Furthermore, the sets $P = \{p_1, p_2, \dots, p_N\}$ and $Q = \{q_1, q_2, \dots, q_M\}$ of these nodes are adequately dense with respect to the selected partitions, i.e., for each $i = 1, 2, \dots, N$ there exists an index $k \in \{1, \dots, n\}$ such that $\xi_k(p_i) > 0$ and for each $j = 1, 2, \dots, M$ there exists an index $l \in \{1, \dots, m\}$ such that $\psi_l(q_j) > 0$.

In this case, we may define the matrix $[F_{kl}]$ to be the discrete F -transform which is the extension of (4.3.3), of f with respect to $\xi_1, \xi_2, \dots, \xi_n$ and $\psi_1, \psi_2, \dots, \psi_m$ if we have for each $k = 1, 2, \dots, n$ and $l = 1, 2, \dots, m$:

$$F_{kl} = \frac{\sum_{j=1}^M \sum_{i=1}^N f(p_i, q_j) \xi_k(p_i) \psi_l(q_j)}{\sum_{j=1}^M \sum_{i=1}^N \xi_k(p_i) \psi_l(q_j)}. \quad (4.3.6)$$

Similarly, by extending (4.3.4) to the case of two variables, we provide the discrete inverse F -transform of f with respect to $\xi_1, \xi_2, \dots, \xi_n$ and $\psi_1, \psi_2, \dots, \psi_m$ to be the following function explained in the same points $(p_j, q_j) \in [c_1, d_1] \times [c_2, d_2]$, with $i = 1, 2, \dots, N$ and $j = 1, 2, \dots, M$, as

$$f_{nm}^F(p_i, q_j) = \sum_{k=1}^n \sum_{l=1}^m F_{kl} \xi_k(p_i) \psi_l(q_j). \quad (4.3.7)$$

4.4 Image Compression using F-Transform Method

Assume an image Z of the dimension $Y \times X$ pixels be illustrated by a function of two variables (a fuzzy relation) $f_Z : Y \times Y \rightarrow [0, 1]$ partially explained at nodes $(i, j) \in [1, Y] \times [1, X]$. The value $f_Z(i, j)$ described an intensity range of each pixel. Further, the compression of the image Z is characterized by the $n \times m$ matrix $F_{nm}[f_Z]$ of the discrete F -transform elements of f_Z :

$$F_{nm}[f_Z] = \begin{pmatrix} F_{11} & \cdots & F_{1m} \\ \vdots & \vdots & \vdots \\ F_{n1} & \cdots & F_{nm} \end{pmatrix}$$

where

$$F_{kl} = \frac{\sum_{j=1}^X \sum_{i=1}^Y f_Z(i, j) \xi_k(i) \psi_l(j)}{\sum_{j=1}^X \sum_{i=1}^Y \xi_k(i) \psi_l(j)}. \quad (4.4.1)$$

for each pair $k = 1, 2, \dots, n$; $l = 1, 2, \dots, m$. The basic functions $\xi_1, \xi_2, \dots, \xi_n$ and $\psi_1, \psi_2, \dots, \psi_m$ create fuzzy partitions of $[1, Y]$ and $[1, X]$ respectively, and $n < Y$, $m < X$. The value $\rho = \frac{nm}{YX}$ is known as the compression ratio.

A reconstruction of the image Z (function f_Z) can be represented by the inverse F -transform of f_Z adapted to the domain $[1, Y] \times [1, X]$:

$$f_{nm}^F(i, j) = \sum_{k=1}^n \sum_{l=1}^m F_{kl} \xi_k(i) \psi_l(j). \quad (4.4.2)$$

Remark 2 *A comparison among three techniques namely JPEG , F-transform and FEQ have been performed in [50]. It has been depicts that the approach of F-transform is better than FEQ method, but it is awful than the JPEG approach. Nevertheless, a complexity of the F-transform based compression is less than the complexity of JPEG technique.*

4.5 Proposed Algorithm

The block based CMFD techniques, the majority of the techniques are analogous to that developed by Popescu and Farid [2]. It indicates that more computation efforts are necessary for dimension lessening, matching control as well as similarity filtering for big number of image blocks. Generally, as input images grow bigger, the nature of copy-move forgery detection algorithms requires many iterations and comparisons. For example, suppose that a gray-scale image of size $m \times n$ pixels could be splitted into overlapping blocks of dimension $b \times b$ pixels, then total number of image blocks are $N = (m - b + 1) \times (n - b + 1)$ produced by sliding the window of $b \times b$ pixels over the whole image by one pixel every time from upper left to bottom right corner. MATLAB is working with matrices; however it is less optimized when faced with multiple loops. Therefore, it will be extremely important that the should be minimal. Moreover, CMFD algorithm turn out to be computationally proscribed when the number of image blocks are higher which inexorably leads to high computational load for consequent feature extraction as well as similarity matching. Therefore, CMFD is generally perform on a reduced image size to decrease the computational cost; However, information loss is undeniable.

Based on that scheme, we have develop boosting scheme to decrease the computational overhead and number of obtained blocks every time and it turns out to decrease the time and memory drastically. The developed technique has been applied on gray-scale images as follows:

1. Let Z be a gray image partitioned in $Y \times X$ pixels. It can be seen as a fuzzy relation $Z : (i, j) \in \{1, \dots, Y\}\{1, \dots, X\} \rightarrow [0, 1]$, $I(i, j)$ being the normalized value of the pixel $P(i, j)$, that is $I(i, j) = P(i, j)/255$ if the length of the gray-scale, has 256 levels.
2. The image Z is compressed by using a discrete F -transform in two variables $[F_{kl}]$ defined for every $k = 1, 2, \dots, n$ and $l = 1, 2, \dots, m$, as:

$$F_{kl} = \frac{\sum_{j=1}^X \sum_{i=1}^Y f_I(i, j) \xi_k(i) \psi_l(j)}{\sum_{j=1}^X \sum_{i=1}^Y \xi_k(i) \psi_l(j)}. \quad (4.5.1)$$

The basic functions $\xi_1, \xi_2, \dots, \xi_n$ and $\psi_1, \psi_2, \dots, \psi_m$ demonstrate fuzzy partitions of $[1, Y]$ and $[1, X]$ respectively.

3. Overlapping blocks of size $b \times b$ are generated in reduced image with one pixel shifting and the total number of overlapping blocks is described by $Y_{ovr} = (X - b + 1) \times (X - b + 1)$.
4. Ignore the blocks whose contrast is greater than the predefined threshold ' CTR ' to reduce the false positive.
 - (a) Transform each overlapping $b \times b$ into a $1 - D$ RPT vector of size $R + 1$.
 - (b) Extracts feature from Step (a) are managed into matrix and denoted as A of $(X - b + 1)(Y - b + 1) \times R + 1$.
 - (c) Form another matrix P of two columns for storing top-left coordinates.

5. Lexicographical sort is applied to the matrix A for making similar blocks consecutive.
6. For every adjacent rows of matrix A ,
 - (a) Compute the normalized correlation coefficient between the pair of sorted rows using the equation (3.3.9) in chapter 3
 - (b) If the calculated correlation coefficient exceeds a preset threshold value ' C_t ', then extract the corresponding blocks position from the matrix P , and marked the location of these doctored blocks in the original image by setting pixel values to zero.
7. Finally, the copy-move region is detected automatically without applying post-processing operation.

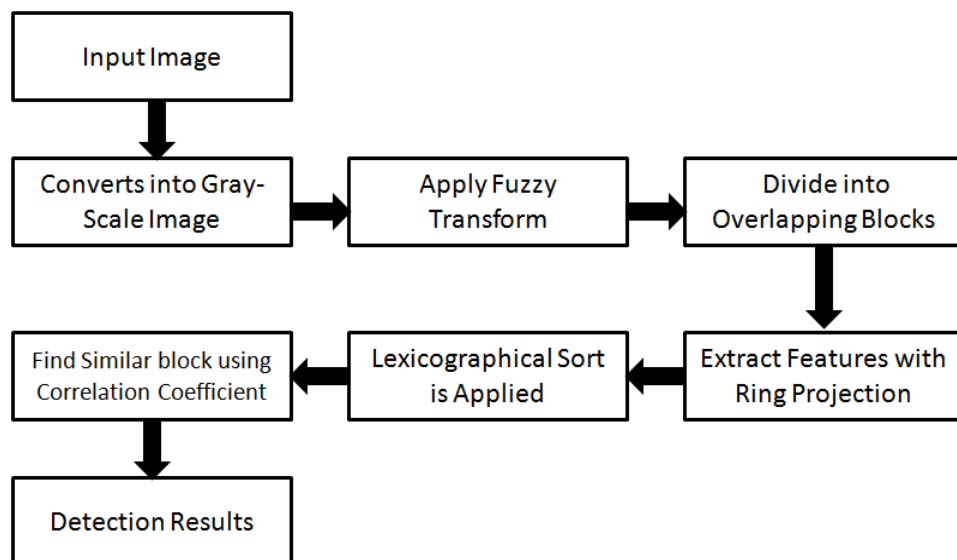


Figure 4.3: *Proposed model*

4.6 Results and Discussion

Accuracy, True Positive Rate (TPR), False Positive Rate (FPR) were calculated to prove the robustness of proposed algorithm. The experimental results were carried out on Matlab R2013a, RAM 4 GB and core i3 processor. The database of 100 images were composed where 50 images were original and 50 were tempered. This database are having different type of image format (.jpg, .png and .tiff) and various resolutions like 256×256 , 512×512 , 640×480 etc.

The forged images are constructed with the help of Photoshop in which the forge area or object is randomly selected and pasted into the same image. Furthermore, one public database MICC-F220 [102] was also used for the comparative analysis of proposed algorithm with other reported techniques. This database are having total 220 images, from them 110 are original and 110 are forged. Additionally, various types of attacks such as scaling, rotation and blurring were also applied on tempered images of both databases to check the robustness of proposed algorithm.

The image is converted into gray-scale then direct fuzzy transform is employed and basic function is used to establish fuzzy partitions. The number of points covered by basis functions are different. It may be noted that the less number of points covered by basic functions may give the less detection results and also increases execution time of algorithm. As we increases the number of points covered by basic functions, the size of original image will reduces, consequently the execution time of algorithm will be decreases. However, higher number of points covered by the basic functions may also give the false detection results. Therefore, baseLen parameter was used in proposed algorithm to control the quality of detection results as well as execution time of algorithm. Optimal value of baseLen parameter leads to the better detection results in a very less time, which shows the feasibility and effectiveness of proposed method. In proposed algorithm, the

parameter ‘CTR’ was also introduced to ignore the low contrast blocks, which reduces the false positive. Lesser the number of blocks are, the faster is the process.

The performance of proposed method is shown in Table 4.1, Table 4.2 and Table 4.3, which shows that proposed method perform better than state of the art techniques [1, 2]. Table 4.1 display the accuracy of developed algorithm in 100 images with various attacks and varying block sizes. The overall accuracy of proposed method was 91.25 %. Table 4.2 shows the accuracy of proposed algorithm and execution time on MICC-F220 database. Moreover, Table 4.3 shows that the proposed algorithm is able to reduce dimensions drastically in comparison to other reported methods[1, 2, 12, 22, 24]. Reduced dimension leads to less of computational time; Therefore, proposed algorithm is faster as compare to other existing algorithm as shown in Table 4.2.

Next, the images are depicted in Figure 4.4 to Figure 4.8 represent the results of copy move forgery marked on the doctored image. The row consist of four images. original image, doctored image, fuzzy transform image and detection of forgery image from left to right, respectively. The Complexity of this algorithm is $O(n^2 \log n)$.

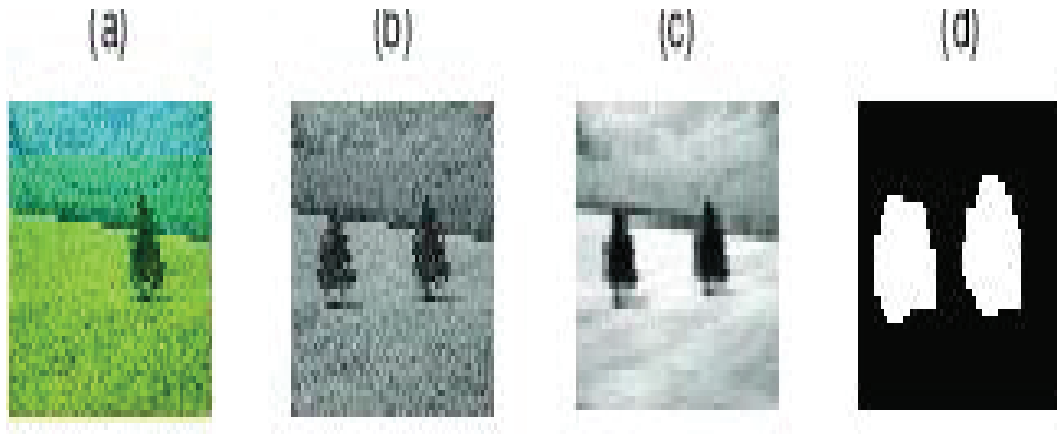


Figure 4.4: (a) *Real image*, (b) *Doctored image* (c) *Fuzzy Transform image* and (d) *Forgery detection*

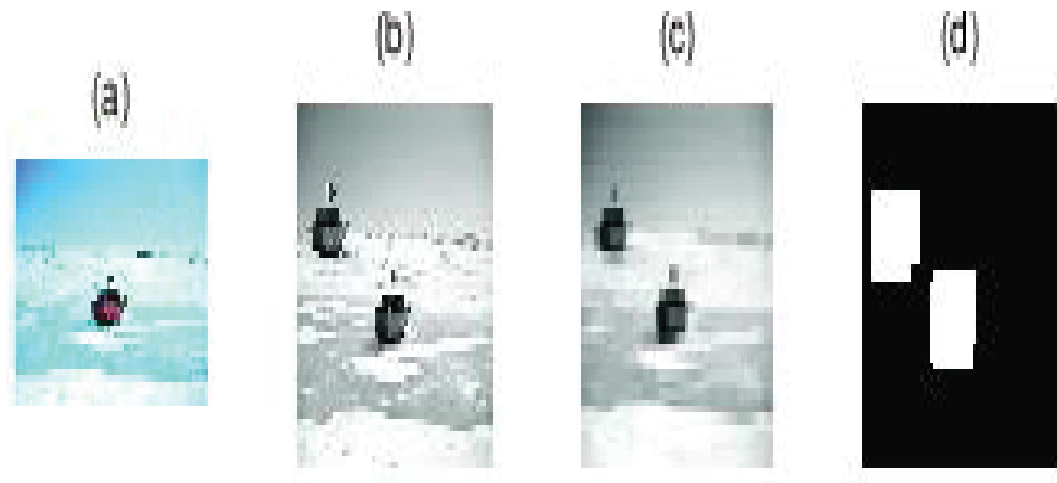


Figure 4.5: (a) *Real image*, (b) *Doctored image* (c) *Fuzzy Transform image* and (d) *Forgery detection*

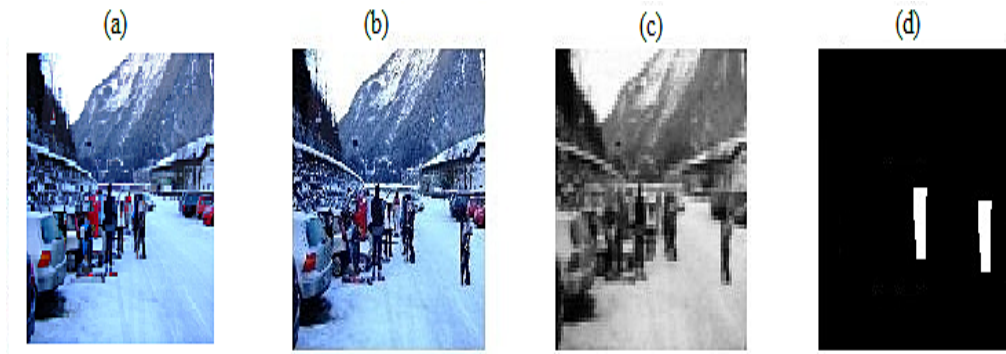


Figure 4.6: *Forgery detection on MICC-220 Database (a) Real image, (b) Forgery image (c) Fuzzy Transform image and (d) Forgery detection*



Figure 4.7: *Forgery detection on MICC-220 Database (a) Real image (b) Forgery image (c) Fuzzy Transform image and (d) Forgery detection*



Figure 4.8: *Forgery detection on MICC-220 Database (a) Real image (b) Forgery image (c) Fuzzy Transform image and (d) Forgery detection*

Table 4.1: Accuracy Results

| Block-Size | No. of Images | Identified Correctly | Identified Incorrectly | Accuracy |
|----------------|---------------|----------------------|------------------------|----------|
| 4×4 | 100 | 94 | 6 | 94 % |
| 8×8 | 100 | 93 | 7 | 93 % |
| 16×16 | 100 | 91 | 9 | 91 % |
| 32×32 | 100 | 87 | 13 | 87 % |
| Total | 400 | 365 | 35 | 91.25 % |

Table 4.2: TPR, FPR and Execution Time Comparison for every Technique on MICC-F220 Database

| Techniques | TPR | FPR | Execution Time in Seconds |
|---------------------|-----|-----|---------------------------|
| Fridrich et al [1] | 89 | 84 | 294.96 |
| Popescu & Farid [2] | 87 | 86 | 70.97 |
| Pan et al. [46] | 89 | 1 | 10 |
| Amerini et al. [22] | 100 | 8 | 4.94 |
| Proposed Method | 90 | 34 | 3.80 |

Table 4.3: Feature Dimension Comparison with Existing Algorithm

| Techniques | Extraction Domain | Total Blocks | Feature Dimension |
|---------------------|-------------------|-----------------|-------------------|
| Fridrich et al.[1] | DCT | 255025 | 64 |
| Popescu & Farid [2] | PCA | 255025 | 32 |
| Amerini et al. [22] | SIFT | 2700 key points | 128 |
| Zimba et al. [21] | DWT-PCA | 12789 | 16 |
| Ghorbani et al. [8] | DWT-DCT | 12769 | 16 |
| Jiu Hu et al. [55] | Grouped DCT | 45024 | 8 |
| Lou et al. [12] | Spatial Domain | 247009 | 5 |
| Proposed Method | FT and RPT | 1156 | 4 |

4.7 Conclusion

A novel method for detecting cloning forgery with the help of fuzzy as well as ring projection transform is presented. The comprises scheme of fuzzy transform and ring projection transform greatly improved the time and memory. Because of the inherently rotation-invariant feature of the RPT technique, large angle rotation of doctored area are detected efficiently. Additionally, the developed technique is able to detect copy-move region effectively with various attack i.e. scaling, rotation and gaussian noise. Moreover, it drastically reduces the computational time as well as feature dimensions compare to other reported algorithms. In future, proposed algorithm can be applied for detecting copy move forgery in color, highly compressed and noisy images.

Chapter 5

Intuitionistic Fuzzy Local Binary Pattern using Texture Feature Extraction

5.1 Summary

This chapter presents texture feature extraction with the help of intuitionistic fuzzy local binary (IFLBP) to encode local texture from the input image. The developed technique extends fuzzy local binary pattern (FLBP) method employing intuitionistic fuzzy set, illustration of local patterns of the input images. Further, IFS-LBP contributes to more than one bin in the dissemination of IFS-LBP values which can be applied as a feature vector in the various fields of image processing. The performance of the proposed method has been demonstrated on various medical images and processing images of size 256×256 . Additionally, the obtained results justify the effectiveness as well as usefulness of proposed method over the other reported techniques and new improvements have been suggested.

5.2 Introduction

Feature extraction is a process to extract the compact and essential information from an image. The major objective of feature extraction is to find the most significant information from original or raw data. When the input image or data to an approach is excessively bulky to be processed as well as it is supposed to be repetitious (a large amount of data, but a little information). Afterwards, the input data will be transformed into a highly reduced dimension representation or a set of features (also known as features vector). These extracted feature vectors represents the whole image. If extracted features are anxiously selected then it is expected that the features set will extract significant information in order to carry out the preferred task using this reduced representation instead of input image or full data. Extracted features have been used in various field of image processing and signal processing such as image forensics, remote sensing, pattern recognition, visual inspection, object discrimination, bio-medical image processing, character recognition, terrain delimitation, image classification, document verification, reading bank deposit slips, applications for credit cards and script recognition etc. [28, 29, 30, 60, 64, 74, 75, 76, 80].

5.3 Local Binary Pattern

Local binary pattern is a kind of gray-scale texture operator which is employed for describing the spatial structure of an image texture [63]. The LBP texture model is depend on the comparison of an pixel values of a pixel neighbourhood. Further, a binary value is appointed to every pixel p_x , belonging to a local neighbourhood.

It is computed by comparing the value of an pixel intensity g_x with a center pixel intensity g_c , which is the same for all pixels in the neighbourhood. Thus, two crisp sets of pixels can be determine for every pixel neighbourhood as follows:

Let $U = \{0, 1 \dots, n - 1\}$ be the universal set of all pixels in the $n \times n$ pixel-neighborhood. Let $A = \{p_x \in U : \ell_A(x)\}$, where $\ell_A(x)$ is a predicate described as $g_x \geq g_c$, be the set of all pixels p_x and B be the set of all neighbourhood pixels p_x with gray value g_x less than or equal to g_c under the universal set U , respectively. Hence, set B is the complement of set A relative to the universal set U .

Logically, for crisp set A , characteristic function $\chi(x) = 0, p_x \notin A$ and $\chi(x) = 1, p_x \in A$. Similarly, the respective characteristic function for set B as $\chi(x) = 0, p_x \in B$ and $\chi(x) = 1, p_x \notin B$.

Based on these binary values of the typical function $\chi(x)$ for a neighbourhood of n pixels, a unique LBP code can be computed as above:

$$LBP_{code} = \sum_{x=0}^{k-1} d_x \cdot w_x, \quad (5.3.1)$$

where $d_x = \chi(x), k \in (0, n]$ being the number of pixels in the neighbourhood that were treated for the generation of binary pattern and $w_x = 2^x, x \in \{0, 1, \dots, k\}$ is a weight function, which select a weight value at each pixel of the neighbourhood. Every pixel of the local neighborhood is described by a single LBP code out of 2^k possible codes.

5.4 Intuitionistic Fuzzy Local Binary Pattern

In order to generalize the Fuzzy Local Binary Pattern technique, it is able to manage the uncertainty with hesitancy arising from either imperfect or imprecise information. In this section, we present the proposed intuitionistic fuzzy local binary pattern (IFS-LBP) for texture illustration with help of intuitionistic fuzzy sets as follows:

Let $U = \{0, 1, \dots, n-1\}$ be the universal set for n -pixels neighborhood. Then an intuitionistic fuzzy set \tilde{A} under the universal set U is given by:

$$\tilde{A} = \{\langle p_x, \mu_{\tilde{A}}(x), \nu_{\tilde{A}}(x) \rangle | p_x \in U\}, \quad (5.4.1)$$

where $\mu_{\tilde{A}} : U \rightarrow [0, 1]$ and $\nu_{\tilde{A}} : U \rightarrow [0, 1]$ express the degree of membership and non-membership to which an element p_x has either greater or less grey value than g_c in \tilde{A} , respectively, with the condition $0 \leq \mu_{\tilde{A}}(x) + \nu_{\tilde{A}}(x) \leq 1$. The amount $\pi_{\tilde{A}}(x) = 1 - \mu_{\tilde{A}}(x) - \nu_{\tilde{A}}(x), \forall p_x \in U$ is known as the degree of indeterminacy (hesitation part). It is the degree of uncertainty whether p_x corresponds to \tilde{A} or not.

The membership and non-membership functions of IFS \tilde{A} can be described as above:

$$\mu_{\tilde{A}}(x) = \begin{cases} 0 & \text{if } g_x < g_c - T, \\ 0.5(1 + h) \left(1 + \frac{g_x - g_c}{T}\right) & \text{if } g_x \in [g_c - T, g_c], T \neq 0, \\ 0.5 \left[\left(1 + \frac{g_x - g_c}{T}\right) + h \left(\frac{g_x - g_c}{T} - 1\right) \right] & \text{if } g_x \in (g_c, g_c + T], T \neq 0, \\ 1 & \text{if } g_x \geq g_c + T, \end{cases} \quad (5.4.2)$$

and

$$\nu_{\tilde{A}}(x) = \begin{cases} 1 & \text{if } g_x < g_c - T, \\ 0.5 \left[\left(1 - \frac{(g_x - g_c)}{T} \right) - h \left(1 + \frac{(g_x - g_c)}{T} \right) \right] & \text{if } g_x \in [g_c - T, g_c], T \neq 0, \\ 0.5(1 + h) \left(1 - \frac{(g_x - g_c)}{T} \right) & \text{if } g_x \in (g_c, g_c + T], T \neq 0, \\ 0 & \text{if } g_x \geq g_c + T. \end{cases} \quad (5.4.3)$$

For an $n \times n$ pixel-neighborhood, the contribution C_{IFLBP} of each IFLBP code in a single bin of intuitionistic fuzzy local binary pattern (IFLBP) histogram is calculated as above:

$$C_{IFLBP}(x, y, i) = \prod_{r=0}^{k-1} [b_r(i)\mu_{\tilde{A}}(x) + (1 - b_r(i))\nu_{\tilde{A}}(x)], \quad (5.4.4)$$

where $k \in (0, n]$, (x, y) and $b_r(i) \in \{0, 1\}$ demonstrate the number of neighboring pixels, the coordinates of a pixel and numerical value of r^{th} bit of binary demonstration of bin i , respectively. The complete IFLBP histogram is described by

$$H_{IFLBP}(i) = \sum_{x, y} C_{IFLBP}(x, y, i), \quad i = 0, 1, \dots, 2^k - 1. \quad (5.4.5)$$

It can be observe that applying the crisp LBP operator, in which every $n \times n$ pixel surroundings always provide one bin of the histogram. On the other hand, FLBP and IFS-LBP histogram of every $n \times n$ pixel surroundings typically provides more than one bin of the histogram. However, the sum of contribution of every $n \times n$ pixel surroundings (IFS-LBP code) to the bins of IFS-LBP histogram is equal to 1, defined as:

$$\sum_{i=0}^{2^k-1} C_{IFLBP}(x, y, i) = 1. \quad (5.4.6)$$

An example of IFS-LBP calculation scheme for a 3×3 -pixel surroundings is depicted in figure 5.1.

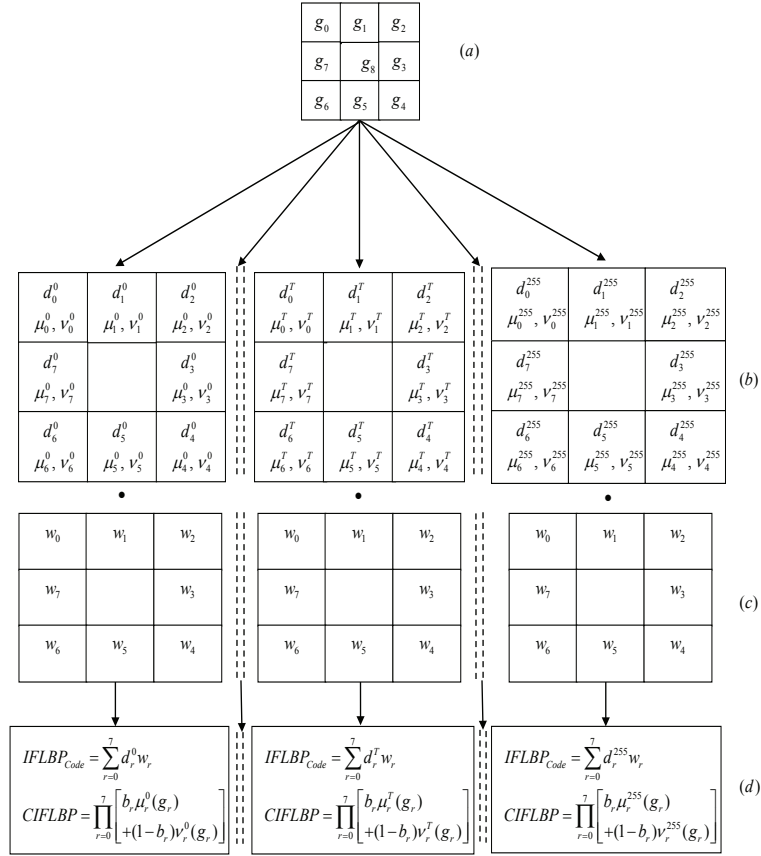


Figure 5.1: IFLBP calculation scheme for a 3×3 pixel neighborhood. (a) Gray-levels of a 3×3 pixels neighborhood. (b) Intuitionistic Fuzzy threshold values along with membership as well as non-membership values. (c) Binomial weights matrix. (d) IFLBP codes and CIFLBP.

Remark 3 When $T \neq 0$, $h = 0$, the resulting intuitionistic fuzzy membership as well as non-membership functions is describe by the Equations 2, 3 are nearly similar to the fuzzy membership function $\mu_A(x)$, the difference being that $\mu_{\bar{A}}(x) = \nu_{\bar{A}}(x) = 0.5$ whereas $\mu_A(x) = 1$ when $g_i = g_c$.

Remark 4 When $T = 0$, the resulting intuitionistic fuzzy membership as well as non-membership functions are similar to the crisp thresholding function $\chi_A(x)$.

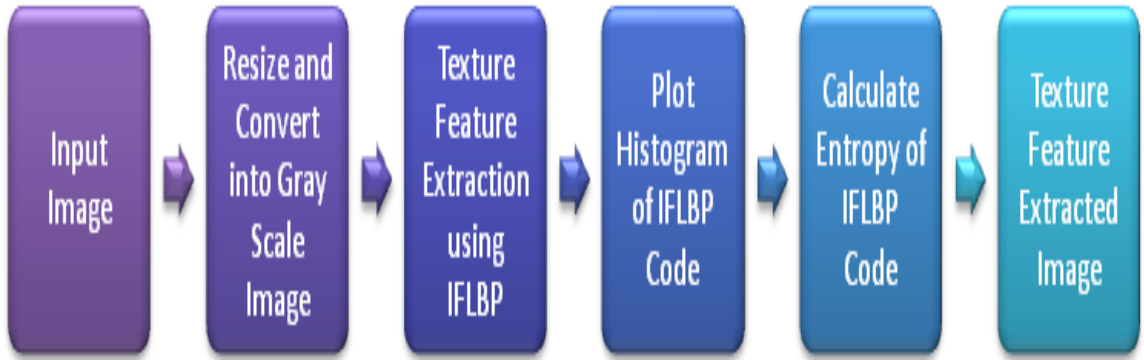


Figure 5.2: Proposed model

5.5 Performance Metrics: Entropy of IFLBP Features

Information content of an image is usually measured by computing the uncertainty as well as entropy of an image. The magnitude of entropy maximize, more information gain is correlate with the image. Moreover, the entropy find the average, global information content of an image in terms of average bits per pixel. Shannon entropy [99] is given as:

$$H = - \sum_{i=0}^{255} p_i \log p_i \quad (5.5.1)$$

where p_i is the probability of the i^{th} pattern. It is worth mentioning that the logarithmic entropic measure (5.5.1) that as $p_i \rightarrow 0$ it's analogous self information of this event, $I(p_i) = -\log p_i \rightarrow \infty$ but $I(p_i = 1) = \log p_i \rightarrow 0$. Thus, we see that information gain from an event is neither bounded at both ends nor defined at all points.

In exercise, the clinch in information from an event, either thoroughly possible or highly improbable, is expected to lie between two finite limits. For example, as more and more pixels in an image are analyzed, the gain in information increases and when all the pixels are inspected the gain attains its maximum value, irrespective of the content of an image. Shannon's entropy which is highly praised, we discover that the measure of self information of an event with probability p_i is taken as $\log p_i$, a decreasing function of p_i . Moreover, similar minimizing character alternately can be cultivate by examine it as a function of $(1 - p_i)$ rather than of $1/p_i$.

The additive property, which examine essential of Shannon's approach, of the self information function for independent events may not have a substantial importance (impact) in practice as well as in some conditions. By choice, as in the case of probability law, the joint self information may be product rather than sum of the self information in two independent cases.

Additionally, the above considerations recommend the self information as an exponential function of $(1 - p_i)$ instead of logarithmic behaviour. This is also appropriate while considering the concept of information gain in an image. Pal and Pal entropy [100] is defined by

$$H = \sum_{i=0}^{255} p_i e^{1-p_i} \quad (5.5.2)$$

5.6 Experimental Results and Analysis

It can be observed that Keramidas et al. method [30] has zero values for some bins out of 255 bins. However, proposed method histograms is not having bins with zero values as well as there are more spikes, though limited in magnitude. Additionally, it specify that proposed method is having additional information than existing methods. Entropy is a measure of uncertainty associated with the random occurrences.

However, it considered as the measure of ‘disorder’. Pal and Pal entropy [100] is a statistical measure of randomness which is carried out to illustrates the texture of a given image.

The more diversified signal indicate the higher entropy as well as the more actual information gain. Generally, If all the bins of histogram having equal probability then the maximum entropy will be attained. Apparently, for the fixed threshold T , proposed method’s histograms always give greater entropy than the existing method’s histograms. Therefore, IFLBP histogram gain more information than other reported method’s histograms.

Additionally, we apply proposed IFLBP approach on various images as shown in Figures 5.3 to 5.7 of size 256×256 to calculate the histograms feature vectors for different threshold values and varying hesitation ($h \in [0, 1]$) as well as computed entropies from these histograms, finally the results are shown in Tables 5.1 to 5.5. We can examine from these tables that the maximum entropy obtain in Table 5.1 for the $T = 6$, $T = 10$ are at $h = 0.3$, for $T = 2$, $T = 14$, $T = 20$, $T = 12$ are at $h = 0.1$. We fellow the same procedure for remaining images, results are shown in Tables 5.2 to 5.5 and Figures 5.4 to 5.7 respectively. Therefore, the entropies obtained by proposed method are always greater than the entropies obtained by existing methods. We plot the histograms of IFLBP codes of every image where we have found the maximum entropy as shown in Figures 5.3 to 5.7. From these histograms we can observe that the IFLBP histograms do not have bins with zero values. In addition to that, the IFLBP features of all images are more informative than existing features. The complexity of this algorithm is $O(n^2)$.

Table 5.1: The Entropy Values at Different Threshold and Hesitation for X-Ray image

| Methods | Hesitation (h)↓ | Thresholds (T)→ | | | | |
|----------------------|-----------------|-----------------|---------------|---------------|---------------|---------------|
| | | 2 | 6 | 10 | 14 | 20 |
| Keramidas et al.[30] | 0.0 | 1.9016 | 1.68193 | 0.8708 | 0.5800 | 0.3889 |
| Proposed Method | 0.1 | 2.6884 | 2.6999 | 2.6999 | 2.7058 | 2.7068 |
| | 0.3 | 2.6877 | 2.7001 | 2.7040 | 2.7056 | 2.7065 |
| | 0.5 | 2.6844 | 2.6983 | 2.7024 | 2.7040 | 2.7048 |
| | 0.7 | 2.6751 | 2.6923 | 2.6970 | 2.6987 | 2.6995 |
| | 1.0 | 2.6167 | 2.6474 | 2.6538 | 2.6549 | 2.6540 |

Table 5.2: The Entropy Values at Different Threshold and Hesitation for Thyroid Image

| Methods | Hesitation (h)↓ | Thresholds (T)→ | | | | |
|----------------------|-----------------|-----------------|---------------|---------------|---------------|---------------|
| | | 2 | 6 | 10 | 14 | 20 |
| Keramidas et al.[30] | 0.0 | 1.6859 | 1.9053 | 1.6529 | 0.8107 | 0.5882 |
| Proposed Method | 0.1 | 2.6854 | 2.6938 | 2.6997 | 2.7031 | 2.7055 |
| | 0.3 | 2.6842 | 2.6938 | 2.7000 | 2.7033 | 2.7054 |
| | 0.5 | 2.6800 | 2.6914 | 2.6982 | 2.7016 | 2.7037 |
| | 0.7 | 2.6669 | 2.6822 | 2.6902 | 2.6940 | 2.6961 |
| | 1.0 | 2.5672 | 2.5988 | 2.6106 | 2.6152 | 2.6169 |

Table 5.3: The Entropy Values at Different Threshold and Hesitation for Brain CT Scan Image

| Methods | Hesitation (h)↓ | Thresholds (T)→ | | | | |
|----------------------|-----------------|-----------------|---------------|---------------|---------------|---------------|
| | | 2 | 6 | 10 | 14 | 20 |
| Keramidas et al.[30] | 0.0 | 1.6118 | 1.4533 | 0.8742 | 0.7741 | 0.5749 |
| Proposed Method | 0.1 | 2.6978 | 2.6998 | 2.7020 | 2.7038 | 2.7055 |
| | 0.3 | 2.6933 | 2.6958 | 2.6987 | 2.7009 | 2.7131 |
| | 0.5 | 2.6784 | 2.6822 | 2.6865 | 2.6901 | 2.6935 |
| | 0.7 | 2.6290 | 2.6362 | 2.6441 | 2.6505 | 2.6567 |
| | 1.0 | 2.2237 | 2.2478 | 2.6888 | 2.2903 | 2.2979 |

Table 5.4: The Entropy Values at Different Threshold and Hesitation for Lena Image

| Methods | Hesitation (h)↓ | Thresholds (T)→ | | | | |
|----------------------|-----------------|-----------------|---------------|---------------|---------------|---------------|
| | | 2 | 6 | 10 | 14 | 20 |
| Keramidas et al.[30] | 0.0 | 1.7785 | 1.6843 | 1.1374 | 0.6021 | 0.4921 |
| Proposed Method | 0.1 | 2.6764 | 2.6936 | 2.6998 | 2.7029 | 2.7051 |
| | 0.3 | 2.6676 | 2.6959 | 2.7016 | 2.7041 | 2.7059 |
| | 0.5 | 2.6776 | 2.6959 | 2.7016 | 2.7041 | 2.7059 |
| | 0.7 | 2.6678 | 2.6970 | 2.7017 | 2.7036 | 2.7048 |
| | 1.0 | 2.6769 | 2.6965 | 2.7000 | 2.7008 | 2.7007 |

Table 5.5: The Entropy Values at Different Threshold and Hesitation for JUIT Logo

| Methods | Hesitation (h)↓ | Thresholds (T)→ | | | | |
|----------------------|-----------------|-----------------|---------------|---------------|---------------|---------------|
| | | 2 | 6 | 10 | 16 | 20 |
| Keramidas et al.[30] | 0.0 | 0.7454 | 0.7087 | 0.6803 | 0.6768 | 0.6258 |
| Proposed Method | 0.1 | 2.7010 | 2.7032 | 2.7040 | 2.7046 | 2.7051 |
| | 0.3 | 2.6969 | 2.6996 | 2.7005 | 2.7010 | 2.7016 |
| | 0.5 | 2.6822 | 2.6858 | 2.6867 | 2.6871 | 2.6876 |
| | 0.7 | 2.6302 | 2.6341 | 2.6340 | 2.6337 | 2.6333 |
| | 1.0 | 2.1837 | 2.1643 | 2.1480 | 2.1369 | 2.1266 |

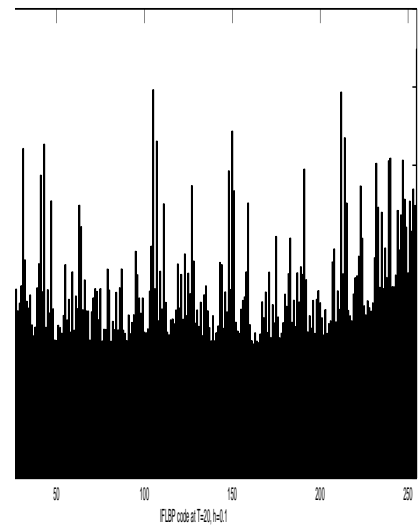
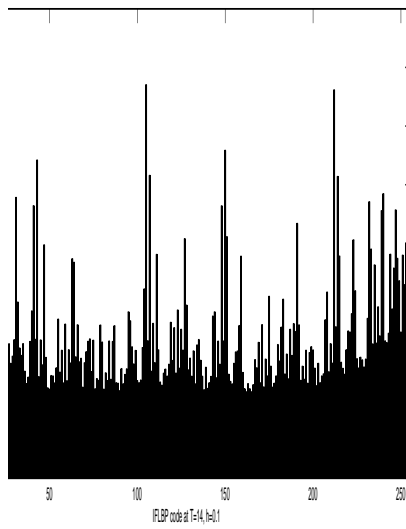
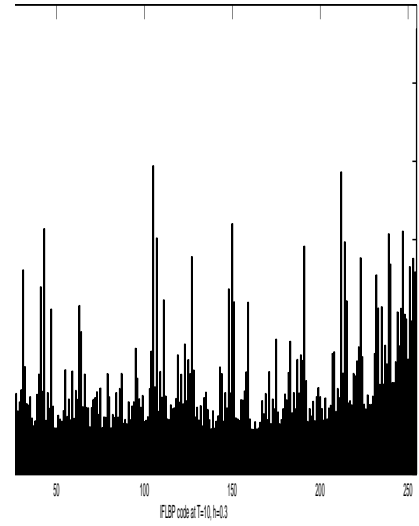
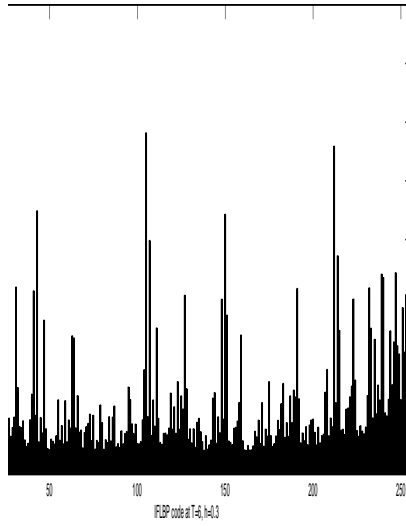
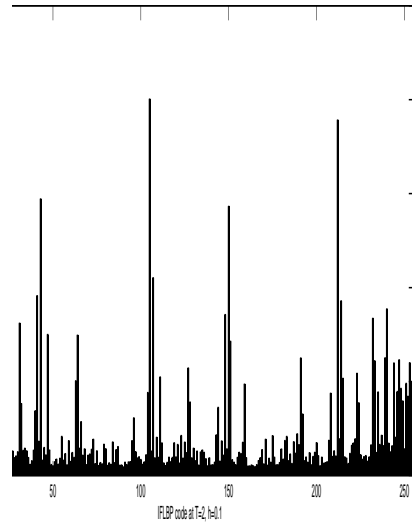
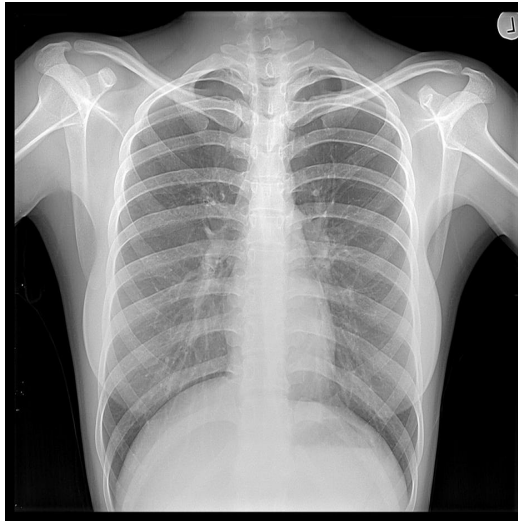


Figure 5.3: Histograms Plot of IFLBP Codes for X-Ray Image

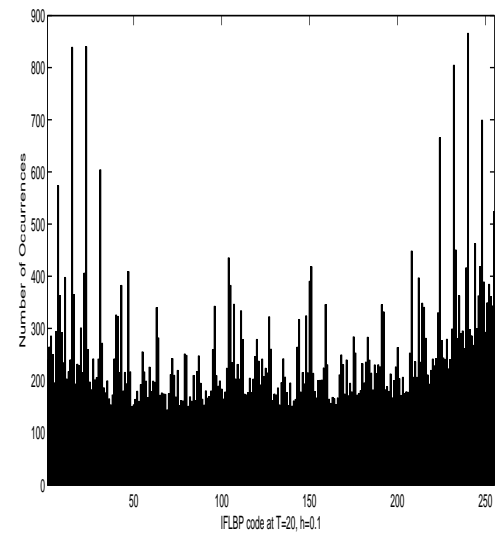
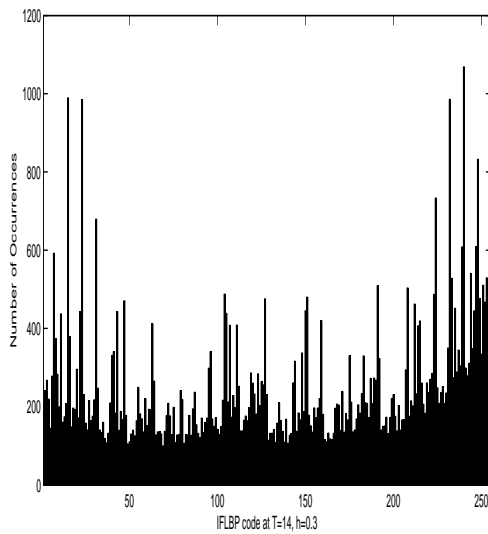
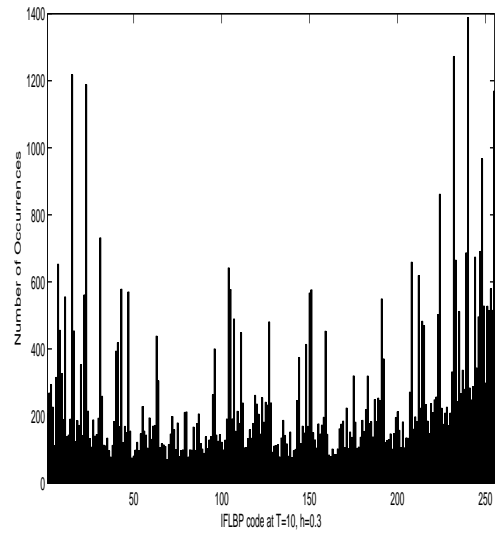
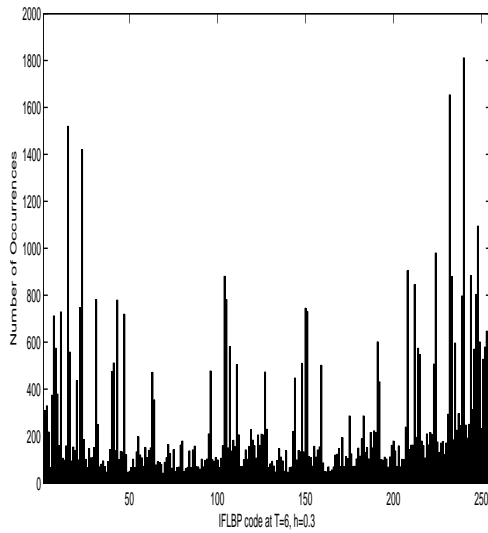
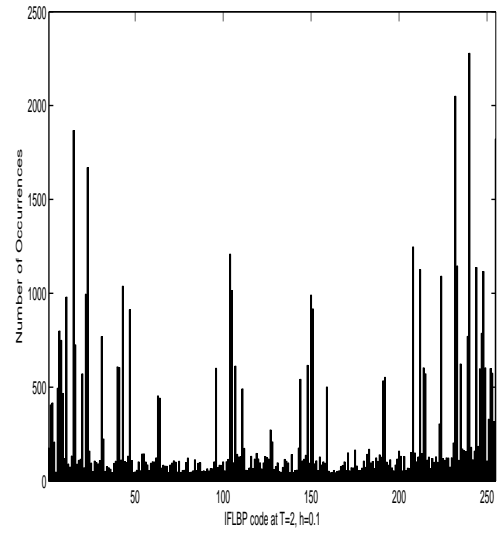
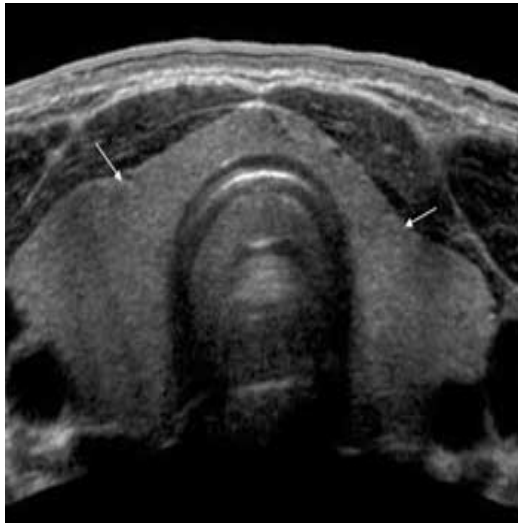


Figure 5.4: Histograms Plot of IFLBP Codes for Thyroid Image

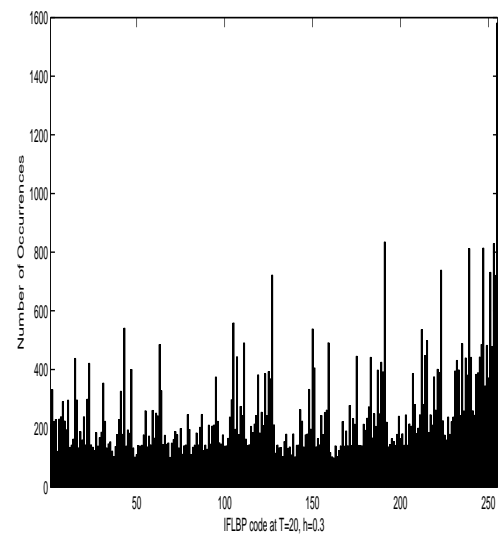
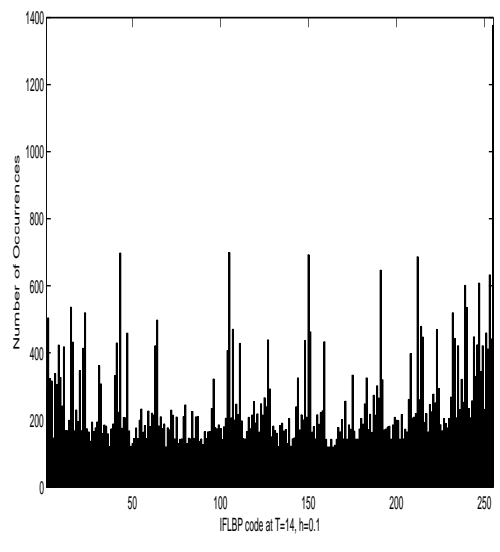
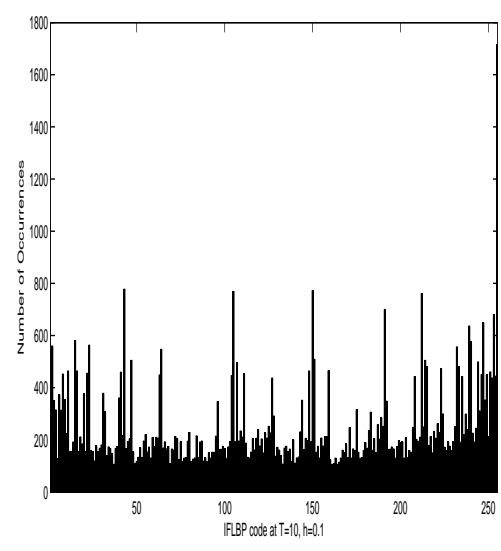
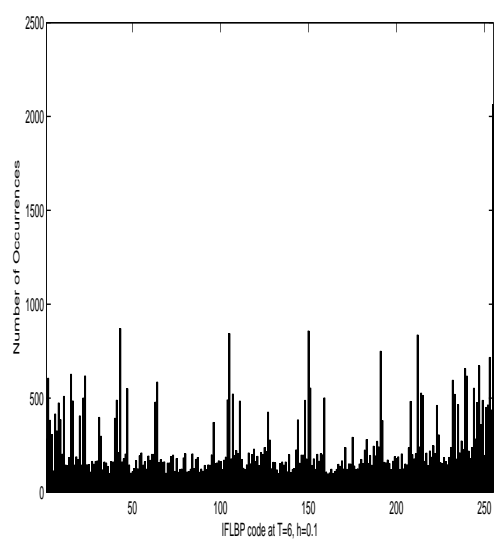
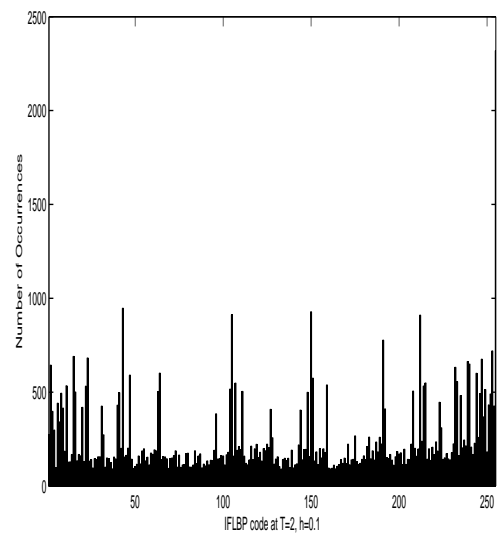


Figure 5.5: Histograms Plot of IFLBP Codes for Brain CT-Scan Image

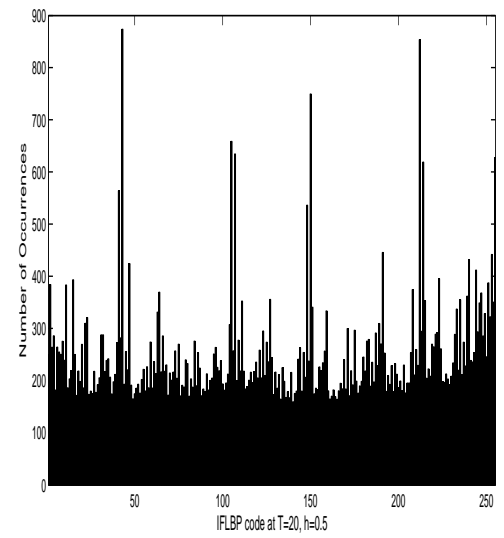
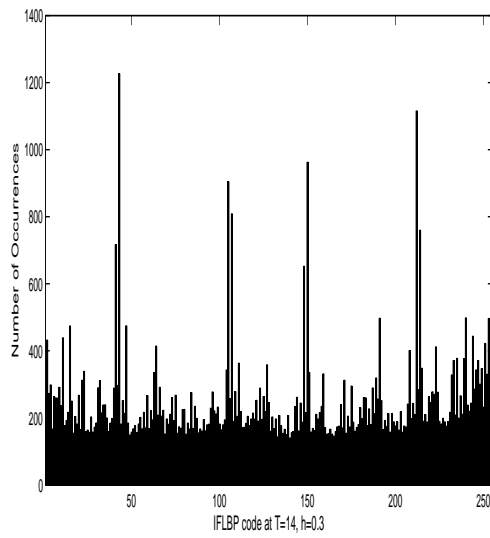
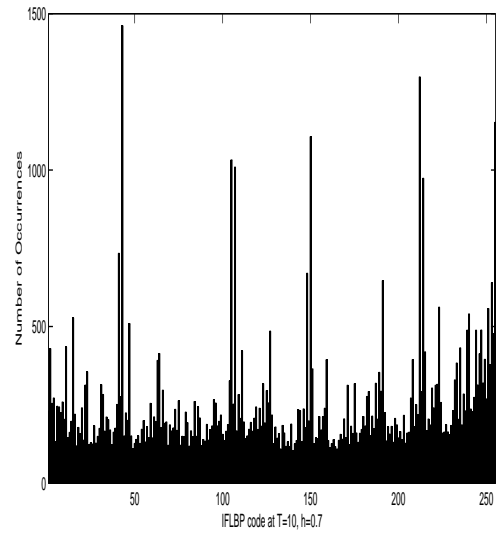
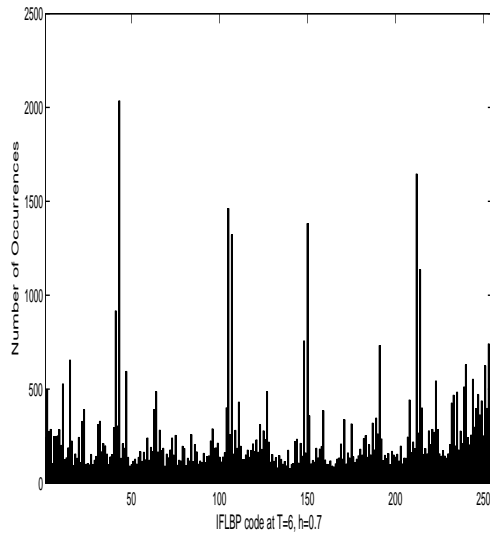
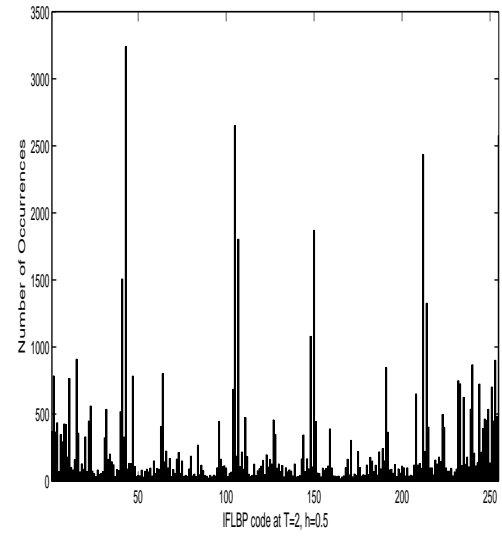


Figure 5.6: Histograms Plot of IFLBP Codes for Lena Image

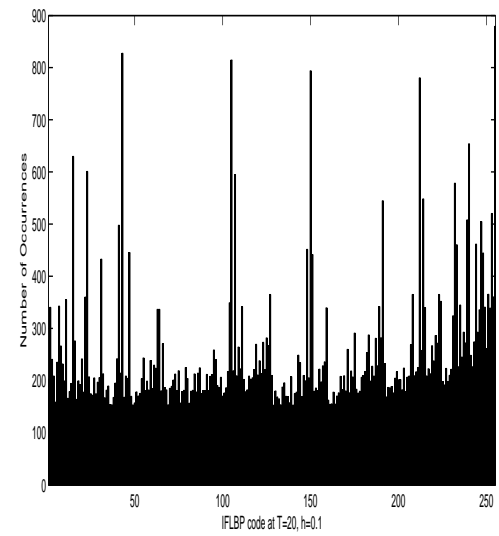
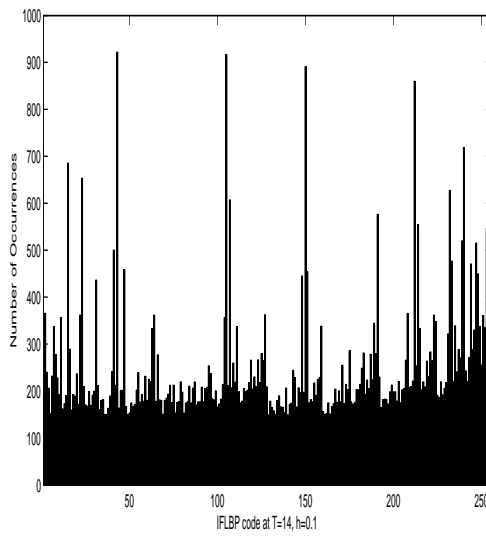
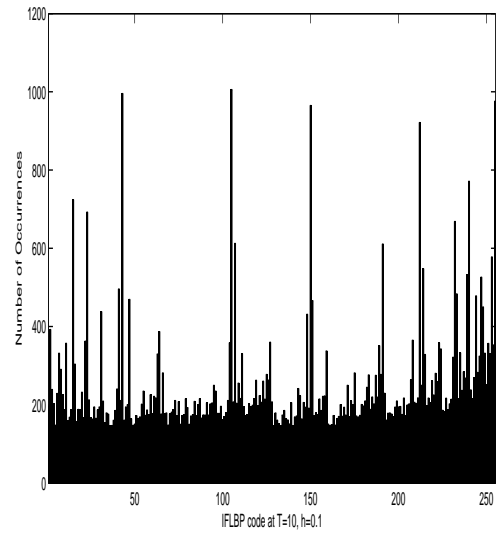
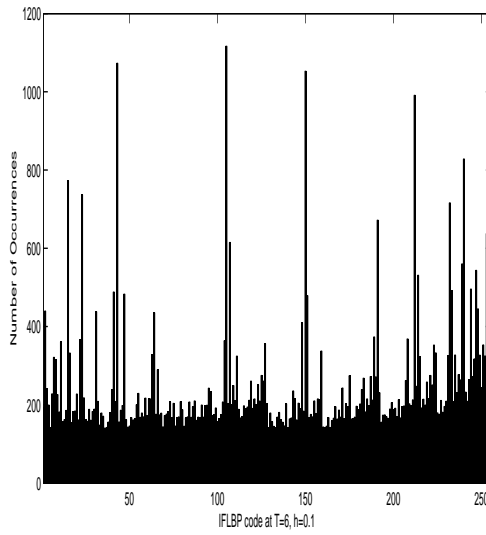
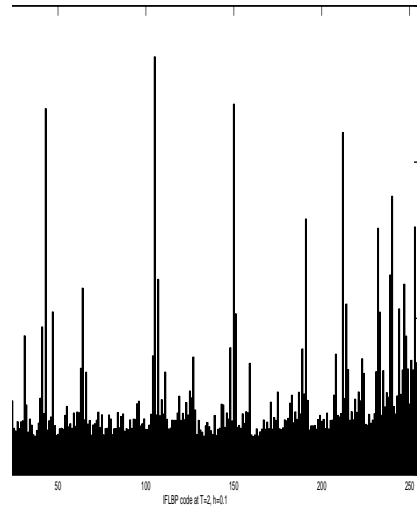
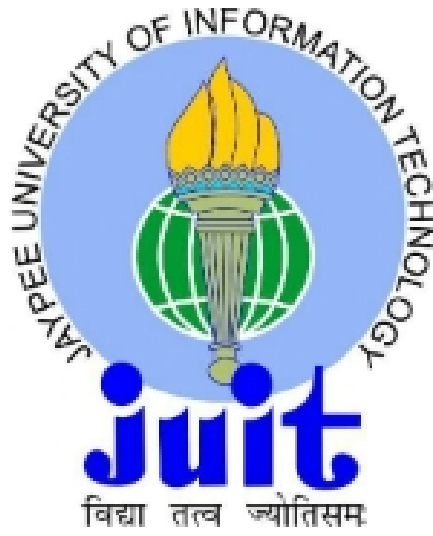


Figure 5.7: Histograms Plot of IFLBP Codes for JUIT Logo

5.7 Conclusion

We have developed a novel intuitionistic fuzzy local binary pattern for texture feature extraction to encode local texture from an image with the help of intuitionistic fuzzy set theory in the representation of local patterns of texture in the images. The developed approach is the extended version of FLBP method. IFS-LBP also devote to more than one bin in the distribution of the IFS-LBP values. Further, it can be used as a feature vector in various field of image processing. The proposed IFS-LBP technique is experimentally evaluated for various medical and image processing images of the size 256×256 . It can be observed from Tables 1-5, the entropy values of the proposed method is always greater than the existing approaches. The obtained results validate the effectiveness as well as usefulness of our proposed method over the existing feature extraction methods. The proposed IFS-LBP approach can be applied for feature extraction in the various fields of image processing and bio-medical image processing i.e. image de-noising problems, image forgery detection, pattern classification and recognition, image segmentation etc.

Chapter 6

Conclusions and Future Scope

6.1 Conclusions

This thesis emphasizes on copy move image forgery detection techniques. New approaches have been proposed to address open issues such as accuracy and execution time.

Chapter 2 presents projection profiling based cloning detection. A fast algorithm for detecting copy move region which is tested on more than 50 images of various sizes such as 256×256 and 512×512 etc. The accuracy of the proposed algorithm is 88 %. The execution time is comparative less with the various existing algorithms. The new improvements have been suggested in terms of accuracy as well as execution time compare with existing techniques.

In chapter 3, we have designed a hybrid method for cloning detection using ring projection and modified fast discrete haar wavelet transform. It is used to detect copy-move image forgery by comprises scheme of haar wavelet and RPT, the time efficiency can be greatly improved. The accuracy of proposed method is 90.75 % and execution time is also improved.

In chapter 4, we have developed a direct fuzzy transform and ring projection based copy-move image forgery detection method for detecting copy-move forgery. This approach is successfully able to improve the accuracy as well as reduce the execution time and robust to attacks such as rotation, scaling and blurring etc. The accuracy is 91.25 %.

Chapter 5 presents the texture features extraction method using intuitionistic fuzzy local binary pattern. These extracted features are found more informative and efficient compare to other reported algorithms. This technique can be used in many applications areas of image processing.

6.2 Future Scope

In future, proposed algorithm can be tested on color images and texture feature extraction technique can be applied to extract feature vector. Further, these features may be used to detect forgery as well as the other image processing areas such as pattern recognition, medical imaging, face detection and so on.

Publications

Journal Papers

1. Mohd Dilshad Ansari, Satya Prakash Ghrera and Vipin Tyagi, "Pixel-Based Image Forgery Detection: A Review", IETE Journal of Education, Vol. 55(1), 2014. [Published By Taylor & Francis] Citations: 45
2. Mohd Dilshad Ansari, Satya Prakash Ghrera and Mohd Wajid "An Approach for Identification of Copy-Move Regions based on Image Projection Profiling", Pertanika Journal of Science and Technology,(JST), Malaysia, Vol. 25(2), pp.507-508, 2017. [Indexed in Scopus, ESCI-Thomson Reuters] Citations: 3
3. Mohd Dilshad Ansari and Satya Prakash Ghrera "Intuitionistic Fuzzy Local Binary Pattern for Features Extraction", International Journal of Information and Communication Technology (IJICT), Inderscience, Vol. 13(1), pp.83-99, 2018. [Indexing in Scopus, ACM] Citations: 7
4. Mohd Dilshad Ansari and Satya Prakash Ghrera "Copy-Move Image Forgery Detection using Ring Projection and Modified Fast Discrete Haar Wavelet Transform", International Journal on Electrical Engineering and Informatics, Indonesia, Vol.9(3), pp.542-552, 2017. [Indexed in Scopus, DOAJ]
5. Mohd Dilshad Ansari and Satya Prakash Ghrera "Direct Fuzzy Transform and RPT Based Copy-Move Image Forgery Detection", International Journal of Signal and Imaging Systems Engineering(IJSISE), Inderscience. [Indexed in Scopus, ESCI] (Accepted)
6. Mohd Dilshad Ansari, Satya Prakash Ghrera "Texture Feature Extraction using Intuitionistic Fuzzy Local Binary Pattern", Pertanika Journal of Science and Technology, Malaysia. [Indexed in Scopus, ESCI] (Under Review)

Conference Papers

1. Mohd Dilshad Ansari and Satya Prakash Ghrera "Feature Extraction Method for Digital Images Based on Intuitionistic Fuzzy Local Binary Pattern" 5th IEEE International Conference on System Modeling & Advancement in Recent Trends (SMART- 25-27 Nov 2016), pp. 345-349, 2016. TMU, Moradabad, Uttar Pradesh, India. [Indexed in Scopus, ISI]
2. Mohd Dilshad Ansari and Satya Prakash Ghrera "On Copy Move Image Forgery Detection using Modified Fast Discrete Haar Wavelet Transform" 4th IEEE International Conference on Computing for Sustainable Global Development (IndiaCom- 1-3 March 2017) Bharati Vidhyapeeth, New Delhi, India. (Accepted & Presented) [Indexed in Scopus, IET]

Bibliography

- [1] Fridrich, J., Soukal D., & Lukas, J. "Detection of copy move forgery in digital images," Proceedings of the Digital Forensic Research Workshop, pp.5-8, August 2003.
- [2] Popescu, A. C. & Farid, H. "Exposing digital forgeries by detecting duplicated image regions", Technical Report, TR2004-515, Dartmouth College, 2004.
- [3] Gonzalez, R.C., Woods, R.E. "Digital Image Processing", 2nd edn. (2002)
- [4] Lin, S. D., & Wu, T. "An Integrated Technique for Splicing and Copy-move Forgery Image Detection," 4th International Congress on Image and Signal Processing (CISP), vol. 2, pp. 1086-1090. IEEE, 2011
- [5] Kang, X., & Wei, S, "Identifying Tampered regions using singular value decomposition in Digital image forensics," International Conference on Computer Science and Software Engineering, Vol. 3, pp. 926-930, 2008.
- [6] Huang, H., Guo , W., & Zhang ,Y. "Detection of copy-move forgery in digital images using SIFT algorithm," Pacific-Asia Workshop on Computational Intelligence and Industrial Application, Vol. 2, pp. 272-276, 2008.
- [7] Li, G., Wu, Q., Tu, D., & Sun, S. "A Sorted Neighborhood Approach for Detecting Duplicated Regions in Image Forgeries based on DWT and SVD,"

- International Conference on Multimedia and Expo, China, pp.1750-1753, 2007.
- [8] Ghorbani, M., Firouzmand, M., & Faraahi, A. "DWT-DCT (QCD) Based Copy-move Image Forgery Detection", 18th International Conference on Systems, Signals and Image Processing (IWSSIP), pp. 1-4, 2011.
- [9] Farid, H. "A survey of image forgery detection," IEEE Signal Process. Mag., vol. 26(2), pp. 16-25, 2009.
- [10] Redi, J. A., Taktak, W., & Dugelay, J. L. "Digital Image forensic: a booklet for beginners" Multimedia tools and application, Vol. 51(1), pp.133-162, 2011.
- [11] Lin, H. J., Wang, C. W., & Kao, Y. T. "Fast Copy-Move Forgery Detection," WSEAS Trans. Signal Process, Vol. 5(5), pp.188-197, 2009.
- [12] Luo, W., Huang, J., & Qiu, G. "Robust detection of region-duplication forgery in digital image," 18th International Conference on Pattern Recognition (ICPR2006), Vol. 4, pp. 746-749, 2006.
- [13] Zhang, J., Feng, Z., & Su, Y. "A New Approach for Detecting Copy-Move forgery in Digital Images". International Conf. on Comm. Sys., Singapore, pp. 362-366, 2008.
- [14] Kang, L., & Cheng, X. P. "Copy-move Forgery Detection in Digital Image," International Congress on Image and Signal Processing (CISP2010) IEEE Computer Society, pp. 2419-2421. 2010.
- [15] Qu, Z., Qiu, G., & Huang, J. "Detect Digital Image Splicing with Visual Cues" International workshop on information hiding, Springer, Berlin, Heidelberg, pp 247-261, 2009

- [16] Lin, Z., He, J., Tang, X., & Tang, C. K. "Fast, automatic and fine-grained tampered JPEG image detection via DCT coefficient analysis" *Pattern Recognition*, Vol.42 (11), pp. 2492-2501, 2009.
- [17] Huang, Y., Lu, W., Sun, W., & Long, D. "Improved DCT-based detection of copy-move forgery in images," *Forensic Science International*, vol. 206 (1), pp. 178-184, 2011.
- [18] Qiao, M., Sung, A., Liu, Q., & Ribeiro, B. "A novel approach for detection of copy-move forgery", *Fifth International Conference on Advanced Engineering Computing and Applications in Sciences (ADVCOMP 2011)*, pp. 44-47, 2011
- [19] Ryu, S. J., Lee, M. J., & Lee, H. K. "Detection of copy-rotate-move forgery using zernike moments," *International Workshop on Information Hiding*, Vol.6387, pp.51-65, 2010.
- [20] Chuang, W. H., Swaminathan, A., & Wu, M. "Tampering identification using empirical frequency response," *International Conference on Acoustics, Speech, and Signal Processing (ICASSP'09)*, pp. 1517-1520, 2009.
- [21] Zimba, M., & Xingming, S. "DWT-PCA (EVD) based copy-move image forgery detection", *International Journal of Digital Content Technology and its Applications*, Vol.5 (1), pp.251-258, 2011.
- [22] Amerini, I., Ballan, L., Caldelli, R., Del Bimbo, A., & Serra, G. "A SIFT-based forensic method for copy move attack and transformation recovery", *IEEE Transactions on Information Forensics and Security* Vol.6 (3), pp.1099-1110, 2011.
- [23] Zhang, C., & Zhang, H. "Exposing Digital Image Forgeries by Using Canonical Correlation Analysis", *International Conference on Pattern Recognition (ICPR)*, pp.838-841, 2010

- [24] Bayram, S., Sencar, H. T., & Memon, N. "An efficient and robust method for detecting copy-move forgery", International Conference on Acoustics, Speech and Signal Processing (ICASSP), pp. 1053-1056, 2009.
- [25] Bayram, S., Sencar, H. T., & Memon, N. "A survey of copy-move forgery detection techniques," IEEE Western New York Image Processing Workshop, Rochester, NY, pp. 538-542, 2008.
- [26] Popescu, A. C. & Farid, H., "Exposing digital forgeries in color fillter array interpolated images," IEEE Transactions on Signal Processing, Vol. 53 (10), 3948-3959, 2005.
- [27] Popescu, A.C.,& Farid, H. "Exposing digital forgeries by detecting traces of resampling". IEEE Transactions on Signal Processing, Vol.53 (2), pp.758-767, 2005.
- [28] Barcelo,A., Montseny,E., & Sobrevilla,P. "Fuzzy Texture Unit and Fuzzy Texture Spectrum for texture characterization", Fuzzy Sets and System, Vol.158 (3), pp.239-252, 2007.
- [29] Ahonen, T., & Pietikinen, M. "Soft histograms for local binary patterns", Finnish Signal Processing Symposium, Vol. 5 (9), pp. 1-5, 2007.
- [30] Keramidis, E., Iakovidis, D., & Maroulis, D. "Fuzzy binary patterns for uncertainty-aware texture representation", Electronic Letters on Computer Vision and Image Analysis, Vol.10 (1), pp.63-78, 2011.
- [31] Zadeh, L., "Fuzzy Sets", Journal of Information and Control, Vol.8(3), pp.338-353, 1965.
- [32] Mahdian, B., & Saic, S. "Detection of copy-move forgery using a method based on blur moment invariants", Forensic science international, vol. 171(2), pp. 180-189, 2007.

- [33] Roeser, P. R., & Jernigan, M. E. "Fast Haar Transform Algorithm", IEEE Transactions on Computer", Vol. 31 (2), pp.175-177, 1982.
- [34] Kaiser, G. "The Fast Haar Transform: Gateway to Wavelet", IEEE Potentials, Vol.17 (2), pp.34-37, 1998.
- [35] Wajid, M., Abdullah, M. W., & Farooq, O. "Imprinted Braille-character pattern recognition using image processing techniques" International Conference on Image Information Processing (ICIIP), pp. 1-5, 2011.
- [36] Tang, Y. Y., Cheng, H. D., & Suen, C. Y. "Transformation-ring projection (TPR) algorithm and its VLSI implementation," International Journal of Pattern Recognition Artificial Intelligence, Vol. 5(2), pp.25-56, 1991.
- [37] Tang, Y. Y., Li, B. F., Ma, H., & Liu, J. "Ring-projection-wavelet fractal signatures: a novel approach to feature extraction," IEEE Transaction on Circuits System: Analog and Digital Signal Processing, Vol.45 (8), pp.1130-1134, 1998.
- [38] Perfilieva, I. "Fuzzy transforms." Transactions on Rough Sets II, Springer Berlin, Heidelberg, Vol.3135, pp.63-81, 2004.
- [39] Perfilieva, I. "Fuzzy Transforms: theory and applications", Fuzzy Sets and Systems, Vol.157(8), pp.993-1023. 2006.
- [40] Di Martino, F., Loia, V., Perfilieva, I., & Sessa, S. "An image coding/decoding method based on direct and inverse fuzzy transforms." International Journal of Approximate Reasoning, Vol.48 (1), pp.110-131, 2008.
- [41] Novk, V., Perfilieva, I., & Mockor, J. "Mathematical principles of fuzzy logic" Springer Science & Business Media, Vol. 517, 2012.
- [42] Pal, N. R. & Pal, S. K. "Object-background segmentation using new definitions of entropy", IEE Proceeding E (Computers and Digital Technique), Vol.136 (4), pp.284-295, 1989.

- [43] Wang, X., Zhang, X., Li, Z., & Wang, S. "A DWT-DCT based passive forensics method for copy-move attacks", 3rd IEEE International Conference on Multimedia Information Networking and Security, pp. 304-308, 2011.
- [44] Chow, T. W., & Rahman, M. K. M. "A new image classification technique using tree-structured regional features", *Neurocomputing*, vol.70(4), pp. 1040-1050, 2007.
- [45] Hashmi, M. F., & Keskar, A. G. "Block and Fuzzy Techniques Based Forensic Tool for Detection and Classification of Image Forgery", *Journal of Electrical Engineering and Technology*, Vol.10 (4), pp.1886-1898 , 2015.
- [46] Pan, X. & Lyu, S. "Region duplication detection using image feature matching" *IEEE Transaction on Information Forensics and Security*, Vol.5 (4), pp.857-867, 2010.
- [47] Heikkila, M., & Pietikainen, M. "A texture-based method for modeling the background and detecting moving objects", *IEEE transactions on pattern analysis and machine intelligence*, Vol.28(4), pp. 657-662, 2006
- [48] Sertel, O., Kong, J., Shimada, H., Catalyurek, U. V., Saltz, J. H., & Gurcan, M. N. "Computer-aided prognosis of neuroblastoma on whole-slide images: Classification of stromal development", *Pattern recognition*, Vol. 42(6), pp.1093-1103, 2009.
- [49] Chang, P. & Piau, P. "Modified Fast and Exact Algorithm for Fast Haar Transform", *Proceedings of World Academy of Science, Engineering and Technology*, Vol.26, pp.509-512, 2007.
- [50] Bhardwaj, A. & Ali, R. "Image Compression Using Modified Fast Haar Wavelet Transform", *World Applied Sciences Journal*, Vol.7(5), pp.647-653, 2009.

- [51] Tsai, D. M. & Chiang, C. H. "Rotation-invariant pattern matching using wavelet decomposition", *Pattern Recogn. Lett.*, Vol.23(1), pp.191-201, 2002.
- [52] Choi, M.S. & Kim, W.Y. "A novel two stage template matching method for rotation and illumination invariance", *Pattern Recogn.*, Vol.35, pp.119-129, 2002.
- [53] Battiato, S., Farinella, G.M., Messina, E. & Puglisi, G. "Robust image alignment for tampering detection". *IEEE Trans. Inf. Forensics Secur.*, Vol.7(4), pp.1105-1117, 2012.
- [54] Ibrahim, R.W., Moghaddasi, Z., Jalab, H.A. & Noor, R.M. "Fractional differential texture descriptors based on the machado entropy for image splicing detection", *Entropy*, vol. 17(7), pp.4775-4785, 2015.
- [55] Hu, J., Zhang, H., Gao, Q. & Huang, H. "An improved lexicographical sort algorithm of copy-move forgery detection" *Second International Conference on Networking and Distributed Computing (ICNDC)*, pp. 23-27, 2011.
- [56] Lee, J. C., Chang, C. P., & Chen, W. K. "Detection of copy-move image forgery using histogram of orientated gradients" *Information Sciences*, Vol.321, pp.250-262, 2015
- [57] Liu, G., Wang, J., Lian, S. & Wang, Z. "A passive image authentication scheme for detecting region-duplication forgery with rotation." *Journal of Network and Computer Applications*, Vol.34(5), pp.1557-1565, 2011.
- [58] Castellano, G., Bonilha, L., Li, L. M., & Cendes, F. "Texture analysis of medical images" *Clinical radiology*, Vol. 59(12), pp.1061-1069, 2004.
- [59] Tsymbal, O. V., Lukin, V. V., Ponomarenko, N. N., Zelensky, A. A., Egiazarian, K. O., & Astola, J. T "Three-State Locally Adaptive Texture Preserving Filter for Radar and Optical Image Processing", *EURASIP Journ. on Ap. Sign. Proc.*, Vol.8, pp.1185-1204, 2005.

- [60] Li, Y., & Peng, J. X. "Remote Sensing Texture Analysis Using Multi-Parameter and Multi-Scale Features", *Photo. Engin. & Remote Sens.*, Vol. 69(4), pp.351-356, 2003.
- [61] Wang, Z. Z., & Yong, J. H. "Texture Analysis and Classification With Linear Regression Model Based on Wavelet Transform", *IEEE Transactions on Image Processing*, Vol.17(8), pp.1421-1430, 2008.
- [62] Wagner, T. "Texture Analysis" *Handbook of Computer Vision and Application*, Academic Press, 1999.
- [63] Petrou, M. & Sevilla, P. G. "Image Processing: Dealing With Texture", New York: Wiley, 2006.
- [64] Ojala, T., Pietikinen, M., & Harwood, D. "A comparative study of texture measures with classification based on featured distribution", *Pattern Recognition*, Vol.29(1), pp.51-59, 1996 .
- [65] Chan, C. H., Kittler, J., & Messer, K. "Multi-Scale Local Binary Pattern Histograms for Face Recognition", *Advances in biometrics*, Seoul, Korea, LNCS 4642, Springer, pp.809-818, 2007.
- [66] Pok, G., Ryu, K. H., & Lyu, J. C. "Rotation and Gray-Scale Invariant Classification of Textures Improved by Spatial Distribution of Features", *DEXA 2005*, Copenhagen, Denmark, LNCS 3588, pp.250-259, 2005.
- [67] Fehr, J. "Rotational Invariant Uniform Local Binary Patterns For Full 3D Volume Texture Analysis", *Finnish signal processing symposium (FINSIG)*, Oulu, Finland (2007).
- [68] Wu, W., Li, J., Wang, T., & Zhang, Y. "Markov chain local binary pattern and its application to video concept detection." In *15th IEEE International Conference on Image Processing*, pp. 2524-2527, 2008.

- [69] Li, M., & Staunton, R. C. "Optimum Gabor filter design and local binary patterns for texture segmentation", *Pattern Recognition Letters*, Vol.29(5), pp.664-672, 2008.
- [70] Yao, C. H., & Chen, S. Y. "Retrieval of translated, rotated and scaled color textures", *Pattern Recognition*, Vol.36(4), pp.913-929, 2003.
- [71] Hafiane, A., Seetharaman, G., & Zavidovique, B. "Median binary pattern for textures Classification", *International Conference Image Analysis and Recognition*, Springer, Berlin, Heidelberg, pp.387-398, 2007.
- [72] Hafiane, A., Seetharaman, G., Palaniappan, K., & Zavidovique, B. "Rotationally Invariant Hashing of Median Binary Patterns for Texture Classification", *Proc. Image Analysis and Recognition*, LNCS, pp.619-629, 2008.
- [73] Iivarinen, J. "Surface defect detection with histogram-based texture features" *Intelligent Robots and Computer Vision XIX: Algorithms, Techniques, and Active Vision*, Vol.4197, pp.140-145, 2000.
- [74] Silvén, O., Niskanen, M., & Kauppinen, H. "Wood inspection with non-supervised clustering" *Machine Vision and Applications*, Vol.13(5), pp.275-285, 2003.
- [75] Tajeripour, F., Kabir, E., & Sheikhi, A. "Fabric Defect Detection Using Modified Local Binary Patterns", *EURASIP Journal on Advances in Signal Processing*, Vol. 1, pp.783-898, 2008.
- [76] Hadizadeh, H., & Shokouhi, S. B. "Random Texture Defect Detection Using 1-D Hidden Markov Models Based on Local Binary Patterns" *IEICE Transactions on Information and Systems*, Vol.91(7), pp.1937-1945, 2008.
- [77] Grabner, H., Nguyen, T. T., Gruber, B., & Bischof, H. "On-line boosting-based car detection from aerial images", *ISPRS Journal of Photogrammetry and Remote Sensing*, Vol.63(3), pp.382-396, 2008.

- [78] Liao, C. J., & Chen, S. Y. "Complementary retrieval for distorted images", *Pattern Recognition*, Vol.35(8), pp.1705-1722,2002.
- [79] Jiang, J., Armstrong, A., & Feng, G. C. "Web-based Image Indexing and Retrieval in JPEG compressed domain", *Multimedia Systems*, Vol.9(5),pp.424-432, 2004.
- [80] Grangier, D., & Bengio, S. "A Discriminative Kernel-Based Approach to Rank Images from Text Queries", *IEEE Transactions on Pattern Analysis and Machine Intelligence*, Vol.30(8), pp.1371-1384, 2008.
- [81] Li, S. Z., Chu, R., Liao, S., & Zhang, L. "Illumination Invariant Face Recognition Using Near-Infrared Images", *IEEE Transactions on Pattern Analysis and Machine Intelligence*, Vol.29(4), pp.627-639, 2007.
- [82] Zhang, X., Gao, Y., & Leung, M. K. "Recognizing Rotated Faces From Frontal and Side Views: An Approach Toward Effective Use of Mugshot Databases", *IEEE Transactions on Information Forensics and Security*, Vol.3(4), pp.684-697, 2008.
- [83] Destrero, A., De Mol, C., Odone, F., & Verri, A. "A regularized framework for feature selection in face detection and authentication" *International journal of computer vision*, Vol.83(2), pp.164-177, 2009.
- [84] Shan, C., Gong, S., & McOwan, P. W. "Facial expression recognition based on local binary patterns: A comprehensive study" *Image and Vision Computing*, Vol.27(6), pp.803-816, 2009.
- [85] Iakovidis, D. K., Maroulis, D. E., & Karkanis, S. A. "An intelligent system for automatic detection of gastrointestinal adenomas in video endoscopy", *Computers in Biology and Medicine*, Vol.36(10), pp.1084-1103, 2006.
- [86] Nanni, L., & Lumini, A. "A reliable method for cell phenotype image classification", *Artificial Intelligence in Medicine*, Vol.43(2), pp.87-97, 2008.

- [87] Sertel, O., Kong, J., Shimada, H., Catalyurek, U. V., Saltz, J. H., & Gurcan, M. N. "Computer-aided prognosis of neuroblastoma on whole-slide images: Classification of stromal development", *Pattern Recognition*, Vol.42(6), pp.1093-1103, 2009.
- [88] Garcia, R., Xevi, C., & Battle, J. "Detection of matchings in a sequence of underwater images through texture analysis", *Proc. IEEE International Conference on Image Processing*, Vol.1, pp.361-364, 2001.
- [89] Heikkila, M., & Pietikainen, M. "A texture-based method for modeling the background and detecting moving objects", *IEEE Transactions on Pattern Analysis and Machine Intelligence*, Vol.28(4), pp.657-662, 2006.
- [90] Petrovic, N., Jovanov, L., Piurica, A., & Philips, W. "Object Tracking Using Naive Bayesian Classifiers", *Proc. Advanced Concepts for Intelligent Vision Systems*, LNCS 5259, pp.775-784, 2008.
- [91] Barcelo, A., Montseny, E., & Sobrevilla, P. "Fuzzy Texture Unit and Fuzzy Texture Spectrum for texture characterization", *Fuzzy Sets System*, Vol. 158(3), pp.239-252, 2007.
- [92] Keramidas, E.G. "Ultrasound Image Processing and Analysis Framework", MSc thesis, University of Athens, Greece, 2007.
- [93] Keramidas, E. G., Iakovidis, D. K., Maroulis, D., & Dimitropoulos, N. "Thyroid Texture Representation via Noise Resistant Image Features", *IEEE International Symposium on Computer-Based Medical Systems*, pp.560-565, 2008.
- [94] Keramidas, E. G., Iakovidis, D. K., & Maroulis, D. "Noise-robust statistical feature distributions for texture analysis." In *16th European IEEE Conference on Signal Processing*, pp. 1-5, 2008.

- [95] Iakovidis, D. K., Keramidas, E. G., & Maroulis, D. "Fuzzy local binary patterns for ultrasound texture characterization", *Image Analysis and Recognition*. Springer Berlin Heidelberg, pp.750-759, 2008.
- [96] Zadeh, L. A. "Fuzzy Sets" *Journal of Information and Control*, Vol.8(3), pp.338-353, 1965.
- [97] Atanassov, K. T. "Intuitionistic Fuzzy Sets", *Fuzzy Sets and Systems*, Vol.20(1),pp.87-96, 1986.
- [98] Atanassov, K., & Gargov, G. "Interval-Valued Intuitionistic Fuzzy Sets", *Fuzzy Sets and Systems*, Vol.31(3), pp.343-349, 1989.
- [99] Shannon, C. E. "A Mathematical Theory of Communication" *The Bell System Technical Journal*, Vol.27, pp.623-656, 1948.
- [100] Pal, N. R., & Pal, S. K. "Object-background segmentation using new definitions of entropy" *IEE Proceedings E-Computers and Digital Techniques* Vol.136(4), pp.284-295, 1989.
- [101] ping Tian, D. "A review on image feature extraction and representation techniques" *International Journal of Multimedia and Ubiquitous Engineering*, Vol.8(4), pp.385-396, 2013.
- [102] <http://www.micc.unii.it/ballan/research/image-forensics/>.